

Enhanced Propagation Yield of Influenza Viruses for Vaccine
Production through Cellular MicroRNAs Regulation.



Mr. Suthat Saengchoowong

จุฬาลงกรณ์มหาวิทยาลัย
CHULALONGKORN UNIVERSITY

A Dissertation Submitted in Partial Fulfillment of the Requirements
for the Degree of Doctor of Philosophy in Biomedical Sciences and
Biotechnology

Common Course

FACULTY OF MEDICINE

Chulalongkorn University

Academic Year 2019

Copyright of Chulalongkorn University



จุฬาลงกรณ์มหาวิทยาลัย
CHULALONGKORN UNIVERSITY

การเพิ่มปริมาณเชื้อไวรัสไข้วัดใหญ่เพื่อการผลิตวัคซีนด้วยวิธีการควบคุมระดับไมโครอาร์เอ็นเอ
ของเซลล์



วิทยานิพนธ์นี้เป็นส่วนหนึ่งของการศึกษาตามหลักสูตรปริญญาวิทยาศาสตรดุษฎีบัณฑิต
สาขาวิชาชีวเวชศาสตร์และชีวเทคโนโลยี ไม่สังกัดภาควิชา/เทียบเท่า
คณะแพทยศาสตร์ จุฬาลงกรณ์มหาวิทยาลัย
ปีการศึกษา 2562
ลิขสิทธิ์ของจุฬาลงกรณ์มหาวิทยาลัย

Thesis Title	Enhanced Propagation Yield of Influenza Viruses for Vaccine Production through Cellular MicroRNAs Regulation.
By	Mr. Suthat Saengchoowong
Field of Study	Biomedical Sciences and Biotechnology
Thesis Advisor	Associate Professor SUNCHAI PAYUNGPORN, Ph.D.
Thesis Co Advisor	Professor YONG POOVORAWAN, M.D. Qibo Zhang, Ph.D.

Accepted by the FACULTY OF MEDICINE, Chulalongkorn University in Partial Fulfillment of the Requirement for the Doctor of Philosophy

..... Dean of the FACULTY OF
MEDICINE
(Professor SUTTIPONG WACHARASINDHU, M.D.)

DISSERTATION COMMITTEE

..... Chairman
(Professor KANYA SUPHAPEETIPORN, M.D., Ph.D.)
..... Thesis Advisor
(Associate Professor SUNCHAI PAYUNGPORN, Ph.D.)
..... Thesis Co-Advisor
(Professor YONG POOVORAWAN, M.D.)
..... Thesis Co-Advisor
(Qibo Zhang, Ph.D.)
..... Examiner
(Associate Professor PARVAPAN
BHATTARAKOSOL, Ph.D.)
..... Examiner
(Assistant Professor THANANYA THONGTAN, Ph.D.)
..... External Examiner
(Professor William Anderson Paxton, Ph.D.)
..... External Examiner
(Assistant Professor Nattanan Panjaworayan T-
Thienprasert, Ph.D.)

สุทัศน์ แสงชูวงศ์ : การเพิ่มปริมาณเชื้อไวรัสไข้หวัดใหญ่เพื่อการผลิตวัคซีนด้วยวิธีการควบคุมระดับไมโครอาร์เอ็นเอของเซลล์. (Enhanced Propagation Yield of Influenza Viruses for Vaccine Production through Cellular MicroRNAs Regulation.) อ.ที่ปรึกษาหลัก : รศ. ดร.สัณชัย พงษ์กร, อ.ที่ปรึกษาร่วม : ศ. นพ.ยง ภู่วรวรรณ,ดร.ลิโบ ชาง

การรับวัคซีนไข้หวัดใหญ่ประจำปีช่วยลดความรุนแรงของอาการทางคลินิก และช่วยลดอัตราการตายซึ่งเกิดจากการติดเชื้อไวรัสไข้หวัดใหญ่ ปัจจุบันเซลล์ไตสุนัข Madin-Darby (MDCK) ได้รับการรับรองเพื่อการผลิตวัคซีนไข้หวัดใหญ่ที่ใช้ในมนุษย์ ถึงแม้ว่าไมโครอาร์เอ็นเอจะมีบทบาทสำคัญในการควบคุมการแบ่งตัวของเชื้อไวรัสชนิดต่างๆ แต่ยังไม่มีการศึกษาปฏิสัมพันธ์ระหว่างเชื้อไวรัสไข้หวัดใหญ่ที่ระบาดในมนุษย์กับไมโครอาร์เอ็นเอของโฮสต์ที่พบในเซลล์ไตสุนัขนี้ วัตถุประสงค์หลักของการศึกษานี้เพื่อเพิ่มปริมาณเชื้อไวรัสไข้หวัดใหญ่ด้วยวิธีการควบคุมระดับไมโครอาร์เอ็นเอของเซลล์โฮสต์ โดยนำเซลล์ไตสุนัขมาติดเชื้อไข้หวัดใหญ่สายพันธุ์เอ (ชนิด pH1N1 หรือ H3N2) หรือไข้หวัดใหญ่สายพันธุ์บี (ชนิด Victoria หรือ Yamagata) ด้วยค่า multiplicity of infection (MOI) ที่ 0.01 หลังจากการติดเชื้อ 6, 12 และ 24 ชั่วโมง ทำการตรวจสอบข้อมูลของไมโครอาร์เอ็นเอด้วยเทคโนโลยีหิววิเคราะห์ลำดับเบส Next-generation sequencing ด้วยเครื่อง MiSeq (Illumina) ข้อมูลการเปลี่ยนแปลงระดับของไมโครอาร์เอ็นเอถูกทดสอบยืนยันความถูกต้องอีกครั้งด้วยวิธี RT-qPCR และเพื่อตรวจสอบผลของไมโครอาร์เอ็นเอดังกล่าวที่มีต่อการเพิ่มจำนวนของเชื้อไวรัสไข้หวัดใหญ่ ทำการนำส่งตัวยับยั้งไมโครอาร์เอ็นเอ (microRNA inhibitor) หรือพลาสมิด์ที่กระตุ้นการแสดงออกของไมโครอาร์เอ็นเอชนิดนั้นเข้าไปในเซลล์ไตสุนัข ตามด้วยการติดเชื้อไวรัสไข้หวัดใหญ่สายพันธุ์ต่าง ๆ แล้วทำการเก็บน้ำยาเลี้ยงเซลล์ที่ 48 ชั่วโมง ภายหลังจากการติดเชื้อไวรัส เพื่อตรวจสอบปริมาณการเพิ่มจำนวนของไวรัสด้วยเทคนิค RT-qPCR และ ELISA นอกจากนี้บริเวณตำแหน่งของอินเพ้าหมายที่จับกับไมโครอาร์เอ็นเอถูกทำนายด้วยโปรแกรมคอมพิวเตอร์ และถูกตรวจสอบด้วยเทคนิค 3'-UTR reporter และ dual luciferase assay นอกจากนี้ทำการตรวจสอบลำดับนิวคลีโอไทด์ของอิน HA และ NA ของเชื้อไวรัสไข้หวัดใหญ่ที่ถูกเพิ่มจำนวนด้วยการใส่ microRNA inhibitor จากผลการศึกษาพบว่า ไมโครอาร์เอ็นเอ 4 ชนิด ได้แก่ cfa-miR-340, cfa-miR-146b, cfa-miR-197 และ cfa-miR-215 ที่มีการเปลี่ยนแปลงเพิ่มสูงขึ้น และพบได้บ่อยระหว่างการติดเชื้อไข้หวัดใหญ่หลายสายพันธุ์ ผลการทดลองพบว่า การยับยั้ง cfa-miR-146b สามารถเพิ่มปริมาณเชื้อไวรัสไข้หวัดใหญ่สายพันธุ์เอ ชนิด pH1N1 และสายพันธุ์บี ชนิด Yamagata นอกจากนี้ยังพบว่า การยับยั้ง cfa-miR-215 สามารถเพิ่มปริมาณเชื้อไวรัสสายพันธุ์เอ ชนิด pH1N1 และสายพันธุ์บี ชนิด Victoria ในขณะที่การยับยั้ง cfa-miR-197 ส่งผลให้ปริมาณเชื้อไวรัสสายพันธุ์เอ ชนิด H3N2 เพิ่มขึ้น ผลการศึกษาพบว่า cfa-miR-146b และ cfa-miR-215 สามารถจับกับตำแหน่งบนอิน PB1 ของไข้หวัดใหญ่สายพันธุ์เอ ชนิด pH1N1 ในขณะที่อิน PB2 ของเชื้อไวรัสไข้หวัดใหญ่สายพันธุ์เอ ชนิด H3N2 ถูกยับยั้งการแสดงออกเมื่อถูกจับกับ cfa-miR-197 นอกจากนี้ cfa-miR-146b สามารถจับกับตำแหน่งบนอิน PA ของไวรัสไข้หวัดใหญ่สายพันธุ์บี ชนิด Yamagata ส่วนอิน PB1 ของไวรัสไข้หวัดใหญ่สายพันธุ์บี ชนิด Victoria ถูกยับยั้งการแสดงออกเมื่อจับกับ cfa-miR-215 ผลการตรวจสอบลำดับเบสไม่พบการเปลี่ยนแปลงของลำดับนิวคลีโอไทด์ของอิน HA และ NA ซึ่งเป็นอินที่แสดงความเป็นแอนติเจนของเชื้อไวรัสไข้หวัดใหญ่ระหว่างไวรัสดั้งเดิม (parental) และไวรัสที่ถูกเพิ่มจำนวนด้วยการใส่ microRNA inhibitor การศึกษานี้บ่งชี้ว่า ไมโครอาร์เอ็นเอของเซลล์ MDCK มีแนวโน้มที่จะสามารถจับกับอินของไวรัสไข้หวัดใหญ่แต่ละชนิดที่แตกต่างกัน และไมโครอาร์เอ็นเอดังกล่าวส่งผลให้เกิดการยับยั้งการเพิ่มจำนวนของไวรัส ในทางกลับกันเชื้อไวรัสไข้หวัดใหญ่สามารถกลับถูกเพิ่มจำนวนได้เมื่อมีการเติม microRNA inhibitor ดังกล่าว

สาขาวิชา ชีวเวชศาสตร์และชีวเทคโนโลยี
ปีการศึกษา 2562

ลายมือชื่อนิสิต

ลายมือชื่อ อ.ที่ปรึกษาหลัก

ลายมือชื่อ อ.ที่ปรึกษาร่วม

ลายมือชื่อ อ.ที่ปรึกษาร่วม

5774852630 : MAJOR BIOMEDICAL SCIENCES AND BIOTECHNOLOGY

KEYWORD: MicroRNA, Influenza A Virus, Influenza B Virus, Madin-Darby Canine Kidney Cell, Next-generation Sequencing

Suthat Saengchoowong : Enhanced Propagation Yield of Influenza Viruses for Vaccine Production through Cellular MicroRNAs Regulation.. Advisor: Assoc. Prof. SUNCHAI PAYUNGPORN, Ph.D. Co-advisor: Prof. YONG POOVORAWAN, M.D., Qibo Zhang, Ph.D.

Annual influenza vaccination aims to prevent influenza virus infection thus reduce the incidence of infection and disease in humans. Nowadays, Madin–Darby canine kidney (MDCK) cell culture-based system has been approved as an alternative for influenza vaccine production. Although cellular microRNAs may play an important role in controlling the replication of viruses, the interaction between human seasonal influenza viruses and host microRNAs has not been investigated in this permissive cell line. The primary objective of this study is to improve the yield of seasonal influenza virus (i.e. vaccine virus) production via manipulation of the host microRNAs. MDCK cells were infected with influenza A (pH1N1 or H3N2) or influenza B (Victoria or Yamagata) virus at MOI of 0.01. After collection at 6, 12, and 24 hours post-infection, microRNAs were subjected to massively parallel sequencing using MiSeq platform (Illumina). The profiles of microRNAs were validated by RT-qPCR. To evaluate the effect of candidate microRNAs on viral replication, MDCK cells were transfected with either microRNA inhibitors or microRNA over-expressing plasmids, followed by the infection of influenza viruses. The supernatants were collected at 48 hours post-infection, and the amount of virus was quantified by RT-qPCR and ELISA method. Moreover, *in silico* predicted microRNA binding sites were further verified by 3'-UTR reporter and dual luciferase assays. Furthermore, the effect of microRNA inhibitors on antigenic HA and NA sequences was also investigated. The results showed that four validated microRNAs including *cfa*-miR-340, *cfa*-miR-146b, *cfa*-miR-197, and *cfa*-miR-215 were most commonly upregulated upon infection with different seasonal influenza viruses. Among these microRNAs, *cfa*-miR-146b is a candidate target for microRNA inhibition to increase the production of A/pH1N1 and B/Yamagata viruses. Furthermore, *cfa*-miR-215 inhibition may be another good strategy for enhancing A/pH1N1 and B/Victoria viral production. On the other hand, the inhibition of *cfa*-miR-197 may be useful for the propagation of A/H3N2 virus. Moreover, the dual luciferase assay was used to evaluate microRNA binding sites. The results showed that the PB1 gene of A/pH1N1 virus is a direct target of *cfa*-miR-146b and *cfa*-miR-215, whereas the PB2 gene of A/H3N2 virus was silenced by *cfa*-miR-197. Whilst *cfa*-miR-146b targeted the PA gene of B/Yamagata, *cfa*-miR-215 silenced the PB1 gene of B/Victoria. Lastly, the sequencing results demonstrated that there was no change in antigenic HA and NA sequences between the viruses from the cells treated with microRNA inhibitors and the parental viruses. Taken together, it is demonstrated that microRNAs target viral genes in a strain-specific manner, leading to suppression of viral replication. Conversely, propagation of influenza viruses could be enhanced by the utilisation of microRNA inhibitors.

Field of Study: Biomedical Sciences and
Biotechnology

Academic Year: 2019

Student's Signature

Advisor's Signature

Co-advisor's Signature

Co-advisor's Signature

ACKNOWLEDGEMENTS

Foremost, I would like to express my heartfelt gratitude to my advisors, Assoc. Prof. Sunchai Payungporn from Chulalongkorn University (CU) and Dr. Qibo Zhang from University of Liverpool (UoL) for their competent supervision, patience, motivation, and guidance which have encouraged me to accomplish my doctoral study. Not only academic advice have they provided for me, but they also taught me a great deal about professional and life in general.

In addition, I would like to express my deep appreciation to my co-advisor, Prof. Yong Poovorawan (CU), for being the ultimate role model and inspirational mentor who always gives an opportunity and shares an invaluable experience to many Thai young scientists, including me.

Thanks are also due to the examination committee for their insightful comments and constructive criticism on my dissertation. Moreover, I feel indebted to Prof. Steven Edwards (UoL), Asst. Prof. Thananya Thongtan (CU), as well as postgraduate staff from both universities for their helps and supports.

Besides, I would like to express my deep admiration to postgraduate fellows, especially Dr. Nasamon Wanlapakorn, for encouraging me to persevere. I warmly thank my colleagues at the SP Lab (CU) for all the happiness and fun we have had for several years. Moreover, I am particularly grateful to the QZ (UoL) lab members (Khalid, Miguel, Fadiyah, Rong, Dr. Suttida, and Dr. Shamsher) during my study experience in Liverpool, United Kingdom.

Most importantly, my study would not have been possible without the financial supports from Graduate School, and Faculty of Medicine, Chulalongkorn University: the 100th Anniversary Chulalongkorn University Fund for Doctoral Scholarship; the 90th Anniversary of Chulalongkorn University Ratchadaphiseksomphot Endowment Fund; and the Overseas Research Experience Scholarship for Graduate Students of Chulalongkorn University.

Last but not least, nobody has been more important to me in the pursuit of my Ph.D. journey than the members of my family. I would like to take this chance to express the profound gratitude to my beloved parents, Surathin Saengchoowong and Piyada Lorsirinant, whose love and guidance are with me in whatever I pursue.

Importantly, I wish to thank my loving cousins and friends, particularly Dr. Yaowaluk Techarongrojwong and Vajira Malailoy, who support me emotionally whenever I feel tired. Besides, I really appreciate all my best friends for standing by my side when times get hard.

Suthat Saengchoowong



TABLE OF CONTENTS

	Page
.....	iii
ABSTRACT (THAI)	iii
.....	iv
ABSTRACT (ENGLISH)	iv
ACKNOWLEDGEMENTS	v
TABLE OF CONTENTS	vii
LIST OF FIGURES	x
LIST OF TABLES	xii
ABBREVIATIONS	xiii
CHAPTER I INTRODUCTION	1
1.1. Background and Rationale	1
1.2. Research Questions	4
1.3. Objectives	5
1.4. Hypothesis	5
1.5. Definition	7
1.6. Experimental Design	9
CHAPTER II LITERATURE REVIEWS	10
2.1. Seasonal Influenza Viruses	10
2.1.1. Significance of Seasonal Influenza	10
2.1.2. Classification of Influenza Viruses	10
2.1.3. Virus Structure and Genome Organization	12
2.1.4. Replication Cycle	14
2.1.5. Epidemiology	20
2.1.6. Inactivated Influenza Vaccines	23
2.2. MicroRNAs	25

2.2.1. Biogenesis	25
2.2.2. Mechanisms of Action.....	27
2.2.3. Virus-Host MicroRNA Interplay.....	29
CHAPTER III RESEARCH METHODOLOGY	31
3.1. Ethical Approval	31
3.2. Cell Culture and Virus Inoculations	31
3.3. MicroRNA Extractions	32
3.4. DNA Library Preparation and High-Throughput Sequencing.....	33
3.5. Data Analysis of High-Throughput Sequencing.....	38
3.6. Quantification of MicroRNAs by Reverse Transcriptase-Quantitative Polymerase Chain Reaction (RT-qPCR).....	39
3.7. Transfection of MicroRNA Inhibitors	42
3.8. Construction of Silencing Plasmids.....	43
3.9. Transfection of Silencing Plasmids	47
3.10. Viral RNAs Extraction	47
3.11. Quantification of Viral Genes by RT-qPCR.....	48
3.12. Quantification of Viral Proteins by Enzyme-Linked Immunosorbent Assay (ELISA)	50
3.13. <i>In Silico</i> Analysis of MicroRNA Target Prediction	53
3.14. Construction of Reporter Vectors	53
3.15. Luciferase Reporter Assay.....	56
3.16. Sequencing of HA and NA Genes	57
3.17. Statistical Analysis.....	59
CHAPTER IV RESULTS.....	61
4.1. High-throughput Sequencing of Canine MicroRNAs upon Seasonal Influenza Infection.....	61
4.2. Validation of MicroRNA Profiles	70
4.3. Effect of Candidate MicroRNAs Expression on Viral Propagation Yield	74
4.4. Computational Prediction of Seasonal Influenza Viral Genomes Targeted by Canine MicroRNAs	83

4.5. MicroRNA Target Sites Validation	85
4.6. Effect of MicroRNA Inhibitor Manipulation on microRNA Binding Sites and Antigenic Sequences	92
CHAPTER V DISCUSSION AND CONCLUSIONS	98
APPENDIX A.....	111
APPENDIX B	112
REFERENCES	113
VITA.....	133



LIST OF FIGURES

Figure 1	Enhancing viral replication through manipulation of cellular microRNAs	6
Figure 2	Procedure framework	9
Figure 3	Phylogenetic trees of the hemagglutinin (HA) and neuraminidase (NA) genes of all known influenza A virus subtypes	11
Figure 4	Structure of influenza A virus	13
Figure 5	The life cycle of influenza viruses	18
Figure 6	Pandemic and seasonal viruses demonstrate genetic relationships between human and relevant animal influenza viruses	22
Figure 7	The global circulation of influenza viruses from week 1 of 2009 to week 48 of 2019	23
Figure 8	Drosha-dependent biogenesis of microRNAs	26
Figure 9	Direct and indirect effects of microRNAs on viral replication	30
Figure 10	MicroRNA profile of MDCK cells in response to IAV pH1N1 infection	63
Figure 11	MicroRNA profile of MDCK cells in response to IAV H3N2 infection	65
Figure 12	MicroRNA profile of MDCK cells in response to IBV Victoria infection	66
Figure 13	MicroRNA profile of MDCK cells in response to IBV Yamagata infection	67
Figure 14	Venn Diagram shows (A) upregulated and (B) downregulated microRNAs of MDCK cells upon different strains of seasonal influenza infection.	68
Figure 15	Validation of upregulated microRNAs during IAV infection	70

Figure 16	Validation of upregulated microRNAs during IBV infection	71
Figure 17	Effect of candidate microRNAs on the yield of IAV pH1N1 was determined by RT-qPCR and ELISA	76
Figure 18	Effect of candidate microRNAs on the yield of IAV H3N2 was determined by RT-qPCR and ELISA	78
Figure 19	Effect of candidate microRNAs on the yield of IBV Victoria was determined by RT-qPCR and ELISA	80
Figure 20	Effect of candidate microRNAs on the yield of IBV Yamagata was determined by RT-qPCR and ELISA	81
Figure 21	Schematic diagram of luciferase reporter assay for target site validation.	85
Figure 22	Luciferase assay was assessed for microRNA targets on IAV pH1N1	87
Figure 23	Luciferase assay was assessed for microRNA targets on IAV H3N2	88
Figure 24	Luciferase assay was assessed for microRNA targets on IBV Victoria	89
Figure 25	Luciferase assay was assessed for microRNA targets on IBV Yamagata	90
Figure 26	MicroRNA binding sites of the experimental strains and other seed viral strains used for influenza vaccine manufacturing during 2011-2019	93
Figure 27	HA and NA sequences of the IAV pH1N1 viruses in the presence of microRNA inhibitors	94
Figure 28	HA and NA sequences of the IBV Victoria viruses in the presence of microRNA inhibitors	95
Figure 29	HA and NA sequences of the IBV Yamagata viruses in the presence of microRNA inhibitors	96

LIST OF TABLES

Table 1	Molecular differences between influenza A and B viruses	16
Table 2	Pandemic waves of human influenza	21
Table 3	Inactivated seasonal influenza vaccines registered for use in humans	24
Table 4	Primers and PCR conditions used for microRNA quantification	41
Table 5	Oligonucleotides used for the construction of silencing plasmids	44
Table 6	Primers and PCR conditions used for viral RNA quantification	50
Table 7	Oligonucleotides used for the construction of reporter plasmids	55
Table 8	Primers and PCR conditions used for HA and NA amplification	59
Table 9	Summary statistics of sequencing data obtained from MDCK cells infected with mock and seasonal IAV at different time points.	61
Table 10	Summary statistics of sequencing data obtained from MDCK cells infected with mock and seasonal IBV at different time points.	62
Table 11	Summary of common microRNA validation	73
Table 12	<i>In silico</i> analysis of microRNA target prediction	83
Table 13	Predicted host genes targeted by candidate microRNAs	106

ABBREVIATIONS

ANOVA	Analysis of variance
Ago2	Argonaute-2
bp	Base pair
BS	Bottom strand
BSA	Bovine serum albumin
°C	Degree Celsius
<i>cfa</i>	<i>Canis familiaris</i> (Dog)
CO ₂	Carbon dioxide
Ct	Cycle threshold
cRNA	Complementary RNA
CYLD	Lysine 63 deubiquitinase
ddH ₂ O	Double-distilled water
DGCR8	DiGeorge critical region 8
DMEM	Dulbecco's modified Eagle medium
<i>E. coli</i>	<i>Escherichia coli</i>
EDTA	Ethylenediaminetetraacetic acid
EEEV	Eastern equine encephalitis virus
ELISA	Enzyme-linked immunosorbent assay
EMA	European Medicines Agency
EV71	Enterovirus 71
F	Forward strand
FBS	Fetal bovine serum
FDA	U.S. Food and Drug Administration
GISAID	Global Initiative on Sharing All Influenza Data
GW182	Glycine-tryptophan repeat-containing protein of 182 kDa
h	Hour
HA	Hemagglutinin
HCV	Hepatitis C virus
hpi	Hours post infection
HRP	Horseradish-peroxidase
<i>hsa</i>	<i>Homo sapiens</i> (Human)
H ₂ SO ₄	Sulfuric Acid
HTLV-1	Human T cell leukemia virus type I
IAV	Influenza A viruses
IBV	Influenza B viruses
IKK ϵ	I κ B kinase- ϵ
IRB	Institutional Review Board
IRF3	Interferon regulatory factor 3
JAK1	Janus kinase 1
kb	Kilobase
kcal	Kilocalorie
M	Matrix
M1	Matrix1
M2	Matrix2

MDCK	Madin-Darby canine kidney
MFE	Minimum free energy
mg	Milligram
min	Minute
miR	MicroRNA
ml	Millilitre
mM	Millimolar
MOI	Multiplicity of infection
mol	Mole
mRNA	Messenger RNA
n	Number
N	Normality
NA	Neuraminidase
NCBI	National Centre for Biotechnology Information
ng	Nanogram
NLS	Nuclear localization signal
nm	Nanometre
nM	Nanomolar
NP	Nucleoprotein
NS	Non-structural
NS1	Non-structural 1
NS2/NEP	Non-structural 2 (Nuclear export protein)
OAS2	2'-5'-Oligoadenylate synthetase 2
PA	Polymerase acidic
PACT	protein activator of PKR
PB1	Polymerase basic 1
PB2	Polymerase basic 2
PBS	Phosphate buffer saline
PCR	Polymerase Chain Reaction
pH1N1	Pandemic H1N1 2009
PFV-1	Primate foamy retrovirus type 1
pmol	Picomole
pre-miRNA	Precursor microRNA
pri-miRNA	Primary microRNA
PRRSV	Porcine reproductive and respiratory syndrome virus
R	Reverse strand
RAN	Ras-related nuclear protein
RdRp	RNA-dependent RNA polymerase
RIG-I	Retinoic acid-inducible gene I
RISC	RNA-induced silencing complex
RLC	RISC loading complex
RNU6-2	RNA U6 small nuclear 2
ROCK1	Rho-associated, coiled-coil containing protein kinase 1
rRNA	Ribosomal RNA
SD	Standard deviation
sec	Second
siRNA	Small interfering RNA

svRNA	Small viral RNA
TBK1	Tank-binding kinase-1
TPCK	L-1-Tosylamide-2-phenylethyl chloromethyl ketone
TRAF6	TNF receptor associated factor 6
tRNA	Transfer RNA
TRBP	Tar RNA binding protein
TS	Top strand
U	Unit
UTR	Untranslated region
vRNA	Viral genomic RNA
vRNP	Viral ribonucleoprotein
x g	Times gravity
XIAP	X-chromosome-linked inhibitor of apoptosis
μg	Microgram
μl	Microlitre
μM	Micromolar



CHAPTER I

INTRODUCTION

1.1. Background and Rationale

Influenza A and B viruses are responsible for seasonal influenza, which is characterised by the symptoms of high fever, cough, headache, muscle and joint pain, unwell feeling, sore throat and runny nose (1). Due to the induction of a protective immune response, most people can recover from the illness within a week (2). Nonetheless, disease severity including high death rate is usual in infants, the elderly and the immunocompromised populations, as well (1). As a result, seasonal epidemics affects 3–5 million severe human cases and 250,000 deaths worldwide annually (3). In addition to health issue, seasonal influenza poses remarkably socio-economical impacts such as costs of medical care, and loss of productivity (4).

Influenza viruses are categorized into the family *Orthomyxoviridae* with a pleomorphic enveloped shape of roughly 100 nm in diameter (5). Influenza A Viruses (IAV) demonstrate substantial variations in their surface glycoproteins, hemagglutinin (HA) and neuraminidase (NA). On the basis of the antigenic properties, to date 18 HA and 11 NA subtypes of IAV have been identified (6, 7). In contrast, only one subtype of HA has been found in Influenza B Viruses (IBV) (5). The genomes of IAV and IBV are single-stranded negative-sense and each comprises of eight segments, namely polymerase basic 2 (PB2), polymerase basic 1 (PB1), polymerase acidic (PA), HA, nucleoprotein (NP), NA, matrix (M), non-structural (NS) (8). However, IBV differs from IAV with regard to their countermeasures against innate immunity (8).

Nowadays H1N1 and H3N2 subtypes of IAV along with two types of IBV, Victoria lineage and Yamagata lineage are circulating seasonally in humans (9). However, the emerging strains of influenza viruses arise from antigenic drift due to high frequency of point mutations. Furthermore, antigenic shift could cause pandemic outbreaks, resulted from the creation of novel subtypes derived from the gene reassortments between different influenza viruses, particularly in animal reservoirs (10, 11). As a result of lack of preventive immunity against new strains and subtypes, people can suffer from influenza several times throughout their lives. The most effective strategy to prevent the disease or reduce occurrence of severe complications and deaths is vaccination (3).

Embryonated chicken eggs are currently used for the majority of inactivated influenza vaccine production. The egg-based manufacturing process starts with the WHO Global Influenza Surveillance and Response System providing candidate vaccine viruses (CVVs). To allow these CVVs to replicate, the viruses are injected into embryonated chicken eggs and incubated for a few days. The allantoic fluid containing the viruses is collected from the eggs. For killed influenza vaccines, the harvested viruses are then inactivated using chemical methods or physical modifications, and the virus antigen is purified (12, 13). Although this production process is well-established, it is certainly neither flexible nor scalable enough. Because of limitations in both capacity and egg supply in pandemics e.g. the last 2009 H1N1 outbreak, the traditional production of egg-based vaccines was not able to satisfy the growing demands in a timely manner (14, 15). To overcome this incapacity, cell culture-based production system is now being established (16). In recent years, Madin-Darby Canine Kidney (MDCK) has been approved by both of the

U.S. Food and Drug Administration (FDA) and the European Medicines Agency (EMA) to be used for the production of influenza vaccines (17, 18).

In addition to the investigation of cultivation approach, understanding of virus–host interactions is necessary for the optimisation of cell culture-based vaccine production. More recently, there has been an increasing amount of evidence that microRNAs play critical roles in host-pathogen interactions. MicroRNAs are a class of highly conserved noncoding single-stranded RNA approximately 18–25 nucleotides in length. It has been shown that microRNAs control gene expression post-transcriptionally by either translation inhibition or mRNA deadenylation and degradation, which are dependent on the complementarity between 3'-untranslated region of target mRNA and microRNA sequence (19, 20). Experimental and computational strategies assessing the number of protein-encoding genes under the regulation of microRNAs indicated that most of the genes could be controlled by microRNAs (21). Hence, the identification of microRNA target genes could lead to a better understanding of the microRNA functions in the initiation and progression of several diseases including the infection of viruses (22).

In the context of viral infections, microRNAs could affect viral pathogenesis in either a direct or indirect way. Firstly, microRNAs might serve a direct antiviral function via sequence-specific binding with a viral RNA resulting in silencing a viral gene. Secondly, microRNAs could function indirectly, regulating the host transcriptome to facilitate an environment which suppresses viral replication (23). Recently, it has been evident that the genomes of influenza viruses are directly targeted by host microRNAs. For instance, Song and colleagues (24) showed that microRNA-323, microRNA-491, and microRNA-654 inhibited replication of the

H1N1 IAV through binding to the PB1 gene in H1N1 infected MDCK cell lines. Moreover, mir-let-7c regulates IAV replication via the degradation of viral M1 gene (+) cRNA in H1N1 infected human A549 cell lines (25). Recently, our group demonstrated that human miR-3145 triggered silencing of viral PB1 genes of IAV (pH1N1, H3N2, H5N1), resulted in inhibition of influenza viral replication (26). In addition, Terrier and co-workers (27) performed microRNA global profiling in human lung epithelial cells (A549) infected by IAV (H1N1 and H3N2). They found that a specific anti-miR-146a inhibitor could significantly increase viral propagation.

While the investigations of IAV have extensively used human cell lines as a study model, the studies of microRNAs in MDCK infected with influenza viruses, particularly IBV, are still limited. Besides investigating the interactions between influenza virus genomes and host microRNAs, this study might provide the established MDCK as a promising strategy for cell-based influenza vaccine production with sufficient quantities of seed viruses. Thereby, this investigation is divided into three parts as follows: (i) High-throughput analysis of microRNA profiles in MDCK cells infected with influenza viruses; (ii) Effect of synthetic microRNA inhibitors on viral production. (iii) Identification and validation of host microRNAs targeting influenza viral genomes.

1.2. Research Questions

1.2.1. Which microRNAs are altered upon infection of seasonal influenza A and B viruses in the MDCK cells? Are there any differences or similarities in microRNA profiles between the infection of influenza A and B viruses?

1.2.2. Which microRNAs could target viral genomes?

1.2.3. Could synthetic microRNA inhibitors enhance the production of seasonal influenza viruses?

1.3. Objectives

1.3.1. To increase the production of seasonal influenza viruses through cellular microRNA regulation.

1.3.2. To investigate microRNA profiles in response to the infection of influenza A and B viruses using next-generation sequencing.

1.3.3. To identify some cellular microRNAs which directly target influenza A and B genomes.

1.4. Hypothesis

When influenza viruses infect cells, the replication and transcription of their genome take place inside the nucleus. On the other hand, the release of viral genomic RNAs and the translation process of viral mRNAs occur within the cytoplasm. Meanwhile, host might respond to the infection via the upregulation of cellular microRNAs. Some cellular microRNAs may complementarily bind with some RNAs of influenza viruses, resulting in degradation of viral RNAs or translational repression of viral proteins (Figure 1).

These host microRNAs might lead to the impaired production of viral progeny. On the other hand, microRNA inhibitors may be applied to impede the suppressive effect of microRNAs. As a result, viral genomes still exist and can undergo the translation of proteins essential for the propagation of new virus particles.

Therefore, this study is focusing on the inhibition of upregulated microRNAs which could directly target viral genome.

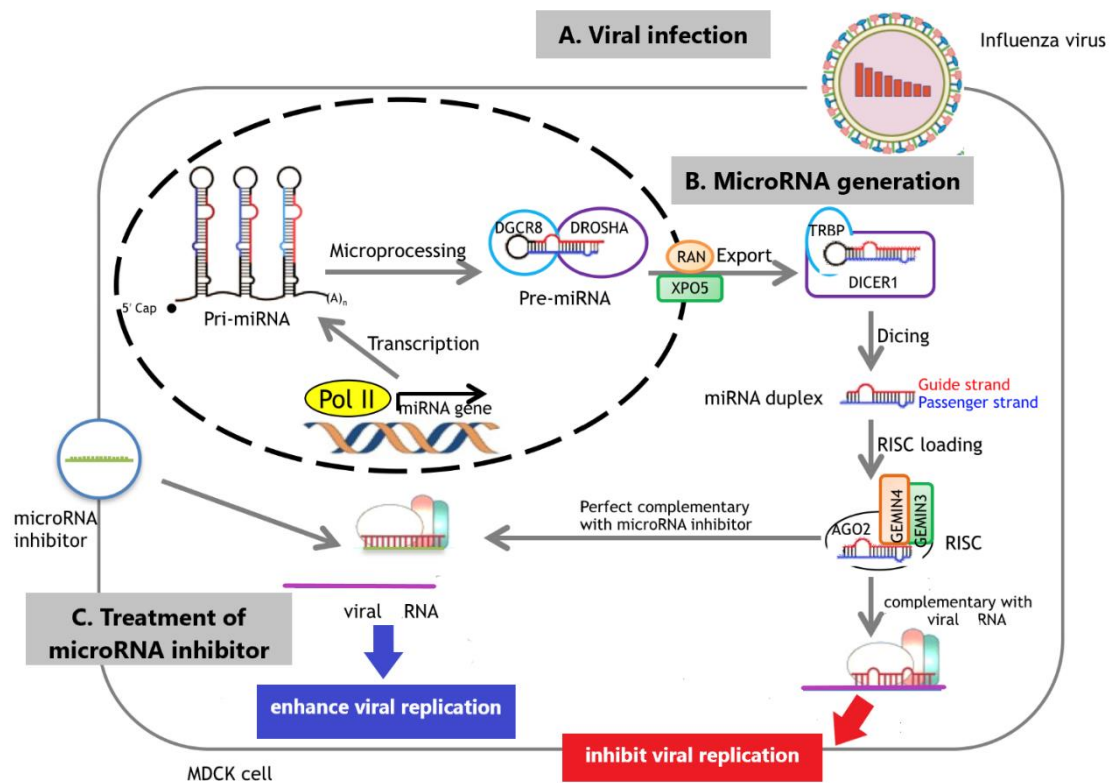


Figure 1 Enhancing viral replication through manipulation of cellular microRNAs.

(A) Influenza virus is taken up into MDCK cell by receptor-mediated endocytosis. During the infection, viral RNAs (purple line) are found in the cytoplasm. (B) Some of the host microRNAs are generated in response to the infection. Most of the primary microRNA transcripts (pri-miRNA) are transcribed from microRNA genes by RNA polymerase II, and then cleaved into a pre-miRNA (precursor-miRNA) by the enzyme complex of Drosha and DGCR8. After nuclear processing, Exportin-5/Ran-GTP complex exports the pre-miRNA into the cytoplasm. The enzyme Dicer further cleaves off the loop of the pre-miRNA, leading to the generation of a roughly 22-nucleotide microRNA duplex. The microRNA duplex is separated into the guide

strand (red line) that is complementary to the viral RNA (purple line) and the passenger strand (blue line) that is subsequently degraded. The viral RNA is directly targeted by the host microRNAs, leading to interfering the replication cycle of the virus. (C) Exogenous microRNA inhibitor (green line) is designed to specifically bind to and inhibit the host microRNAs. Ultimately, microRNA inhibitor facilitates the stability of viral RNAs, which enhances viral replication.

1.5. Definition

MicroRNA: a small noncoding RNA of 18-25 nucleotides that binds to cellular mRNAs and viral RNAs mediates translational repression or RNA degradation, and thereby reducing protein levels within the cells.

Seed region: nucleotides 2–8 at the 5' end of a microRNA that determine the target specificity of the miRNA by binding to complementary sequences in the target RNA. A single microRNA can bind to many different target RNAs based on the seed sequence.

Silencing plasmid: a vector that expresses microRNA within mammalian cells typically use an RNA polymerase III promoter to drive expression of a short hairpin RNA that mimics the structure of an microRNA.

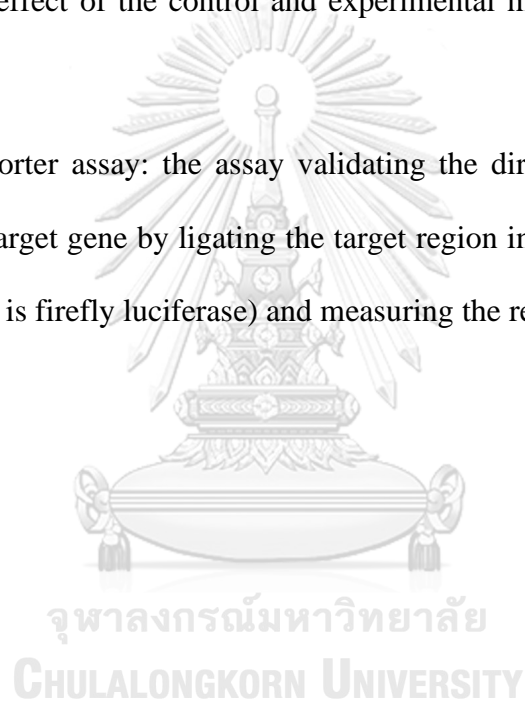
Scramble plasmid: a vector expresses a short hairpin RNA of which designed sequence does not target any known genes in the target organism. Target expression from scramble plasmid-transfected samples is used as a baseline for evaluation of the effect of the control and silencing plasmids on target gene expression.

MicroRNA inhibitor: a small, chemically modified single-stranded RNA molecule is designed to specifically bind to and inhibit endogenous microRNA

molecules and enable microRNA functional analysis by down-regulation of microRNA activity.

Negative control inhibitor: a small, chemically modified single-stranded RNA molecule of which sequence has been tested on mammalian cells and tissues, and is shown to produce no identifiable effects on known microRNA function. Target expression from negative control-transfected samples is used as a baseline for evaluation of the effect of the control and experimental miRNA inhibitors on target gene expression.

3'UTR reporter assay: the assay validating the direct binding of microRNA and its predicted target gene by ligating the target region into the 3'UTR of a reporter gene (in this study is firefly luciferase) and measuring the reporter gene expression.



1.6. Experimental Design

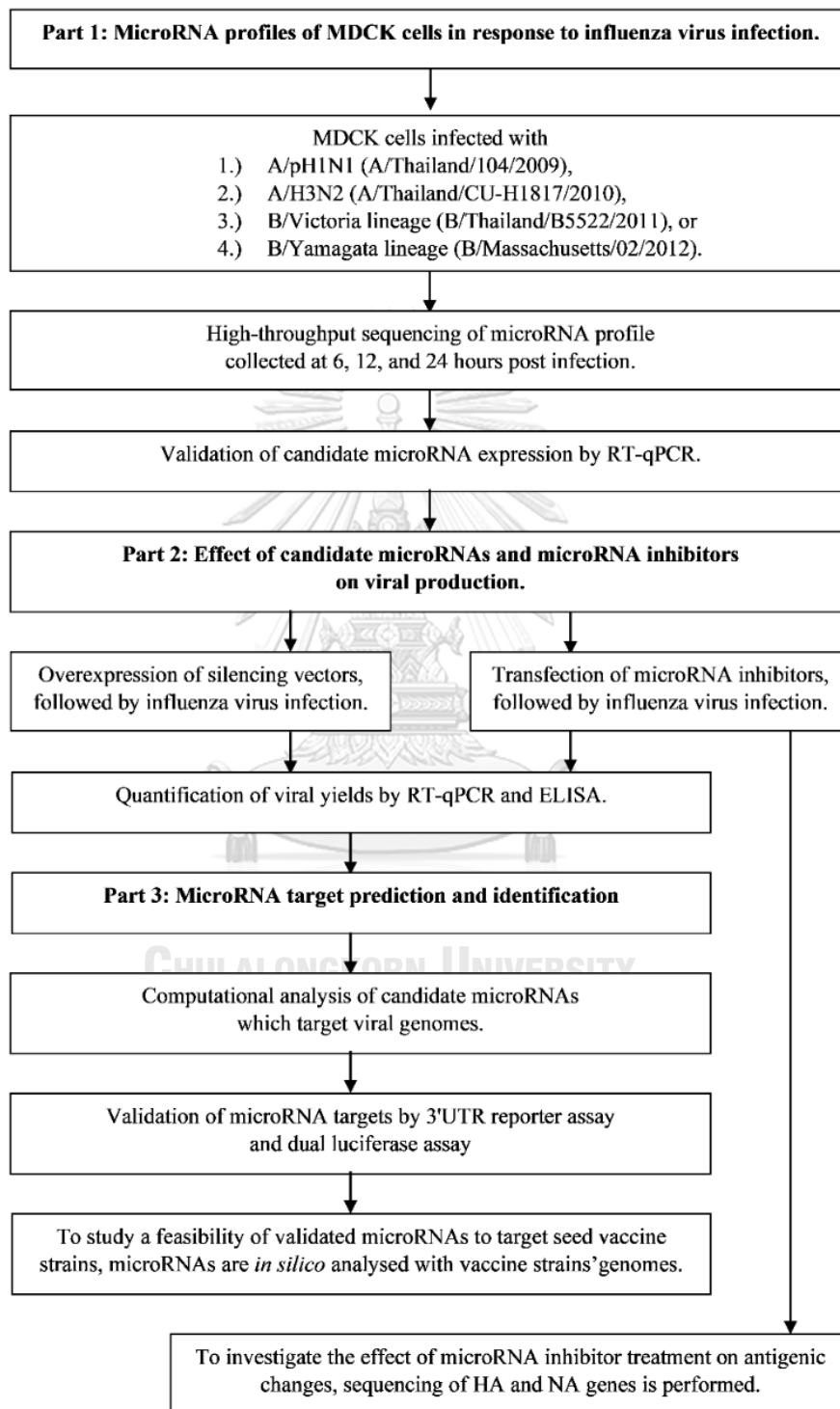


Figure 2 Procedure framework.

CHAPTER II

LITERATURE REVIEWS

2.1. Seasonal Influenza Viruses

2.1.1. Significance of Seasonal Influenza

Influenza A and B viruses cause acute respiratory infections, of which severity ranges from asymptomatic to fatal infections. Typical symptoms include fever, headache, cough, unwell feeling, chills, muscle pain, sore throat, running nose, and less appetite. The range of the incubation period is normally between 1 and 4 days, followed by a symptomatic period of 3–4 days. The clinical outcome is affected by the intrinsic properties of the virus, pre-existing host immunity, and health status. Underlying medical problems including heart or lung disease, immunological disorders, renal failure, diabetes increase the risk of severe outcome (28). Moreover, pregnant women, infants, and the elderly could develop severe disease and complications due to infection (5). As a result, seasonal epidemics affects 3–5 million severe human cases and 250,000 deaths worldwide annually (3). In addition to being a health issue, seasonal influenza poses remarkably socio-economical impacts such as costs of medical care, and loss of productivity (4).

2.1.2. Classification of Influenza Viruses

Alphainfluenzavirus and Betainfluenzavirus genera are the members of the Orthomyxoviridae family. Each genus comprises of only one species: influenza A and influenza B, respectively (29). The two influenzavirus genera can be differentiated on the basis of antigenic differences in nucleoproteins and matrix

proteins (30). Although all of these viruses can naturally infect humans, the range of vertebrate hosts affected by each genus is varied. Influenza A viruses infect a wide range of hosts including humans, avians, dogs, horses, pigs, whales, seals, and bats (6, 7, 31). In contrast, influenza B viruses are isolated almost exclusively from humans. However, it has been evident that influenza B virus infects seals (32), and domestic pigs might be susceptible to influenza B infection (33). Different subtypes of influenza A viruses are further classified by the antigenic variation of surface glycoproteins, hemagglutinin (HA) and neuraminidase (NA). So far there have been 18 known subtypes of HA and 11 subtypes of NA (Figure 3) (6, 7). Interestingly, all subtypes of the influenza A viruses can be isolated from aquatic birds, suggesting avian species are the natural hosts of influenza A viruses, except H17, H18, N10 and N11 exclusively found in bats (34). Of these viruses, only H1N1, H1N2, H2N2, H3N2, H5N1, H7N2, H7N3, H7N7, H7N9, H6N1, H9N2, and H10N7 were isolated from humans (34).

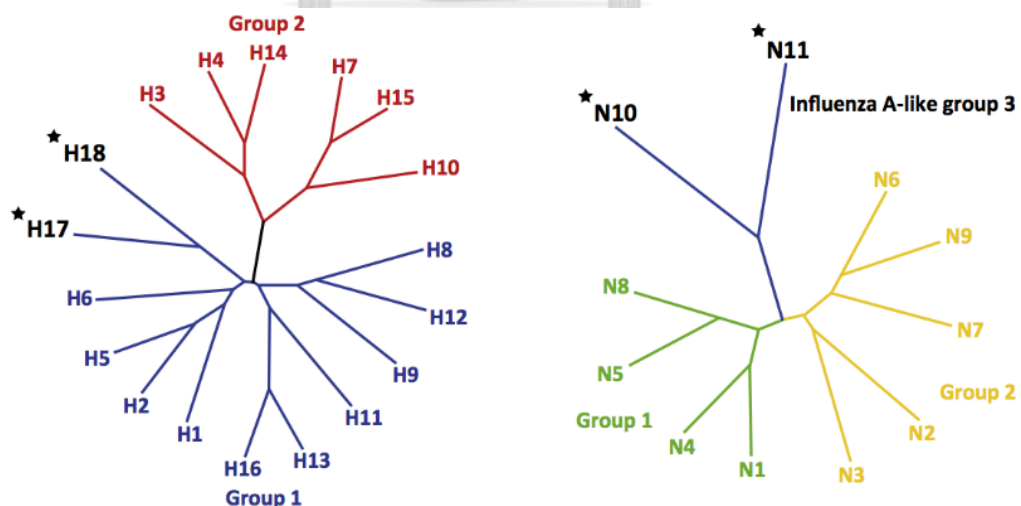


Figure 3 Phylogenetic trees of the hemagglutinin (HA) and neuraminidase (NA) genes of all known influenza A virus subtypes [modified from (35)].

On the other hand, influenza B viruses, which mostly infect humans, are believed to diverge from influenza A viruses at some time point in the past (36). Before two antigenically distinct influenza B lineages emerged, the earliest isolate of influenza B virus had originated in the 1940s (37). Even though influenza B viruses are not categorized into subtypes, the genetic and antigenic discrimination of two distinct lineages is currently based on HA surface glycoprotein: the B/Victoria lineage (named after the B/Victoria/2/1987 strain) and the B/Yamagata lineage (named after the B/Yamagata/16/1988 strain) (37-39). The two lineages are thought to diverge in the 1970s when the B/Victoria lineage gradually emerged in China (39). Since China was the insulated state in the 1970s, the global spread of the B/Victoria lineage may have been delayed. Consequently, the B/Yamagata lineage was dominantly circulating until the B/Victoria appeared globally in the mid of 1980s (39). Ever since, both influenza B virus lineages have been co-circulating with seasonal influenza A virus subtypes H3N2 and H1N1 (9).

2.1.3. Virus Structure and Genome Organization

The size of influenza A and B viruses is approximately 80-120 nm in diameter. Influenza virus contains a lipid envelope, which is derived from the host's cell membrane during the viral budding process (Figure 4). Three structural proteins such as HA, NA, and M2 are anchored in the lipid bilayer (30). The morphology of virions is pleomorphic, ranging from small spherical to long filamentous. The viral shape is a genetic trait and several viral proteins like HA, NA, M1, and M2 are known to affect the morphology of influenza virus particles (40-44). HA and NA are spike glycoproteins embedded in the lipid envelope by the short hydrophobic amino acid sequences. Electron microscopic visualization shows that the spikes of HA and NA

are rod-shaped and mushroom-shaped, respectively. The HA is a homotrimer, of which function is the receptor binding and membrane fusion. In contrast, the NA is a homotetramer, which is responsible for destroying receptors by hydrolyzing sialic acid groups and releasing the viral progeny (45). Homotetramer M2, an integral membrane protein, essentially functions as an ion channel for uncoating—the release of the virus' genetic material into the cytoplasm, while beneath the lipid bilayer is the layer of M1 protein (36). In addition to different size, the M2 ion channels of influenza A viruses are lined with hydrophobic amino acids while those of influenza B viruses are lined with polar serines. Due to a conformational change in the structure of ion channels, influenza A viruses are inhibited by the antiviral drug Amantadine, but not influenza B viruses (46).

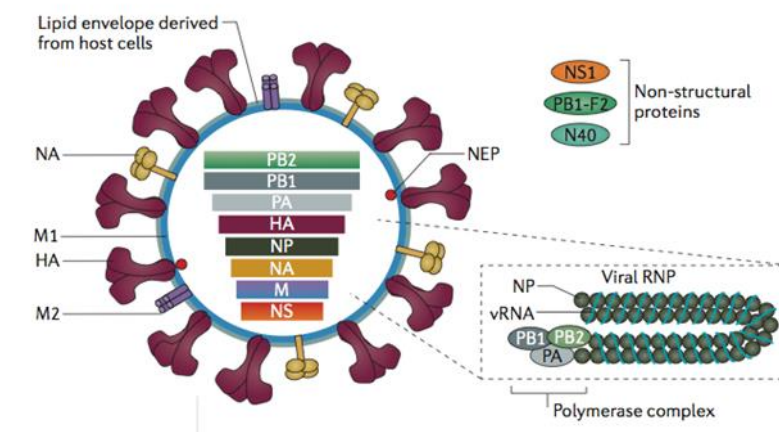


Figure 4 Structure of influenza A virus [modified from (10)]

Inside the virion, influenza A and B viruses contain eight segments of negative-sense single-stranded RNA. The total size of the genome is approximately 13.5 kb, and the size of each RNA segment varies from 890 to 2,341 nucleotides (36, 45). All eight segments of the genomic RNA (vRNA) are bound to the NP and to three viral RNA polymerase subunits (PB2, PB1, and PA), resulting in the formation of viral

ribonucleoprotein (vRNP) complexes (30). The low amount of NS2 protein functions as a nuclear export protein for vRNA in infected cells (47). Influenza A and B viruses utilise the host machinery with various coding strategies such as alternative splicing, ribosomal frameshift and leaky scanning (36). Depending on the isolates, the genome of influenza A viruses could be encoded for 18 proteins, whilst that of influenza B viruses is translated up to 11 proteins (48, 49). The sizes and functions of proteins encoded by each viral RNA segment are overviewed in Table 1.

2.1.4. Replication Cycle

The life cycle of influenza viruses begins with the HA glycoproteins on the viral surface attaching to sialyloligosaccharides receptors on the host cell (Figure 5). Then, the virus is taken up into the host cell by receptor-mediated endocytosis (50). Inside the late endosomes of host cells, a conformational change in the HA triggered by the acidic pH expresses the fusion peptide, resulted in the fusion of the viral and endosomal membranes (51). Subsequently, the viral M2 ion channel equilibrates the interior pH of the virus with that of the acidic endosome, leading to the perturbation of the interactions between the M1 matrix protein and vRNP complex, which is comprised of vRNA and the polymerase subunits and NP proteins. This leads to the release of vRNP complex into the host cytoplasm (52). Due to nuclear localization signals (NLSs) located on the viral proteins NP, PA, PB1 and PB2, vRNP complexes are imported into the host nucleus (53). Unlike most of the other negative-sense RNA viruses, the nucleus is where the genome of the influenza virus is transcribed and replicated by viral RNA-dependent RNA polymerase (RdRp) (53). These processes lead to the creation of four types of RNA species including viral mRNAs, positive-

sense complementary RNA (cRNA), negative-sense viral genomic RNA (vRNA), and negative-sense small viral RNAs (svRNA) (53, 54).



Table 1 Molecular differences between influenza A and B viruses [modified from (36)].

Gene segment	Length (bp)	Influenza A		Influenza B		Features and functions
		Protein	Length (AA)	Protein	Length (AA)	
1	2350	PB2	759	PB2	770	Subunit of viral RNA polymerase; Cap-binding; affect host range and virulence
		PB2-S1	632	-	-	PB2-isoform with an internal deletion; Inhibits interferon signaling pathway
2	2350	PB1	757	PB1	752	Catalytical subunit of viral RNA polymerase; RNA chain elongation
		PB1-N40	718	-	-	N-terminally truncated form of PB1; Balance expression of PB1 & PB1-F2
		PB1-F2	87-90	-	-	Predominantly localized in mitochondria; Induce apoptosis; affect polymerase activity
3	2250	PA	716	PA	726	Subunit of viral RNA polymerase; Endonuclease activity (cap snatching)
		PA-X	252	-	-	Fusion of N-ter of PA and C-ter of X-ORF; Mediate degradation of host mRNAs
		PA-N155	568	-	-	N-terminally truncated form of PA; Might be related to replication
4	1780	PA-N182	535	-	-	N-terminally truncated form of PA; Might be related to replication
		HA	550-560	HA	584	Surface glycoprotein; Antigenic determinant; Receptor binding and membrane fusion
5	1575	NP	498	NP	560	Major component of the viral RNP complex; RNA synthesis & nuclear import

Gene segment	Length (bp)	Influenza A		Influenza B		Features and functions
		Protein	Length (AA)	Protein	Length (AA)	
6	1420	NA	454-465	NA	486	Surface glycoprotein; Antigenic determinant; Neuraminidase, release novel virus
		-	-	NB	100	
7	1050	M1	252	M1	248	Main component of viral membrane; Viral assembly and budding
		M2	97	BM2	109	
		M42	99	-	-	
8	900	NS1	217-230	NS1	281	Multifunctional protein involved in virus-host interactions; Interfere with the anti-viral response; Regulate host and viral gene expression
		NS2/NP	121	NS2/NEP	122	
		NS3	174	-	-	
						Potentially associated with host adaptation

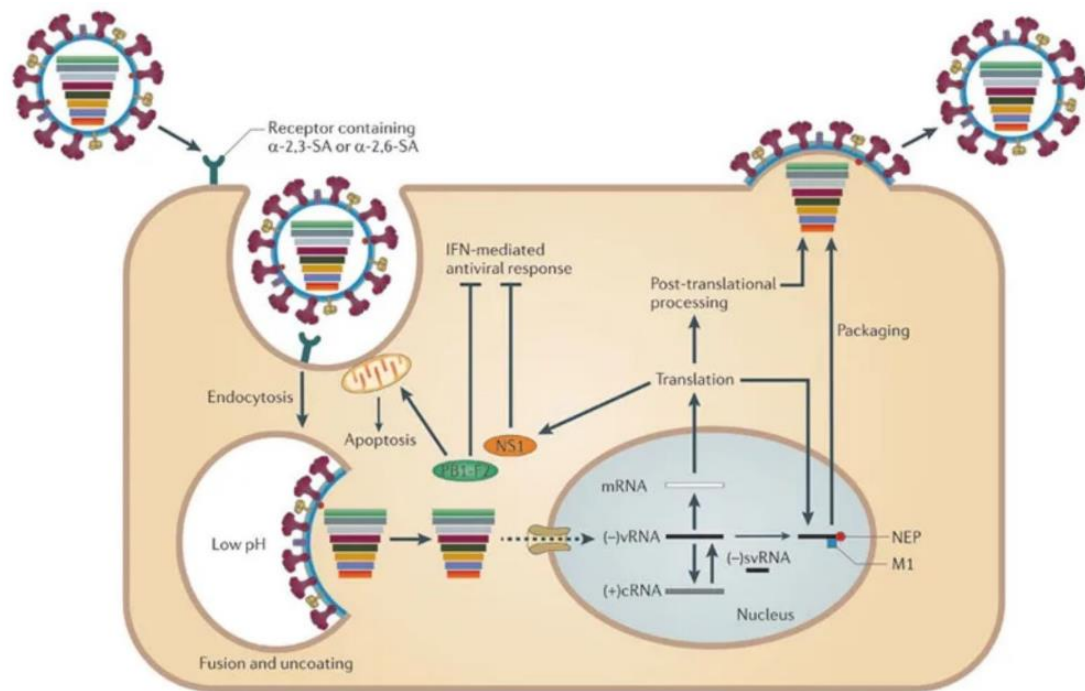


Figure 5 The life cycle of influenza viruses [modified from (10)].

The negative-stranded vRNAs are used as templates for syntheses of both cRNA and mRNA. In general, it is believed that all the polymerase subunits (PB2, PB1, and PA) and NP are required for both viral transcription and replication (55, 56). The svRNAs are believed to have a regulatory effect on switching the function of RdRp between transcription and replication mode (54). During replication, the viral polymerase complex synthesizes the lesser number of cRNA molecules, which are a full-length copy of the vRNA (45). The viral cRNA, which is used as a template for vRNA synthesis, lacks both a 5' cap and the 3' poly-A tail (53). To initiate viral mRNA transcription, a capped RNA fragment is cleaved from the host mRNA through a cap-snatching mechanism (45). This short-capped oligonucleotide primer is used by the viral polymerase. Transcription is terminated at a track of 5–7 U residues located approximately 17 nucleotides from the 5' end of vRNA and a poly (A) tail is then added to the viral mRNA transcript (57). Unlike cRNA, viral mRNA is an

incomplete copy of the vRNA, lacking approximately 17 bases of the complementary viral 3' sequence (45). The viral mRNAs are then exported to the cytoplasm and translated by the host machinery.

Whilst the viral mRNA use the host translation machinery for translation in the cytoplasm, alternative splicing of the viral genome utilizes the host splicing machinery (58). The PB2, PB1, PA, NP, M1, NS1, and NS2/NEP proteins are translocated back into the nucleus in order to transcription, replication, and vRNP assembly. Meanwhile, the envelope proteins HA, NA and M2 are produced on endoplasmic-reticulum-bound ribosomes, where they are folded and trafficked into the Golgi body for post-translational modifications (59-61). After nuclear import, the NP protein bind to the vRNAs, together with three RNA polymerase subunits at one end, to assembly the vRNPs. In the late stage of infection, the interaction between NS2/NEP and the host nuclear export machinery allows these vRNPs to export out of the nucleus (47). Besides, viral protein M1 also participates in the nuclear export of vRNPs (62). When all of the vRNPs exist in the cytoplasm and the envelope proteins reach the host cell membrane, the assembly of virus particles takes place at the cell membrane (53). When the virions are assembled on the host-cell membrane, the M2 protein is also essential for budding influenza virus particles by pinching them off from the host-cell membrane (63). Moreover, the binding between the host sialic acid molecules and the viral HA protein is cleaved by the NA protein, thus releasing the virus particles (10).

2.1.5. Epidemiology

Annual epidemics of influenza is caused by influenza A and B viruses; however, the segmented RNA genome of influenza A viruses can quickly accumulate mutations due to the error-prone nature of the viral RNA polymerase and to the exchange of genome segments with other influenza A virus strains (64). This allows the virus to develop resistance against antivirals, escape the host immune response, and cross the host species barrier (65-67). Introduction of new influenza virus strains into the human population from other species leads to pandemics due to the absence of pre-existing immunity (68). Therefore, influenza A viruses cause pandemics at random intervals, while influenza B viruses, which almost restrictively infect humans, cause only seasonal epidemics (5).

Pandemics are global-scale outbreaks caused by viruses possessing HA proteins to which human populations have no pre-existing immunity (5). All of the human influenza pandemics are summarised in Table 2. During the last century, the H1N1, H3N2, H2N2, and H1N2 subtypes of influenza A viruses have circulated in humans (Figure 6).

Table 2 Pandemic waves of human influenza.

Timeline	Pandemics Name	Subtypes	Origins
1918-1919	Spanish Flu	H1N1	- An avian-descended H1N1 virus (69, 70).
1957-1958	Asian Flu	H2N2	<ul style="list-style-type: none"> - The gene segments encoding HA and NA were replaced by an avian-like H2 subtype HA and an N2 subtype NA (71). - The gene segment encoding the PB1 polymerase was also replaced with an avian-like gene segment (72). - The other five gene segments retained from the 1918-derived H1N1 lineage.
1968	Hongkong Flu	H3N2	<ul style="list-style-type: none"> - A reassortment event between a circulating human H2N2 virus and an avian IAV, acquiring novel HA (H3 subtype) and PB1 gene segments (71, 72). - The other six gene segments, including the NA gene segment, were retained from the 1957 H2N2 virus (including five segments-PB2, PA, NP, M, and NS-retained from the 1918 H1N1 lineage).
1977-1978	Russian Flu	H1N1	- The re-emergence of a descendant of the 1918 H1N1 virus that had been absent from circulation for 20 years since 1957 (73).
2009-2010	2009 Flu	Novel H1N1 (pH1N1)	<ul style="list-style-type: none"> - The virus derived its NA and M gene segments from the European avian-like H1N1 lineage and its remaining six gene segments (PB2, PB1, PA, HA, NP, and NS) from the North American swine H1N2 “triple” reassortant lineage. - The HA, NP, and NS gene segments of this lineage are derived from the North American classical swine H1N1 (1918 origin) lineage, while the polymerase gene segments have different origins: PB2 and PA were derived from an avian IAV source and PB1 from a human seasonal H3N2 virus when the “triple” reassortant swine lineage emerged in the late 1990s (74).

Figure 7, pH1N1 and H3N2 subtypes of influenza A viruses together with Victoria and Yamagata lineages of influenza B viruses are presently circulating in humans (9).

Global circulation of influenza viruses

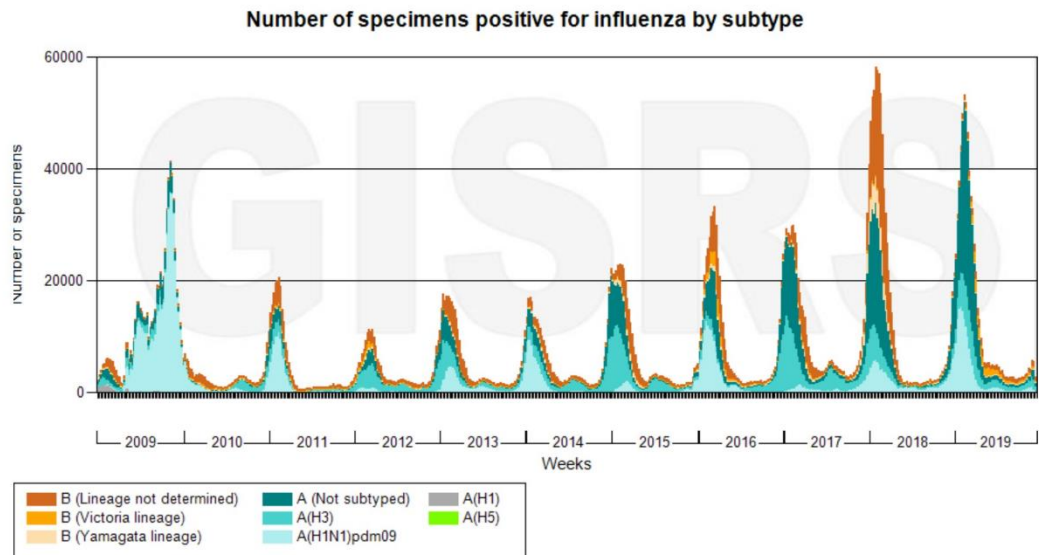


Figure 7 The global circulation of influenza viruses from week 1 of 2009 to week 48 of 2019 (The data from WHO's Global Influenza Surveillance and Response System is shown as of December 2019).

2.1.6. Inactivated Influenza Vaccines

The most effective strategy to prevent the disease or reduce the occurrence of severe complications and deaths is vaccination (3). The majority of inactivated influenza vaccines registered for use in humans are obtained by growing the influenza viruses in embryonated eggs. The process of inactivated influenza vaccines involves several steps. First, WHO provides candidate vaccine viruses (CVVs) grown in eggs to pharmaceutical companies. Next, the CVVs are inoculated into embryonated eggs and allowed to propagate for several days. Then, the virus-containing fluid is harvested and inactivated by chemical methods (e.g. formaldehyde or β -

propiolactone) or physical methods (e.g. ultraviolet radiation or gamma-irradiation) (12, 13). The downstream process continues with purification and testing. Although this production process is well-established, it is certainly neither flexible nor scalable enough. Because of limitations in both capacity and egg supply in a pandemics situation e.g. the last 2009 H1N1 outbreak, the traditional production of egg-based vaccines was not able to satisfy the growing demands in a timely manner (14, 15).

Table 3 Inactivated seasonal influenza vaccines registered for use in humans.

Host factory	Virus strains	Product tradename	Approval authority
Embryonated chicken eggs	Trivalentes	Agriflu [®] Fluvirin [®]	FDA
		Influvac [®] Vaxigrip [®] Intanza [®]	EMA
	Quadrivalentes	Afluria [®] Fluarix [®] Flulaval [®] FluMist [®] Fluzone [®]	FDA
		Vaxigrip [®]	EMA
MDCK	Trivalentes	Optaflu [®] (discontinued)	EMA
	Quadrivalentes	Flucelvax [®]	FDA
Vero	Trivalentes	Preflucel [®] (discontinued)	EMA
	pH1N1	Celvapan [®] (discontinued)	EMA
ExpresSF+ [®]	Quadrivalentes (recombinant HA)	Flubock [®]	FDA

Note: FDA; United States Food and Drug Administration, EMA; European Medicines Agency.

To overcome this incapacity, cell culture-based production systems are now being established (15, 16). Novel inactivated influenza vaccines have been developed by growing the influenza viruses in continuous cell lines, such as Madin-Darby canine kidney (MDCK) epithelial cell line (78). This MDCK cell-based vaccine production has several advantages. For example, some of the influenza strains recommended for seasonal vaccines grow poorly in eggs, whilst the majority of them can be cultured in cell lines (79). Importantly, influenza isolates from egg-based manufactures undergo amino acid changes, which may affect their immunogenicity and finally their efficacy of the usage (79). Besides MDCK cells, some of these vaccines derived from African green monkey kidney (Vero) cell line and Sf9 insect cell line have been licensed in Europe or the USA (Table 3).

2.2. MicroRNAs

2.2.1. Biogenesis

Primary microRNA transcripts (pri-miRNA) are synthesised from the transcription of microRNA genes by either RNA polymerase II or RNA polymerase III (Figure 8) (80, 81). The hallmarks of the pri-miRNAs transcribed by RNA polymerase II are polyadenylated and capped (82). Mostly, a several hundred nucleotides long pri-miRNA contains a hairpin stem of 33 base-pairs, a terminal loop and two single-stranded flanking regions upstream and downstream of the hairpin (83).

Following the transcription process, pri-miRNA is cleaved by the endonucleolytic activity of the nuclear microprocessor complex incorporated by the RNase III enzyme Drosha and the DGCR8 (DiGeorge critical region 8) protein (82).

The resulting shortened hairpin product termed as a pre-miRNA (precursor-miRNA) has a two-nucleotide overhang at its 3' end (81). Alternatively, Drosha-mediated processing is not compulsory for the generation of pre-miRNAs in some non-canonical pathways. A hairpin pre-miRNA might be formed and further processed in the cytoplasm with the bypass of Drosha cleavage when the transcript from the intron is processed by the action of the splicing machinery and the lariat debranching enzyme (83, 84). This Drosha-independent processing of the intron generates finally the microRNAs called mirtrons.

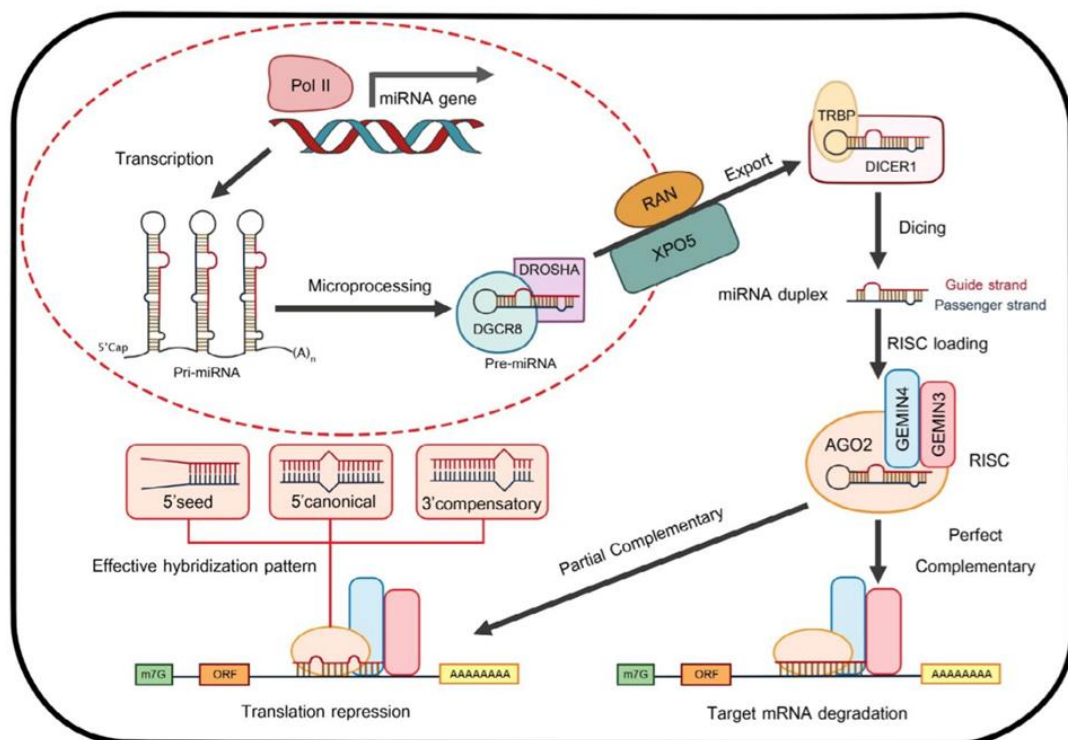


Figure 8 Droscha-dependent biogenesis of microRNAs. MicroRNA genes are transcribed as pri-miRNAs by RNA Pol II in the nucleus. The pri-miRNAs are cleaved by Microprocessor, which includes DROSHA and DGCR8, to produce pre-miRNAs. The pre-miRNAs are then translocated from the nucleus to the cytoplasm by XPO5 and further cleaved by DICER1. The guide strand of the miRNA duplex is

loaded into the RISC, which targets mRNAs by sequence complementary binding and mediates gene regulation through mRNA degradation and translational repression.

After nuclear processing, Exportin-5/Ran-GTP complex exports the pre-miRNA into the cytoplasm (84). The pre-miRNA is also protected by Exportin-5 from nuclear digestion (84, 85). When pre-miRNA arrives in the cytoplasm, the assembly of the RNA-induced silencing complex (RISC) is processed by the RISC loading complex (RLC). RLC is a multiple-protein complex including the RNase Dicer, the core component Argonaute-2 (Ago2), the double-stranded RNA-binding domain proteins TRBP (Tar RNA binding protein) and PACT (protein activator of PKR) (86-89). The RNase III Dicer further cleaves off the loop of the pre-miRNA, resulting in the generation of a roughly 22-nucleotide microRNA duplex with two nucleotides overhangs at each 3' end (90).

After Dicer-dependent processing, the dissociation of Dicer and TRBP or PACT from the microRNA duplex takes place. Prior to the formation of RISC, the microRNA duplex is unwound and then separated into the guide strand that is complementary to the target mRNA and the passenger strand that is subsequently degraded. The functional asymmetry bias is affected by the thermodynamic stability of the base pairs at the two ends of the duplex. Therefore, the mature microRNA strand with the less stable base pair at its 5' end in the duplex is loaded to form the active RISC that performs gene silencing (91).

2.2.2. Mechanisms of Action

MicroRNA is a small ~22-nucleotide-long noncoding RNA that controls gene expression post-transcriptionally in animals, plants, and protozoa. In mammals, the

activity of more than 60% of all protein-coding genes are controlled by microRNA; therefore, this small non-coding RNA regulates almost every cellular process (92, 93). Base-pairing between microRNAs and their target mRNAs determines the fate of the target mRNAs (Figure 8). To illustrate, perfect complementary leads to direct endonucleolytic cleavage of the target mRNAs, whereas translation repression is a result of imperfect matching (94). In animals, Most of the 5'-proximal "seed" region (positions 2–8) located in the microRNA imperfectly hybridises with sequences in the 3'-untranslated region (3'-UTR) of mRNAs (95).

Therefore, microRNA generally represses the synthesis of proteins either by translation inhibition and/or deadenylation along with subsequent degradation of mRNA targets (96, 97). Mature microRNAs function when incorporated into RISC with Ago2 and GW182 (glycine-tryptophan repeat-containing protein of 182 kDa) family proteins (96, 97). In the cytoplasm, components of RISC and mRNAs are accumulated into processing bodies (P bodies, also known as GW bodies), which is involved in the degradation of repressed mRNAs (98, 99). More specifically, the CCR4-NOT1 deadenylase complex interacts with the RISC to facilitate deadenylation. In addition, the 5'-terminal cap (m^7G) is removed by the decapping DCP1-DCP2 complex, leading to instability and degradation of mRNA (100).

For microRNA-mediated repression of translation initiation, the RISC interferes with the recognition of eIF4F-cap together with the recruitment of 40S small ribosomal subunit. Moreover, the RISC prevents the formation of 80S ribosomal complex by antagonising 60S subunit joining (100). Besides the translational initiation step, The RISC represses translation at the step of post-

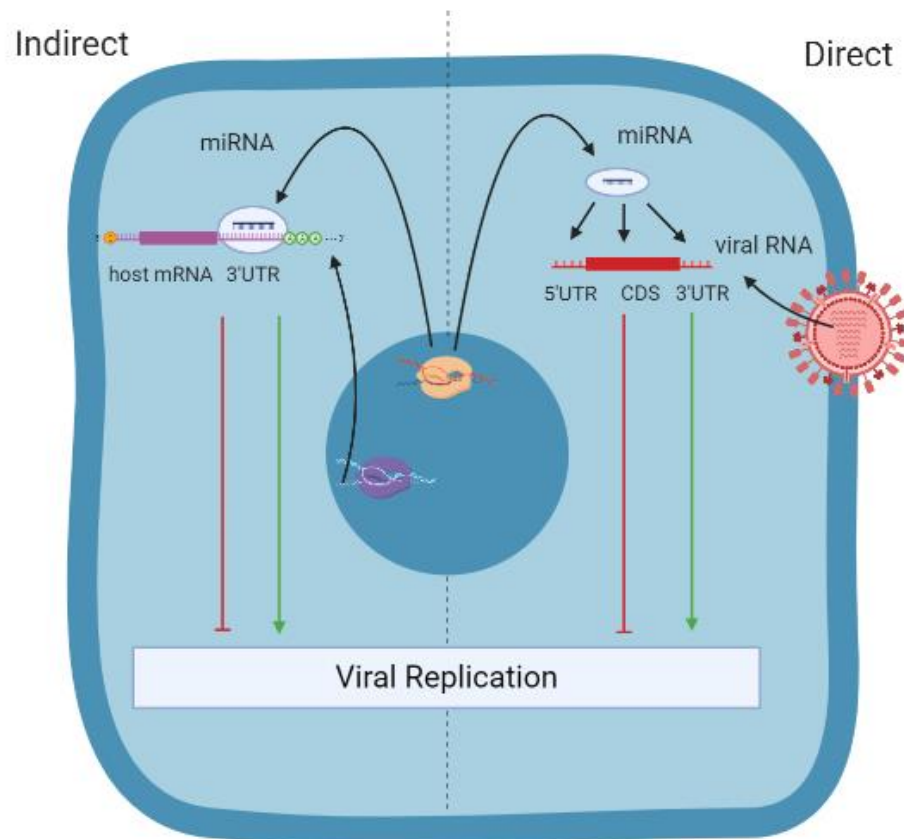
initiation such as inhibition of ribosome elongation, induction of ribosome drop-off, or facilitating proteolysis of nascent polypeptides (100).

2.2.3. Virus-Host MicroRNA Interplay

MicroRNAs play important roles in cell fate determination, proliferation, and cell death. In addition to these vital processes, microRNAs involve in diverse cellular activities, such as immune response (101), insulin secretion (102), and viral replication (103). Upon viral infections, host microRNAs could modulate the infection in one of two ways (Figure 9). First, direct effect on viral regulation takes place when host microRNAs directly target different regions of viral RNAs. For instance, miRNA-17 binds to the 3' UTR of the Bovine Viral Diarrhea Virus genome, resulted in enhanced translation (104). On the other hand, miRNA-122 could stabilize Hepatitis C Virus RNA, thus enhancing translation through binding to the 5' UTR (105). Besides, the coding sequences of Porcine Reproductive and Respiratory Virus (PRRSV) could be directly targeted by microRNA-181, leading to impaired viral replication (106).

Second, indirect effect involves modulation of cellular mRNA encoding a host factor required for one or several steps in the viral cycle. For example, miRNA-181 could modulate viral receptor expression, regulating the entry of PRRSV (106). MicroRNA-33a regulates cofactors required for Japanese Encephalitis Virus replication (107), whilst microRNA-141 modulates cofactors involved in protein translation of Enterovirus 71 (108). In addition, microRNA-532 inhibits signaling factors related to self-defense apoptosis, thus enhancing the replication of West Nile

Virus (109). Moreover, microRNA-144 could facilitate Influenza A virus replication through suppressing interferon-related genes (110).



CHULALONGKORN UNIVERSITY

Figure 9 Direct and indirect effects of microRNAs on viral replication. Host microRNAs can affect viral infection directly by interacting with various regions of viral RNAs including the 3'-UTR, 5'-UTR, and the coding regions. On the other hand, microRNAs could indirectly impact viral infection by regulating host genes that play a role in viral replication. As a result, cellular microRNAs could have an enhancing (Green line-arrow) or inhibitory (Red T-bar) effect on viral infection.

CHAPTER III

RESEARCH METHODOLOGY

3.1. Ethical Approval

This experimental study was not conducted in either animal models or human subjects. Therefore, the requirement for ethical clearance was exempted (IRB No. 152/59) from the review of the Institutional Review Board (IRB) Faculty of Medicine, Chulalongkorn University.

3.2. Cell Culture and Virus Inoculations

MDCK cells (ATCC; #CCL-34) were cultured in Dulbecco's modified Eagle medium (DMEM; GE Healthcare Life Sciences) containing 10% fetal bovine serum (FBS; Gibco) and 1% (v/v) penicillin/streptomycin (Gibco) under 5% CO₂ at 37°C. Upon reaching confluence, 5x10⁴ cells were re-seeded per well in DMEM medium without antibiotics in 24-well plates. IAV subtypes pH1N1 (A/Thailand/104/2009), H3N2 (A/Thailand/CU-H1817/2010), IBV Victoria lineage (B/Thailand/CU-B5522/2011), or IBV Yamagata lineage (B/Massachusetts/02/2012) was then prepared at the multiplicity of infection (MOI) of 0.01. When the cells reached approximately 80% confluences, the media were removed, and the cultures were washed with Phosphate Buffer Saline (PBS; Amresco). Each viral infection was performed in sextuplicate. One hundred microlitres of each viral suspension in overlay medium (DMEM supplemented with 0.2 µg/ml TPCK-treat trypsin (Sigma-Aldrich)) was added into each well and then incubated under 5% CO₂ at 37°C for 1 h

with periodically shaking. After incubation, the viral suspensions were removed from each well and then washed with PBS. Finally, the cells were cultured with fresh infection medium (DMEM supplemented with 0.2% (w/v) bovine serum albumin (BSA; Merck Millipore), and 0.2 $\mu\text{g/ml}$ TPCK-treated trypsin) and incubated under 5% CO_2 at 37°C for 48 h.

3.3. MicroRNA Extractions

The cells were collected at 6, 12, and 24 hours post-infection (hpi). Briefly, the cells were washed twice with PBS and then dissociated with 0.05% trypsin/EDTA (Gibco). To extract microRNAs from the cell pellets, microRNA purification kit (Geneaid) was used according to the manufacturer's instruction.

Step 1 Cell lysis: Two hundred μl of lysis buffer (Geneaid) was added to the cell pellets, and then vortexed vigorously until the pellets were dissolved completely. The mixture was incubated at room temperature for 10 minutes.

Step 2 RNA precipitation: The mixture was added with 20 μl of Mi buffer (Geneaid) and 180 μl of ddH₂O saturated phenol (Invitrogen) and 40 μl of chloroform (Merck Millipore). The mixture was vortexed vigorously for 2 minutes and then centrifuged at 14,000 x g for 3 minutes. The upper phase was transferred to a clean 1.5 ml microcentrifuge tube. A 35% volume of absolute ethanol (Merck Millipore) was added to the upper phase and mixed well by shaking vigorously.

Step 3 RNA binding: An RNA column (Geneaid) was placed in a 2 ml collection tube (Geneaid), the ethanol-added mixture was added to the RNA column. After incubated for one minute at room temperature, the RNA column was then centrifuged at 14,000 x g for 30 seconds. The filtrate was transferred to a new 1.5 ml

microcentrifuge tube. A 70% volume of absolute ethanol was added to the filtrate and mixed well by shaking vigorously. A new RNA column was placed in a 2 ml collection tube, then the ethanol-added mixture was added to the RNA column. After incubated for one minute at room temperature, the column was centrifuged at 14,000 x g for 30 seconds to allow the microRNA to bind to the RNA column membrane.

Step 4 Washing: Ethanol-added wash buffer (Geneaid) was added to the RNA column. After incubated for one minute at room temperature, the column was centrifuged at 14,000 x g for one minute to completely remove the liquid residue. After that, the RNA column was placed in a clean 1.5 ml microcentrifuge tube.

Step 5 MicroRNA elution: Fifty μ l of release buffer (pre-heated to 65°C) was added into the centre of the RNA column. After incubated for 3 minutes at room temperature, the column was centrifuged at 14,000 x g for 3 minutes to recover the microRNA. The concentration of microRNAs was quantified using Qubit fluorometer (Invitrogen) with a Qubit™ microRNA assay kit (Invitrogen).

3.4. DNA Library Preparation and High-Throughput Sequencing

Purified microRNAs from the cells infected with the same viral strains and the same time-point were pooled together (n = 6). One hundred ng of the microRNAs from each group were used to construct the libraries with different indexes, according to a NEBNext® Multiplex Small RNA Library Prep Set for Illumina® (New England BioLabs).

Step 1 The 3' SR Adaptor ligation:

- (a) The 3' SR Adaptor for Illumina was diluted (1:2) with nuclease-free water.

(b) The following components were prepared in a total volume of 7 μ l in a sterile nuclease-free PCR tube:

- Input microRNA (100 ng) 1–6 μ l
- Diluted 3' SR Adaptor for Illumina 1 μ l
- Nuclease-free water variable

(c) The mixture was incubated in a preheated thermal cycler for 2 minutes at 70°C and then transferred the tube to ice.

(d) To make a total volume of 20 μ l, the following components were added into the mixture:

- 3' Ligation Reaction Buffer (2X) 10 μ l
- 3' Ligation Enzyme Mix 3 μ l

(e) The mixture was incubated for 1 hour at 25°C in a thermal cycler.

Step 2 The reverse transcription primer hybridization:

(a) The SR RT Primer for Illumina was diluted (1:2) with nuclease-free water.

(b) To make a total volume of 25.5 μ l, the following components were added into the ligation mixture from the step 1 and mixed well:

- Nuclease-Free Water 4.5 μ l
- SR RT Primer for Illumina 1 μ l

(c) The samples were placed in a Nexus GSX1 (Eppendorf) thermocycler with heated lid set to > 85°C, and heated with the following program: 5 minutes at 75°C; 15 minutes at 37°C; 15 minutes at 25°C; hold at 4°C.

Step 3 The 5' SR Adaptor ligation:

- (a) With 5 minutes remaining, the 5' SR Adaptor was resuspended in 120 μ l of nuclease-free water. After that, the 5' SR Adaptor was diluted (1:2) with nuclease-free water.
- (b) The 5' SR Adaptor was aliquoted into a separate, nuclease-free 200 μ l PCR tube, for the number of samples in the experiment plus an excess of 10%.
- (c) The aliquoted 5' SR Adaptor was denatured in the thermal cycler at 70°C for 2 minutes and then immediately placed on ice.
- (d) To make a total volume of 30 μ l, the following components were added into the ligation mixture from the step 2 and mixed well:
- 5' SR Adaptor for Illumina (denatured) 1 μ l
 - 5' Ligation Reaction Buffer (10X) 1 μ l
 - 5' Ligation Enzyme Mix 2.5 μ l
- (e) The samples were incubated for 1 h at 25°C in the thermal cycler.

Step 4 First-strand synthesis:

- (a) To make a total volume of 40 μ l, the following components were mixed in a sterile, nuclease-free tube:
- Adaptor Ligated RNA from Step 3 30 μ l
 - First-Strand Synthesis Reaction Buffer 8 μ l
 - Murine RNase Inhibitor 1 μ l
 - ProtoScript II Reverse Transcriptase 1 μ l
- (b) The mixture was incubated for 60 minutes at 50°C, followed by immediately proceeded to PCR amplification.

Step 5 PCR amplification:

discarded, and the QIAquick column was placed back into the same tube.

- (d) The QIAquick column was centrifuged at 17,900 x g once more in the provided 2 ml collection tube for 1 min to remove residual wash buffer.
- (e) Each QIAquick column was placed in a new clean 1.5 ml microcentrifuge tube. To elute the amplified DNA, 27.5 μ l of nuclease-free water to the center of the QIAquick membrane and centrifuge the column for 1 min.

Step 7 Size selection:

- (f) The purified PCR reaction (25 μ l) was added with 32.5 μ l (1.3X volume) of resuspended AMPure XP beads (Beckman Coulter) and mixed well on by pipetting up and down at least 10 times.
- (g) The mixture was incubated for 5 minutes at room temperature.
- (h) The tube was placed on a magnetic stand (Invitrogen) to separate beads from the supernatant. After the solution was clear (about 5 minutes), the supernatant (57.5 μ l) was carefully transferred to a new tube. The beads that contain the large DNA fragments were discarded.
- (i) The supernatant (57.5 μ l) was mixed well with 92.5 μ l (3.7X volume) of resuspended AMPure XP beads and incubated for 5 minutes at room temperature.
- (j) The tube was placed on the magnetic stand to separate beads from supernatant. After the solution is clear (about 5 minutes), the

supernatant was carefully removed and discarded. The beads that contain DNA targets were kept in the tube.

- (k) Two hundred μl of freshly prepared 80% ethanol was added to the tube with beads while in the magnetic stand. The sample was incubated at room temperature for 30 seconds, and then the supernatant was carefully removed and discarded.
- (l) Step (h) was repeated once.
- (m) The tube was briefly spun and then put back in the magnetic stand.
- (n) The residual ethanol was completely removed, and the beads were air-dried for up to 10 minutes while the tube was on the magnetic stand with lid open.
- (o) The DNA target was eluted from the beads with 15 μl nuclease-free water, and mixed well by pipetting up and down, incubate for 2 minutes and put the tube in the magnetic stand until the solution was clear.
- (p) The supernatant was transferred to a clean PCR tube.

The concentration of DNA libraries was quantified by using KAPA Library Quantification Kits for Illumina[®] Platform (Kapa Biosystems). The DNA libraries were pooled together with equal concentration, and then single-end sequenced (50 cycles) on a MiSeq Benchtop Sequencer (Illumina).

3.5. Data Analysis of High-Throughput Sequencing

The primary analysis of sequencing data was performed using MiSeq reporter software version 2.4. While low-quality reads with Q-score < 30 were excluded, low-quality regions of sequences were trimmed by the software. The passing filtered reads

with Q-score ≥ 30 were aligned with canine genomic DNA from CanFam 3.1, mature & precursor canine microRNAs from miRbase (111) and contaminant RNA (tRNA, rRNA and mRNA). The sequencing reads matching to canine genomic DNA and contaminant RNA were discarded, whereas the reads matching to the microRNA database were considered as microRNAs. The microRNAs were identified and counted based on the number of reads matching to the miRBase (www.miRbase.org/). As described in previous work (112), differential expression compared between the virus-infected group and mock-infected control was calculated in terms of fold changes.

$$\text{Normalised expression (virus infection)} = \frac{\text{microRNA of interest (virus infection)}}{\text{Total count of microRNAs (virus infection)}}$$

$$\text{Normalised expression (mock infection)} = \frac{\text{microRNA of interest (mock infection)}}{\text{Total count of microRNAs (mock infection)}}$$

$$\text{Fold change} = \text{Log}_2 \frac{\text{Normalised expression (virus infection)}}{\text{Normalised expression (mock infection)}}$$

3.6. Quantification of MicroRNAs by Reverse Transcriptase-Quantitative Polymerase Chain Reaction (RT-qPCR)

Prior to detecting the expression levels of candidate microRNAs, 100 μg of the microRNAs was polyuridylated by poly(U) polymerase (New England Biolabs).

The following components were combined in a sterile microcentrifuge tube:

- 10X NE buffer 2 (New England Biolabs) 2.5 μl
- 50 mM UTP (Thermo Scientific) 0.25 μl
- Small RNAs 100 ng

- 40 U/ μ l RiboLock RNase Inhibitor (Thermo Scientific) 1 μ l
- 2 U/ μ l Poly(U) Polymerase (New England Biolabs) 1 μ l
- Nuclease-free water up to 25 μ l

The mixture was incubated at 37°C for 10 min. To generate cDNA, 12.3 μ l of the microRNAs tailed with poly(U) was added with 0.2 μ l of 10 μ M stem-loop (SL) poly(A) primer (5'-GTCGTATCCAGTGCAGGGTCCGAGGTATTTCGCACTGGATACGAC-3') (113). The mixture was then incubated at 65°C for 5 min, chilled on ice for 2 min. After that, the following components for reverse transcription were combined:

- 5X Reaction Buffer (Thermo Scientific) 4 μ l
- 40 U/ μ l RiboLock RNase Inhibitor (Thermo Scientific) 0.25 μ l
- dNTPs Mix, 10 mM each (Thermo Scientific) 2 μ l
- 200 U/ μ l RevertAid Reverse Transcriptase (Thermo Scientific) 1 μ L

The reverse transcription was performed at 42°C for 1 hour, followed by heat inactivation at 70°C for 10 min. The expression of microRNAs was determined by real-time PCR. The following components were prepared for the qPCR reaction:

- 2X Luna qPCR Master Mix (New England BioLabs) 5 μ l
- 10 μ M MicroRNA-specific forward primers 0.25 μ l
(Primer sequences are shown in Table 4.)
- 10 μ M Reverse primer (miRNA-qPCR_R) 0.25 μ l
- cDNA template 1 μ l
- Nuclease free water Up to 10 μ l

The real-time PCR amplification was conducted on Step One Plus™ Real-time PCR Systems (Applied Biosystems). The real-time PCR conditions were described as follows: initial denaturation stage (95°C, 5 min); cycling stage (Table 4); and the melt curve stage. The expression of canine RNA U6 Small Nuclear 2 (RNU6-2) was measured as an internal control for microRNAs and mock-infected group were used as a calibrator sample. The results were analyzed using StepOne™ Software v.2.2 analysis. The expression ratio was calculated by comparative $\Delta\Delta C_t$ method. All samples were evaluated in triplicate.

Table 4 Primers and PCR conditions used for microRNA quantification.

Primers	Nucleotide Sequences (5'-3')	PCR Cycling Stage (40 cycles)
<i>Cfa</i> -miR-17_F	GCAGTGAAGGCACTTGTAG	95°C 15 sec, 58°C 30 sec, 62°C 30 sec
<i>Cfa</i> -miR-33b_F	TGCATTGCTGTTGCATTGC	95°C 15 sec, 58°C 30 sec, 62°C 30 sec
<i>Cfa</i> -miR-122_F	TGGAGTGTGACAATGGTGT	95°C 15 sec, 60°C 30 sec, 62°C 30 sec
<i>Cfa</i> -miR-125b-2//125b-1_F	CCTGAGACCCTAACTTGTG	95°C 15 sec, 60°C 30 sec, 62°C 30 sec
<i>Cfa</i> -miR-132_F	CAGTCTACAGCCATGGTGC	95°C 15 sec, 62°C 30 sec, 72°C 30 sec
<i>Cfa</i> -miR-146b_F	GAGAACTGAATTCCATAGGC	95°C 15 sec, 62°C 30 sec, 72°C 30 sec
<i>Cfa</i> -miR-181a_F	ATTCAACGCTGTCCGGTGAG	95°C 15 sec, 58°C 30 sec, 62°C 30 sec
<i>Cfa</i> -miR-197_F	ACCACCTTCTCCACCCAG	95°C 15 sec, 58°C 30 sec, 62°C 30 sec
<i>Cfa</i> -miR-215_F	TGACCTACGAATTGATAGACA	95°C 15 sec, 55°C 30 sec, 62°C 30 sec
<i>Cfa</i> -miR-339-1_F	CCCTGTCCTCCAGGAGC	95°C 15 sec, 62°C 30 sec, 80°C 30 sec
<i>Cfa</i> -miR-320_F	GCTGGGTTGAGAGGGCGA	95°C 15 sec, 58°C 30 sec, 62°C 30 sec
<i>Cfa</i> -miR-340_F	TTATAAAGCAATGAGACTGATT	95°C 15 sec, 60°C 30 sec, 62°C 30 sec
<i>Cfa</i> -miR-361_F	TCAGAATCTCCAGGGGTAC	95°C 15 sec, 58°C 30 sec, 62°C 30 sec
<i>Cfa</i> -miR-500_F	GCACCTGGGCAAGGATTCT	95°C 15 sec, 58°C 30 sec, 62°C 30 sec
<i>Cfa</i> -miR-543_F	CATTCGCGGTGCACTTCTT	95°C 15 sec, 55°C 30 sec, 62°C 30 sec
<i>Cfa</i> -miR-1249_F	CCTTCCCCCCTTCTTCA	95°C 15 sec, 58°C 30 sec, 62°C 30 sec
<i>Cfa</i> -miR-1307_F	GCGTGGCGTCCGGTCCGTG	95°C 15 sec, 58°C 30 sec, 72°C 30 sec
<i>Cfa</i> -miR-1839_F	GGTAGATAGAACAGGTCTTG	95°C 15 sec, 58°C 30 sec, 72°C 30 sec
<i>Cfa</i> -miR-1842_F	CTCTGCGAGGTCAGCTCA	95°C 15 sec, 58°C 30 sec, 62°C 30 sec
<i>Cfa</i> -miR-2483_F	CAACCATCCAGCTGTTTGA	95°C 15 sec, 58°C 30 sec, 62°C 30 sec

Primers	Nucleotide Sequences (5'-3')	PCR Cycling Stage (40 cycles)
<i>Cfa</i> - RNU6-2 _F	CTCGCTTCGGCAGCACACA	95°C 15 sec, 55°C 30 sec, 62°C 30 sec
<i>Cfa</i> -miRNA- qPCR_R	TGCGGATAACAATTTTCACACA	-

3.7. Transfection of MicroRNA Inhibitors

To antagonize the silencing effects of candidate microRNAs on viral genes, miR-146b inhibitor (Dharmacon; #IH-300754-05-0005), miR-197 inhibitor (Ambion; #MH10354), miR-215 inhibitor (Ambion; MH15318), miR-340 inhibitor (Dharmacon; #IH-301081-02-0005) and negative control inhibitor (Dharmacon; #IN-001005-01-05) were transfected into MDCK cells using Lipofectamine[®] 2000 transfection agent (Invitrogen). Briefly, MDCK cells were seeded at 0.5×10^5 cells/well on a 24-well plate and cultured under 5% CO₂ at 37°C for 18 h. After incubation, 20 pmol of each microRNA inhibitor was diluted in 50 µl of Opti-MEM[®] Medium (Invitrogen) without serum. Meanwhile, one µl of Lipofectamine[®] 2000 reagent added with 50 µl of Opti-MEM[®] Medium was incubated for 20 min at room temperature. After the 5-min incubation, the diluted microRNA inhibitor was combined with the diluted Lipofectamine[®] 2000. The mixture was then incubated for 20 min at room temperature. With 5 min remaining, the cell media were replaced with 400 µl of Opti-MEM[®] Medium. Afterwards, 100 µl of the oligomer-Lipofectamine[®] 2000 complex was added to each well containing cells and medium. Following the treatment of microRNA inhibitors under 5% CO₂ at 37°C for 4 h, the cells were then infected at the MOI of 0.01 for 48 h with influenza virus A/Thailand/104/2009 (pH1N1), A/Thailand/CU-H1817/2010 (H3N2), B/Thailand/CU-B5522/2011 (Victoria lineage), and B/Massachusetts/02/2012 (Yamagata lineage). Viral supernatants were subjected

to the determination of viral titer by RT-qPCR and ELISA. The experiments were performed in triplicates.

3.8. Construction of Silencing Plasmids

To produce microRNA expressing vectors, pSilencer 3.0-H1 (Ambion) was used as a vector backbone (Appendix A).

Step 1 Plasmid linearization: pSilencer 3.0-H1 was cut with restriction enzymes *Bam*HI (New England BioLabs) and *Hind*III (New England BioLabs). The following components were prepared in a sterile 1.5-ml microcentrifuge tube:

- | | | |
|--|-------|-------|
| • pSilencer 3.0-H1 | 1 | μg |
| • <i>Bam</i> HI | 1 | μl |
| • <i>Hind</i> III | 1 | μl |
| • 10X Tango buffer (New England BioLabs) | 2 | μl |
| • Nuclease-free water | Up to | 20 μl |

The mixture was then incubated at 37°C for 4 h. After that, the plasmids were purified by 1% agarose gel electrophoresis. The gel slice containing the linearized plasmids (2,795 bp) was cut and extracted by HiYield™ Gel/ PCR Fragments Extraction kit (RBC Bioscience), according to the manufacturer's protocol. Briefly, 300 mg of the gel slice was into a microcentrifuge tube and added with 500 μl of DF Buffer. The gel slice was incubated at 55°C for 10-15 minutes until completely dissolved. Then, 800 μl of the sample mixture was applied into the DF Column which was placed in a collection tube. The tube was centrifuged at 10,000 x g for 30 seconds. The flow-through was discarded, and the DF Column was placed back in the collection tube. After that, 600 μl of Ethanol-added Wash Buffer was added to the DF

Column. The tube was centrifuged at 10,000 x g for 30 seconds. The flow-through was discarded, and the DF Column was placed back in the collection tube. The tube was centrifuged again for 2 minutes at 10,000 x g to dry the column matrix. The dried DF Column was transferred into a new microcentrifuge tube. Thirty μ l of Elution Buffer was added to the center of the column matrix. After being allowed to stand for 2 min, the tube was centrifuged for 2 min at full speed to elute purified DNA.

Step 2 Oligonucleotide annealing: Meanwhile, the top-strand and bottom-strand oligonucleotides (Table 5) were annealed with the following components:

- 10 nM Top-strand oligonucleotide 10 μ l
- 10 nM Bottom-strand oligonucleotide 10 μ l
- 5X rapid Ligation buffer (Thermo Scientific) 5 μ l

The mixture was heated in a thermocycler at 90°C for 5 min, followed by annealing at 25°C for 1 hour.

Table 5 Oligonucleotides used for the construction of silencing plasmids.

Oligonucleotides ¹	Nucleotide sequences (5'-3')
<i>Cfa</i> -miR-146b_TS	GATCCGTGAGAACTGAATTCATAGGCTGTGAGCTTGAGCA AACAGCCTAGGGACTCAGTTCTGGTTTTTTGGAAA
<i>Cfa</i> -miR-146b_BS	AGCTTTTCCAAAAAACCAGAACTGAGTCCCTAGGCTGTTTG CTCAAGCTCACAGCCTATGGAATTCAGTTCTCACG
<i>Cfa</i> -miR-197_TS	GATCCGCGGGTAGAGAGGGCAGTGGGAGGTAAGAGCTCTT CACCTTCACCACCTTCTCCACCCAGCTTTTTTTGGAAA GATCCGCGGGTAGAGAGGGCAGTGGGAGGTAAGAGCTCTT CACCTTCACCACCTACCCAGCTTTTTTTGGAAA
<i>Cfa</i> -miR-197_BS	AGCTTTTCCAAAAAAGCTGGGTGGAGAAGGTGGTGAAGGG TGAAGAGCTCTTACCTCCACTGCCCTCTTACCCGCG
<i>Cfa</i> -miR-215_TS	GATCCATGACCTACGAATTGATAGACAATTTGGCTAAGTTT GTCTGTCAATTTTTGTAGGCCATTTTTTTGGAAA
<i>Cfa</i> -miR-215_BS	AGCTTTTCCAAAAAATGGCCTACAAAAATGACAGACAAACT

Oligonucleotides ¹	Nucleotide sequences (5'-3')
	TAGCCAAATTGCTATCAATTCGTAGGTCATG
<i>Cfa</i> -miR-340_TS	GATCCGTTATAAAGCAATGAGACTGATTGTCATGTGTCGGT TGTGGGATCCGTCTCAGTTACTTTATAGTTTTTTTGGAAA
<i>Cfa</i> -miR-340_BS	AGCTTTTCCAAAAAACTATAAAGTAACTGAGACGGATCCCA CAACCGACACATGACAATCAGTCTCATTGCTTTATAACG
<i>Cfa</i> -miR-Scramble_TS	GATCCGCAGGTCTTTCATCTAGAACGATGCGGGTTCAAGAG ACCCGCATCGTTCTAGATGAAAGACCTGTTTTTTGGAAA
<i>Cfa</i> -miR-Scramble_BS	AGCTTTTCCAAAAAACAGGTCTTTCATCTAGAACGATGCGG GTCTCTTGAACCCGCATCGTTCTAGATGAAAGACCTGCG
siLuc/Luc2_TS	GATCCCACCCCAACATCTTCGACGTTCAAGAGACGTCTGAAG ATGTTGGGGTGTTTTTTTGGAAA
siLuc/Luc2_BS	AGCTTTTCCAAAAAACACCCCAACATCTTCGACGTCTCTTG AACGTCGAAGATGTTGGGGTGG

¹ Abbreviations: TS: Top Strand; BS; Bottom Strand

Step 3 Ligation: The annealed fragment was ligated into linearized pSilencer3.0-H1 at the molar ratio of 3 (DNA insert): 1 (pSilencer3.0-H1). The ligation reaction was performed with T4 DNA ligase (Thermo Scientific) at 22°C for 30 min, according to the manufacturer's protocol.

Step 4 Transformation: The plasmids were transformed into *E. coli* strain JM109 competent cells (RBC Bioscience) by heat shock method. Briefly, 5 µl of DNA ligates was added to 50 µl of competent cells. The mixture was incubated for 30 min on ice, followed by heat shock at 42°C for 45 sec and 5 min on ice. After that, 980 µl of SOC media supplemented with 10 µl of 2 M MgCl₂ and 10 µl of 2 M Glucose was added to the mixture. The transformant was incubated at 37°C with shaking at 200 rpm for 1 h. After that, the transformant was spread on an LB agar plate containing Ampicillin and incubated at 37°C overnight. After incubation, the colonies were picked into a 1.5-ml LB broth for liquid culture and incubated at 37°C with overnight shaking.

Step 5 Plasmid extraction: The plasmid DNA was extracted using HiYield™ Plasmid Mini Kit (RBC Bioscience). Bacterial culture in the LB broth was transferred to a sterile microcentrifuge tube. The tube was centrifuged for 1 min at 10,000 x g, followed by removal of the supernatant. After that, 200 µl of RNase-added PD1 Buffer was added to the cell pellet and resuspended by vortexing. The mixture was added with 200 µl of PD2 Buffer and mixed gently by inverting the tube 10 times, followed by incubation for 2 minutes at room temperature. For neutralization, 300 µl of PD3 Buffer was added and mixed immediately by inverting the tube 10 times. The mixture was then centrifuged for 2 min at 10,000 x g. The supernatant was added to the PD Column which was placed on a 2-ml collection tube. The clear lysate was centrifuged at 10,000 x g for 30 seconds. The flow-through was discarded, and the PD Column was placed back to the collection tube. To wash, 400 µl of W1 Buffer was added in the PD Column and centrifuged at 10,000 x g for 30 seconds. The flow-through was discarded, and the PD Column was returned to the collection tube. After that, 600 µl of Ethanol-added Wash Buffer was applied to PD Column and centrifuged at 10,000 x g for 30 Seconds. The flow-through was discarded, and the PD Column was placed back to the collection tube. To dry the column matrix, the tube was centrifuged again for 3 min at 10,000 x g. The dried PD Column was placed to a clean 1.5ml microcentrifuge tube. Then, 50 µl of Elution Buffer was directly added onto the centre of the membrane. After being allowed to stand for 2 min, the tube was centrifuged for 2 min at 10,000 x g to elute plasmid DNA. The concentration of each plasmid was measured by NanoPhotometer® (Implen). To confirm the recombinant vectors, the nucleotide inserts were investigated by Sanger sequencing.

3.9. Transfection of Silencing Plasmids

For upregulation of microRNA activity, pSilencer 3.0-H1 expressing *cfa*-miRNA-146b (denoted by pSilencer_miR-146b), pSilencer_miR-197, pSilencer_miR-215, pSilencer_miR-340, or pSilencer_Scramble was transfected into MDCK cells using TurboFect™ Transfection reagent. Briefly, MDCK cells were seeded at 0.5×10^5 cells/ well on a 24-well plate and cultured under 5% CO₂ at 37°C for 18 h. After overnight incubation, 1 µg of each silencing plasmid was diluted with 100 µl of Opti-MEM® Medium without serum in a sterile microcentrifuge tube. Two µl of TurboFect™ Transfection reagent was diluted to the plasmid DNA and mixed well immediately. The mixture was incubated for 20 min at room temperature. With 5 min remaining, the cell media were replaced with 900 µl of Opti-MEM® Medium. After incubation, 100 µL of the transfection reagent/silencing plasmid mixture was added to each well containing cells and medium. Following the treatment of silencing plasmids under 5% CO₂ at 37°C for 4 h, the cells were then infected at the MOI of 0.01 for 48 h with influenza virus A/Thailand/104/2009 (pH1N1), A/Thailand/CU-H1817/2010 (H3N2), B/Thailand/CU-B5522/2011 (Victoria lineage), and B/Massachusetts/02/2012 (Yamagata lineage). Viral supernatants were subjected to the determination of viral titer by RT-qPCR and ELISA. The experiments were performed in triplicate.

3.10. Viral RNAs Extraction

To isolate viral RNAs, GenUP™ viral RNA extraction kit (Biotechrabbit) was used, following the manufacturer's instruction. Firstly, 450 µl of fresh CARRIER-Buffer LYSIS LR mix was transferred to a sterile microcentrifuge tube. One-hundred

fifty microlitres of each viral supernatant was applied to the tube, followed by the addition of 20 μ l of Proteinase K. After incubated at room temperature for 10 min, the sample mixture was centrifuged at 12,000 x g for 1 min to collect the liquid phase at the bottom of the tube. After that, 600 μ l of Buffer BINDING BR was added to the lysate. The mixture was applied to a MiniFilter placed in a collection tube, then centrifuged at 10,000 x g for 1 min. The MiniFilter was placed in a new collection tube and was added with 500 μ l of Ethanol-added WASH A Buffer. After centrifuged at 10,000 x g for 1 min, the MiniFilter was placed in a new collection tube and added with 650 μ l of Ethanol-added WASH B Buffer. The tube was centrifuged at 10,000 x g for 1 min. To remove residual ethanol, the MiniFilter placed in a new collection tube was centrifuged again for 3 min. After that, the MiniFilter was placed into an Elution tube, and 60 μ l of nuclease-free water (pre-heated at 70°C) was added. After being allowed to stand for 2 min, the tube was centrifuged at 8,000 x g for 1 min to collect viral RNAs.

3.11. Quantification of Viral Genes by RT-qPCR

To generate cDNA, 12.3 μ l of viral RNAs was added with 0.2 μ l of 10 μ M UniFlu_cDNA (5'- IAGCARAAGC-3'). The mixture was then incubated at 65 °C for 5 min, chilled on ice for 2 min. After that, the following components for reverse transcription were combined:

- 5X Reaction Buffer (Thermo Scientific) 4 μ l
- 40 U/ μ l RiboLock RNase Inhibitor (Thermo Scientific) 0.25 μ l
- dNTPs Mix, 10 mM each (Thermo Scientific) 2 μ l

- 200 U/ μ l RevertAid Reverse Transcriptase (Thermo Scientific) 1 μ l

The reverse transcription was performed at 42°C for 1.5 hours, followed by heat inactivation at 70°C for 10 min. The expression of the viral genes was determined by real-time PCR. The following components were prepared for qPCR reaction:

- 2X Luna qPCR Master Mix (New England BioLabs) 5 μ l
 - 10 μ M Forward primer 0.25 μ l
 - 10 μ M Reverse primer 0.25 μ l
- (Primer sequences are shown in Table 6.)
- cDNA template or plasmid 1 μ l
 - Nuclease-free water Up to 10 μ l

The real-time PCR conditions were described as follows: initial denaturation stage (95°C, 2 min); cycling stage (Table 6); and the melt curve stage. RBC T&A cloning vector carrying Flu A M gene or Flu B PB1 gene was constructed and denoted by pFlu A_M or pFlu B_PB1, respectively. The concentration of the plasmids was measured using NanoPhotometer[®] (Implen), and the corresponding copy number was calculated (114). A 10-fold serial dilution series of the pFlu A_M or pFlu B_PB1, ranging from 1×10^9 to 1×10^3 copies/ μ l, was used to create the standard curves.

The real-time PCR amplification was conducted on Step One Plus[™] Real-time PCR Systems (Applied Biosystems). The Ct values were plotted against the logarithm of their initial template copy numbers. Each standard curve was generated by linear regression of the plotted points. Absolute quantification determines the exact

copy concentration of the target genes by relating the Ct value to a standard curve. The copy concentration of M gene was used for quantification of IAV, whereas PB1 copy number was detected for IBV quantification. The results were analyzed using StepOne™ Software v.2.2 analysis, and comparative fold change between each group was reported (115). All samples were evaluated in triplicate.

Table 6 Primers and PCR conditions used for viral RNA quantification.

Primers ¹	Nucleotide Sequences (5'-3')	PCR Cycling Stage (40 cycles)
Flu A_M_F151	CATGGARTGGCTAAAGACAAGACC	
Flu A_M_R276	ATTTAGGTGACACTATAGAGGGCATT YTGGACAAAKCGTCTA	95°C 15 sec, 60°C 20 sec, 72°C 30 sec
Flu B_PB1_F269	AGGCTTTGGATAGAATGGATGA	
Flu B_PB1_R385	AAGTCTGTCTCCCCTGGGTT	95°C 15 sec, 57°C 20 sec, 72°C 30 sec

¹ Abbreviations: F: Forward Strand; R: Reverse Strand

3.12. Quantification of Viral Proteins by Enzyme-Linked Immunosorbent Assay (ELISA)

Influenza A H1N1 (Swine Flu 2009) HA ELISA Pair Set (Sino Biological; #SEK001), Influenza A H3N2 HA ELISA Pair Set (Sino Biological; #SEK11056) and Influenza B HA ELISA Pair Set (Sino Biological; #SEK11053) were used for quantification of viral yields.

Step 1 Plate preparation:

(a) The capture antibody was diluted to the working concentration in

PBS as follows:

- Mouse anti-influenza A H1N1 HA antibody 2 µg/ml
- Rabbit anti-influenza A H3N2 HA antibody 2 µg/ml
- Mouse anti-influenza B HA antibody 2 µg/ml

After coated with 100µl per well of the diluted capture antibody, Nunc-Immuno 96-well plates (Thermo Scientific) were sealed and incubated overnight at 4°C.

- (b) The capture antibody in each well was aspirated, and the wells were washed with at least 300 µl wash buffer (0.05% Tween20 in TBS), repeating the process two times for a total of three washes. After the last wash, the plates were inverted and blotted against clean paper towels to remove the remaining wash buffer.
- (c) The plates were blocked by adding 300 µl of blocking buffer (2% BSA in wash buffer) to each well. Blocking process was performed Incubated at room temperature for 1 hour.
- (d) The blocking buffer in each well was aspirated, and the wells were washed with at least 300 µl wash buffer (0.05% Tween20 in TBS), repeating the process two times for a total of three washes. After the last wash, the plates were inverted and blotted against clean paper towels to remove the remaining wash buffer.

Step 2 Standard preparation: A seven-point standard curve using 2-fold serial dilutions in sample dilution buffer (0.1% BSA in wash buffer) with a high standard of the following concentration was prepared:

- Recombinant influenza A H1N1 HA 1,000 pg/ml
- Recombinant influenza A H3N2 HA 25,000 pg/ml
- Recombinant influenza B HA 4 ng/ml

Step 3 Assay procedure:

- (a) One hundred μL of samples or standards in sample dilution buffer was added per well. The plates were sealed and incubated for 2 h at room temperature.
- (b) The samples or standards in each well were aspirated, and the wells were washed with at least 300 μl wash buffer (0.05% Tween20 in TBS), repeating the process two times for a total of three washes. After the last wash, the plates were inverted and blotted against clean paper towels to remove the remaining wash buffer.
- (c) The detection antibody was diluted to the working concentration in antibody dilution buffer (0.5% BSA in wash buffer) as follows:
- Rabbit anti-influenza A H1N1 HA antibody 0.8 $\mu\text{g/ml}$
 conjugated to horseradish-peroxidase (HRP)
 - Mouse anti-influenza A H3N2 HA antibody 0.8 $\mu\text{g/ml}$
 conjugated to HRP
 - Mouse anti-influenza B HA antibody 0.5 $\mu\text{g/ml}$
 conjugated to HRP
- After added with 100 μl per well of the diluted detection antibody, the plates were sealed and incubated for 1 hour at room temperature.
- (d) The detection antibody in each well was aspirated, and the wells were washed with at least 300 μl wash buffer (0.05% Tween20 in TBS), repeating the process two times for a total of three washes. After the last wash, the plates were inverted and blotted against clean paper towels to remove the remaining wash buffer.

- (e) Two hundred μl of 1-Step™ Turbo TMB-ELISA Substrate Solution (Thermo Scientific) was added to each well, followed by incubation for 20 minutes at room temperature
- (f) Fifty μl of stop solution (2 N H_2SO_4) was added to each well.
- (g) The optical density of each well was immediately determined using a microplate reader set to 450 nm.

3.13. *In Silico* Analysis of MicroRNA Target Prediction

The genomes of influenza viruses A/Thailand/104/2009 (pH1N1), A/Thailand/CU-H1817/2010 (H3N2), B/Thailand/CU-B5522/2011 (Victoria lineage), B/Massachusetts/02/2012 (Yamagata lineage) were retrieved from NCBI and GISAID EpiFlu database. To predict the target sites, two web-based programs including miRBase (111), and RNAhybrid (116) were used on the basis of hybridization patterns between the microRNAs and viral genomes. Therefore, the criteria for the selection of microRNA targets were based on effective hybridization patterns, particularly at the seeding region, and minimum free energy (MFE) for base pairing less than -15.0 kcal/mol. The hybridization patterns obtained from RNAhybrid were classified into 4 categories including 5'-canonical, 5'-seed, 3'-compensatory and ineffective hybridization. Only the targeted viral genomes with patterned hybridization were selected as candidate targets for microRNAs.

3.14. Construction of Reporter Vectors

To produce reporter vectors, pmirGLO (Promega) was used as a vector backbone (Appendix B).

Step 1 Plasmid linearization: pmirGLO was cut with restriction enzymes *NheI* (New England BioLabs) and *XhoI* (New England BioLabs). The following components were prepared in a sterile 1.5-ml microcentrifuge tube:

- pmirGLO 1 μ g
- *NheI* 1 μ l
- *XhoI* 1 μ l
- 10X Tango buffer (New England BioLabs) 2 μ l
- Nuclease-free water Up to 20 μ l

The mixture was then incubated at 37°C for 4 h. Next, the plasmids were treated with 1 μ l of Antarctic phosphatase (New England BioLabs) and 2.2 μ l of 2X Antarctic Phosphatase Buffer (New England BioLabs), followed by incubation at 37°C for 30 min. After that, the plasmids were purified by 1% agarose gel electrophoresis. The gel slice containing the linearized plasmids (2,795 bp) was cut and extracted by HiYield™ Gel/ PCR Fragments Extraction kit (RBC Bioscience), according to the manufacturer's protocol. Briefly, 300 mg of the gel slice was into a microcentrifuge tube and added with 500 μ l of DF Buffer. The gel slice was incubated at 55°C for 10-15 min until completely dissolved. Then, 800 μ l of the sample mixture was applied into the DF Column which was placed in a collection tube. The tube was centrifuged at 10,000 x g for 30 seconds. The flow-through was discarded, and the DF Column was placed back in the collection tube. After that, 600 μ l of Ethanol-added Wash Buffer was added to the DF Column. The tube was centrifuged at 10,000 x g for 30 seconds. The flow-through was discarded, and the DF Column was placed back in the collection tube. The tube was centrifuged again for 2 minutes at 10,000 x g to dry the column matrix. The dried DF Column was transferred into a new microcentrifuge

tube. Thirty microlitres of Elution Buffer was added to the center of the column matrix. After being allowed to stand for 2 min, the tube was centrifuged for 2 min at full speed to elute purified DNA.

Step 2 Oligonucleotide annealing: Meanwhile, the top-strand and bottom-strand oligonucleotides (Table 7) were annealed with the following components:

- 10 nM Top-strand oligonucleotide 10 μ l
- 10 nM Bottom-strand oligonucleotide 10 μ l
- 5X rapid Ligation buffer (Thermo Scientific) 5 μ l
- T4 Polynucleotide Kinase (New England BioLabs) 1 μ l

The mixture was heated in a thermocycler at 90°C for 5 min, 60°C for 2 min, followed by annealing at 37°C for 30 min.

Step 3 Ligation: The annealed fragment was ligated into linearized pmirGLO at the molar ratio of 3 (DNA insert): 1 (pmirGLO). The ligation reaction was performed with T4 DNA ligase (Thermo Scientific) at 22°C for 30 min, according to the manufacturer's protocol. Transformation and plasmid extraction steps were conducted, following the step 4 and step 5 of "3.8. Construction of Silencing Plasmids".

Table 7 Oligonucleotides used for the construction of reporter plasmids.

Virus genes (position)	Nucleotide sequences (5'-3')
pH1N1_PB2_1979_TS	<u>CTAGAGGCAACCAACGACTTACAGTTCTTG</u>
pH1N1_PB2_1979_BS	<u>TCGACAAGAAGTGTAAAGTCGTTTGGTTGCCT</u>
pH1N1_PB1_2191_TS	<u>CTAGGAGTCTGGACGGATCAAGAAAGAAGAGTTCTCT</u>
pH1N1_PB1_2191_BS	<u>TCGAAGAGAACTCTTCTTTCTTGATCCGTCCAGACTC</u>
pH1N1_NA_693_TS	<u>CTAGTGCATGTGTAATGGTTCTTG</u>
pH1N1_NA_693_BS	<u>TCGACAAGAACCATTTACACATGCA</u>
pH1N1_PB2_350_TS	<u>CTAGTAAAACCTATTTGAAAAGGTCGA</u>

pH1N1_PB2_350_BS	<u>TCGATCGACCTTTTCGAAATAAGTTTTA</u>
pH1N1_PB1_2155_TS	<u>CTAGGTGTCTAGGGCCCGGATTGATGCCAGGGTCGA</u>
pH1N1_PB1_2155_BS	<u>TCGATCGACCCTGGCATCAATCCGGGCCCTAGACAC</u>
H3N2_PB2_865_TS	<u>CTAGATTGGCGGAACAAGGATGGTGGAC</u>
H3N2_PB2_865_BS	<u>TCGAGTCCACCATCCTTGTTCGCCAAT</u>
H3N2_PB2_1447_TS	<u>CTAGAATGGGTGTGGATGAATACTCCAGTACAGAGAGGGTGGTGGT</u>
H3N2_PB2_1447_BS	<u>TCGAACCACCACCCTCTCTGTACTGGAGTATTCATCCACACCCATT</u>
B5522_PB1_2101_TS	<u>CTAGAGTGCATCATAACAGGAAGCCAGTGGGTCAA</u>
B5522_PB1_2101_BS	<u>TCGATTGACCCACTGGCTTCCTGTATGATGCACT</u>
B5522_HA_98_TS	<u>CTAGCTGCTACTCAAGGGGAGGTCAA</u>
B5522_HA_98_BS	<u>TCGATTGACCTCCCCTTGAGTAGCAG</u>
B5522_NP_617_TS	<u>CTAGATGTCTGTTTCCAAAGGTCAAA</u>
B5522_NP_617_BS	<u>TCGATTTGACCTTTGGAAACAGACAT</u>
Mass_PA_534_TS	<u>CTAGAACCTATGGCAAGTTCTCAT</u>
Mass_PA_534_BS	<u>TCGAATGAGAACTTGCCATAGGTT</u>
Mass_NP_973_TS	<u>CTAGAGGCCCTCTGTGGCGAGCAAAGTGGTTCTTC</u>
Mass_NP_973_BS	<u>TCGAGAAGAACCCTTTGCTCGCCACAGAGGGCCT</u>
Mass_NP_1290_TS	<u>CTAGTTCTTCTGGAACCTCGGTTTTCT</u>
Mass_NP_1290_BS	<u>TCGAAGAAAACCGAGTTCCAGAAGAA</u>

3.15. Luciferase Reporter Assay

For 3'-UTR reporter assay, MDCK cells were seeded at 10^4 cells/ well in media without antibiotic-antimycotic into 96-well plates and incubated for 24 h. For transfection into each well, pmirGLO and pSilencer were diluted with Opti-MEM (Gibco), and then co-transfected into the MDCK cells by using Turbofect (Thermo Scientific), following the manufacturer's instruction. Briefly, 300 μ g of pSilencer and 75 μ g of pmirGLO was diluted with 20 μ l of Opti-MEM[®] Medium without serum in a sterile microcentrifuge tube. After that, 0.4 μ l of TurboFect[™] Transfection reagent was added to the plasmid DNA and mixed well immediately. The mixture was incubated for 20 min at room temperature. With 5 min remaining, the cell media were replaced with 200 μ l of Opti-MEM[®] Medium. After incubation, 20 μ l of the transfection reagent/plasmid DNAs mixture was added to each well containing cells

and medium. The transfected cells were incubated under 5% CO₂ at 37°C for 48 h, and then harvested. The assay was performed in triplicate.

The dual-luciferase assay was conducted using Dual-Luciferase[®] Reporter Assay System (Promega) according to the manufacturer's protocol. Briefly, the cells were washed with 100 µl of PBS and then added with 20 µl of Passive Lysis Buffer. The suspensions were then transferred into a Nunc[™] F96 white plate (Thermo Scientific). After that, 100 µl of luciferase assay reagent II (LARII) was added into each well. The emission of firefly luciferase activity at 560 nm was measured by Varioskan Flash Multimode (Thermo Scientific). Before measuring *Renilla* luciferase activity at 480 nm, 100 µl of Stop and Glow reagent was added in order to stop firefly luciferase. The assay was done in triplicate. The relative luciferase activity was calculated using signal intensities of firefly luciferase divided by *Renilla* luciferase from a reporter vector, followed by data normalization (117, 118)

3.16. Sequencing of HA and NA Genes

To investigate the effect of microRNA inhibitor treatments on antigenic HA and NA, nucleotide sequencing was performed. To generate cDNA, 12.3 µl of viral RNAs was added with 0.2 µl of either 10µM MBT_Uni12 (5'-ACGCGTGATCAGCAAAAGCAGG-3') for influenza A viruses or 10 µM UniFlu_cDNA (5'- IAGCARAAGC-3') for influenza B viruses. The mixture was then incubated at 65°C for 5 min, chilled on ice for 2 min. After that, the following components for reverse transcription were combined:

- 5X Reaction Buffer (Thermo Scientific) 4 µl
- 40 U/µl RiboLock RNase Inhibitor (Thermo Scientific) 0.25 µl

- dNTPs Mix, 10 mM each (Thermo Scientific) 2 μ l
- 200 U/ μ l RevertAid Reverse Transcriptase (Thermo Scientific) 1 μ L

The reverse transcription was performed at 42°C for influenza A viruses or 37°C for influenza B viruses for 1.5 h, followed by heat inactivation at 70°C for 10 min. The amplification of viral genes was determined by conventional PCR. The following components were prepared for influenza A viruses:

- 5X Phusion HF buffer (Thermo Scientific) 10 μ l
 - 10mM dNTPs 1.75 μ l
 - 10 μ M MBT_Uni12 0.625 μ l
 - 10 μ M MBT_Uni13 0.625 μ l
 - 10 μ M FluA_VMKU-F 0.625 μ l
 - 10 μ M FluA_VMKU-R 0.625 μ l
- (Primer sequences are shown in Table 8)
- Phusion DNA polymerase (Thermo Scientific) 0.5 μ l
 - cDNA Template 7.5 μ l
 - Nuclease free water Up to 50 μ l

The following components were prepared for influenza B viruses:

- 5X Phusion HF buffer (Thermo Scientific) 10 μ l
- 10 mM dNTPs 1.75 μ l
- 10 μ M B-HANA-UniF 1.25 μ l
- 10 μ M B-HANA-UniR 1.25 μ l

(Primer sequences are shown in Table 8)

- Phusion DNA polymerase (Thermo Scientific) 0.5 μ l
- cDNA Template 7.5 μ l
- Nuclease free water Up to 50 μ l

The PCR amplification was conducted on Mastercycler Nexus GSX1 (Eppendorf). The real-time PCR conditions were described as follows: initial denaturation stage (94°C, 2 min); cycling stage (Table 8); and final extension (68°C, 10 min). The PCR products of HA (~1,800 bp) and NA (~1,400 bp) were purified by 1% agarose gel electrophoresis. The gel slice containing HA and NA was cut and extracted by HiYield™ Gel/ PCR Fragments Extraction kit (RBC Bioscience), according to the manufacturer's protocol. The purified PCR products were verified by sequencing, and the results were illustrated by BioEdit version 7.2.

Table 8 Primers and PCR conditions used for HA and NA amplification (119, 120).

Primers	Nucleotide Sequences (5'-3')	PCR Cycling Stage
MBT_Uni12	ACGCGTGATCAGCAAAAGCAGG	(94°C 30 sec, 45°C 30 sec, 68°C 3 min) x 5 cycles, followed by
MBT_Uni13	ACGCGTGATCAGTAGAAACAAGG	
FluA_VMKU-F	GATCGCTCTTCTGGGAGCGAAAGCAG G	(94°C 30 sec, 57°C 30 sec, 68°C 3 min) x 35 cycles
FluA_VMKU-R	CATCGCTCTTCTATTAGTAGAAACAAG	
B-HANA-UniF	GGGGGAGCAGAAGCAGAGC	(94°C 20 sec, 40°C 30 sec, 68°C 3.5 min)
B-HANA-UniR	CCGGGTATTAGTAGTAACAAGAGC	x 5 cycles, followed by (94°C 20 sec, 68°C 30 sec, 68°C 3.5 min) x 35 cycles

3.17. Statistical Analysis

The data were statistically analyzed and visualized by using GraphPad Prism version 8.1. The results were presented as the mean \pm SD (standard deviation) of triplicates. Differences between each group were analyzed using the Student's

unpaired t-test and One-way ANOVA with the Dunnett's multiple comparisons test for gene expression, ELISA, and luciferase activity. The p value less than 0.05 ($p < 0.05$) was considered as statistically significant.



CHAPTER IV

RESULTS

4.1. High-throughput Sequencing of Canine MicroRNAs upon Seasonal Influenza Infection

To investigate microRNA profiles, MDCK cells were mock-infected or infected with either of four seasonal influenza viruses, IAV pH1N1, IAV H3N2, IBV Victoria lineage, or IBV Yamagata lineage. Based on the replication cycle of influenza viruses, release of progeny virus from infected cells is detected at 6 hours post-infection (hpi) (121). Small RNA samples were retrieved at 6, 12, 24 hpi, and were then subject to library preparation for massively parallel sequencing using Illumina MiSeq Platform. The mock-, seasonal IAV-, or IBV-infected small RNA library contained more than 10^4 reads that represented microRNAs (Table 9 and 10). These sequence tags were further evaluated to determine alteration of specific microRNA expression during IAV and IBV infection compared to uninfected state. Since the Dog Genome Sequencing Consortium submitted the genome assembly of domesticated dogs to the database CanFam3.1, 453 mature canine microRNAs were characterised in the database. The high-throughput data identified the range of 147-178 microRNAs in the library of IAV-infected groups (Table 9). On the other hand, 139-174 microRNAs were revealed in the library of IBV-infected groups (Table 10). MicroRNA expression was normalised by total counts of each group, and differential

expression level was then determined by identifying microRNAs that exhibited greater or lesser than 2-fold change in normalised read abundance between the seasonal influenza virus-infected and mock-infected libraries at each time point.

Table 9 Summary statistics of sequencing data obtained from MDCK cells infected with mock and seasonal IAV at different time points.

Group	Reads						Identified miRNA
	Total reads ^(a)	Small RNAs ^(b)	Annotated miRNA ^(c)	Mature 5' ^(d)	Mature 3' ^(e)	Precursor ^(f)	
A/Mock 6 hpi	473694	127596	55478	39096	10465	5917	164
A/pH1N1 6 hpi	218520	66872	27032	20279	4194	2559	151
A/H3N2 6 hpi	334733	99013	17459	10890	4446	2123	147
A/Mock 12 hpi	299794	94330	22351	14806	4716	2829	152
A/pH1N1 12 hpi	517159	132874	81048	61600	11384	8064	169
A/H3N2 12 hpi	297015	101387	12113	6794	3622	1697	147
A/Mock 24 hpi	191885	57246	27248	17911	5991	3346	155
A/pH1N1 24 hpi	491479	147056	65895	48896	10947	6052	178
A/H3N2 24 hpi	351538	117011	17747	12245	3698	1804	151

(a) Total reads aligned to CanFam3.1

(b) Reads annotated to small RNAs

(c) Unique sequences aligned to miRBase

(d) Unique sequences annotated to mature miRNAs from the 5' arm

(e) Unique sequences annotated to mature miRNAs from the 3' arm

(f) Unique sequences annotated to precursor miRNAs

Table 10 Summary statistics of sequencing data obtained from MDCK cells infected with mock and seasonal IBV at different time points.

Group	Reads						Identified miRNA
	Total reads ^(a)	Small RNAs ^(b)	Annotated miRNA ^(c)	Mature 5' ^(d)	Mature 3' ^(e)	Precursor ^(f)	
B/Mock 6 hpi	142980	53775	42440	23824	6247	12369	156
B/Victoria 6 hpi	252245	77122	85623	51530	10458	23635	164
B/Yamagata 6 hpi	133565	55384	24433	12008	5884	6541	139
B/Mock 12 hpi	223322	73817	71551	40935	9497	21119	158
B/Victoria 12 hpi	186716	60702	64329	37901	8940	17488	167
B/Yamagata 12 hpi	204628	75056	59025	34438	7633	16954	151
B/Mock 24 hpi	301204	98428	97355	58146	11471	27738	174
B/Victoria 24 hpi	202549	74715	30069	16720	5913	7436	164
B/Yamagata 24 hpi	298432	121422	50258	30019	5734	14505	147

(a) Total reads aligned to CanFam3.1

(b) Reads annotated to small RNAs

(c) Unique sequences aligned to miRBase

(d) Unique sequences annotated to mature miRNAs from the 5' arm

(e) Unique sequences annotated to mature miRNAs from the 3' arm

(f) Unique sequences annotated to precursor miRNAs

As shown in Figure 10, three microRNAs including *cfa*-miR-543, *cfa*-miR-340, and *cfa*-miR-125b were upregulated at 6, 12, and 24 hours after pH1N1 infection, respectively. On the other hand, the down-expression of 22 microRNAs was revealed upon pH1N1 infection. Among downregulated microRNAs, the expression of *cfa*-miR-1249 was decreased at 12 and 24 hpi.

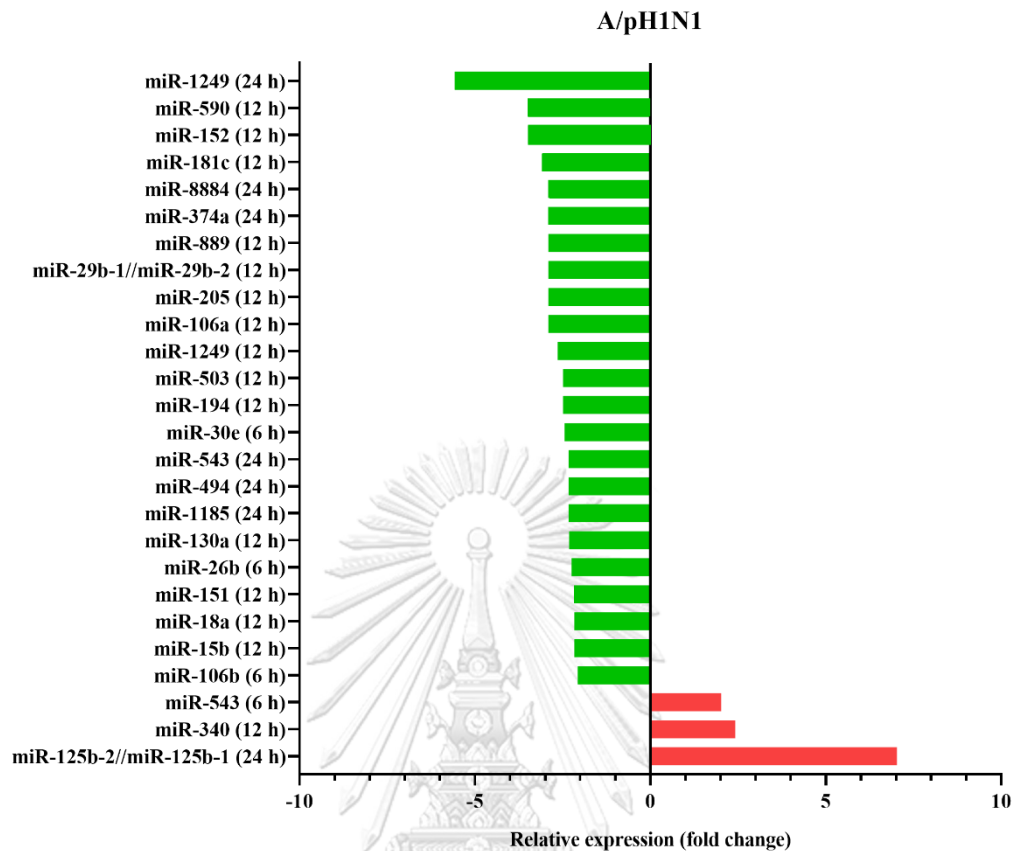


Figure 10 MicroRNA profile of MDCK cells in response to IAV pH1N1 infection.

Meanwhile, the expression of 19 microRNAs increased during the infection of H3N2 (Figure 11). Interestingly, some of the overexpressed microRNAs were demonstrated at different times after H3N2 infection. More specifically, the overexpression of *cfa*-miR-1249 was exhibited at both 6 and 24 hpi, whereas that of *cfa*-miR-146b was found at 6 and 12 hpi. In addition, the expression level of *cfa*-miR-215 rose up at 12 and 24 hpi. In contrast, thirteen microRNAs were downregulated upon H3N2 infection. Among those, the expression of *cfa*-miR-18a decreased at 6 and 24 hpi.

In response to the infection of IBV Victoria lineage (Figure 12), 27 upregulated microRNAs and 14 downregulated microRNAs were expressed. Among these dysregulated microRNAs, the expression of *cfa*-miR-181a increased at 12 and 24 hpi, whereas that of *cfa*-miR-181c decreased at 6 and 24 hpi. During IBV Yamagata lineage infection (Figure 13), high-throughput sequencing revealed that the expression of 14 microRNAs increased and that of 5 microRNAs decreased.

Since we hypothesized that some of host microRNAs could target on viral genomes, upregulated microRNAs were the scope of this study. Intriguingly, next-generation sequencing revealed some of the microRNAs were upregulated upon different influenza virus infections (Figure 14A). For instance, *cfa*-miR-340 was also upregulated at 12 hpi upon infection with different IAV subtypes – pH1N1 and H3N2. On the other hand, the over-expression of *cfa*-miR-361, *cfa*-miR-1841, *cfa*-miR-1842, and *cfa*-miR-330 were shown during infection with different IBV lineages – Yamagata and Victoria lineages. In addition, two microRNAs including *cfa*-miR-129 and *cfa*-miR-1249 were upregulated upon infection of either H3N2 or B/Victoria influenza virus. Furthermore, *cfa*-miR-197, *cfa*-miR-215, and *cfa*-miR-339-1 were overexpressed when the cells were infected with A/H3N2, B/Victoria, or B/Yamagata influenza virus. The upregulated *cfa*-miR-146b was found in H3N2 or B/Yamagata-infected cells. However, the expression of *cfa*-miR-146b was shown increased by greater than 1.5-fold in pH1N1-infected cells as compared to mock infection.

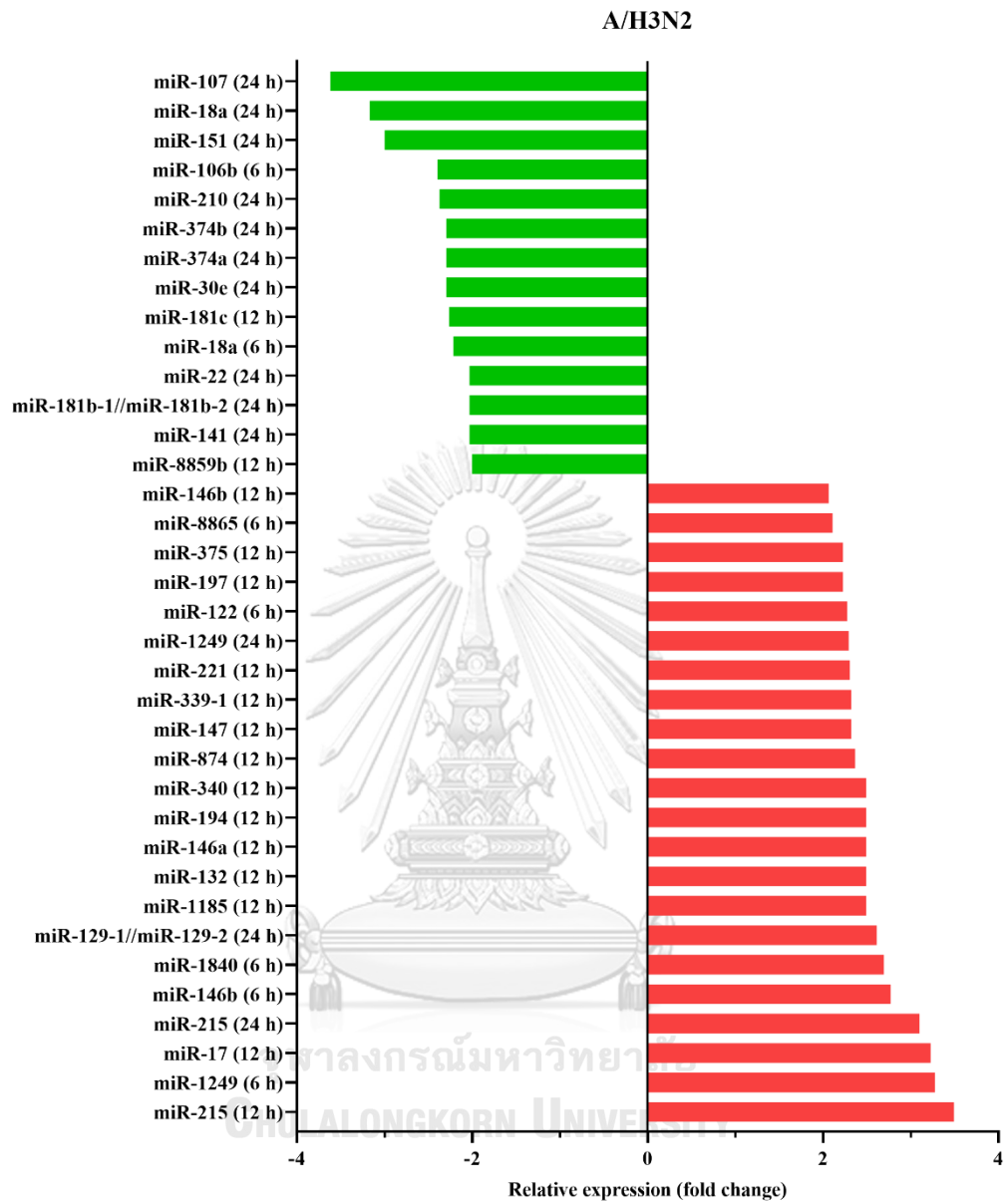


Figure 11 MicroRNA profile of MDCK cells in response to IAV H3N2 infection.

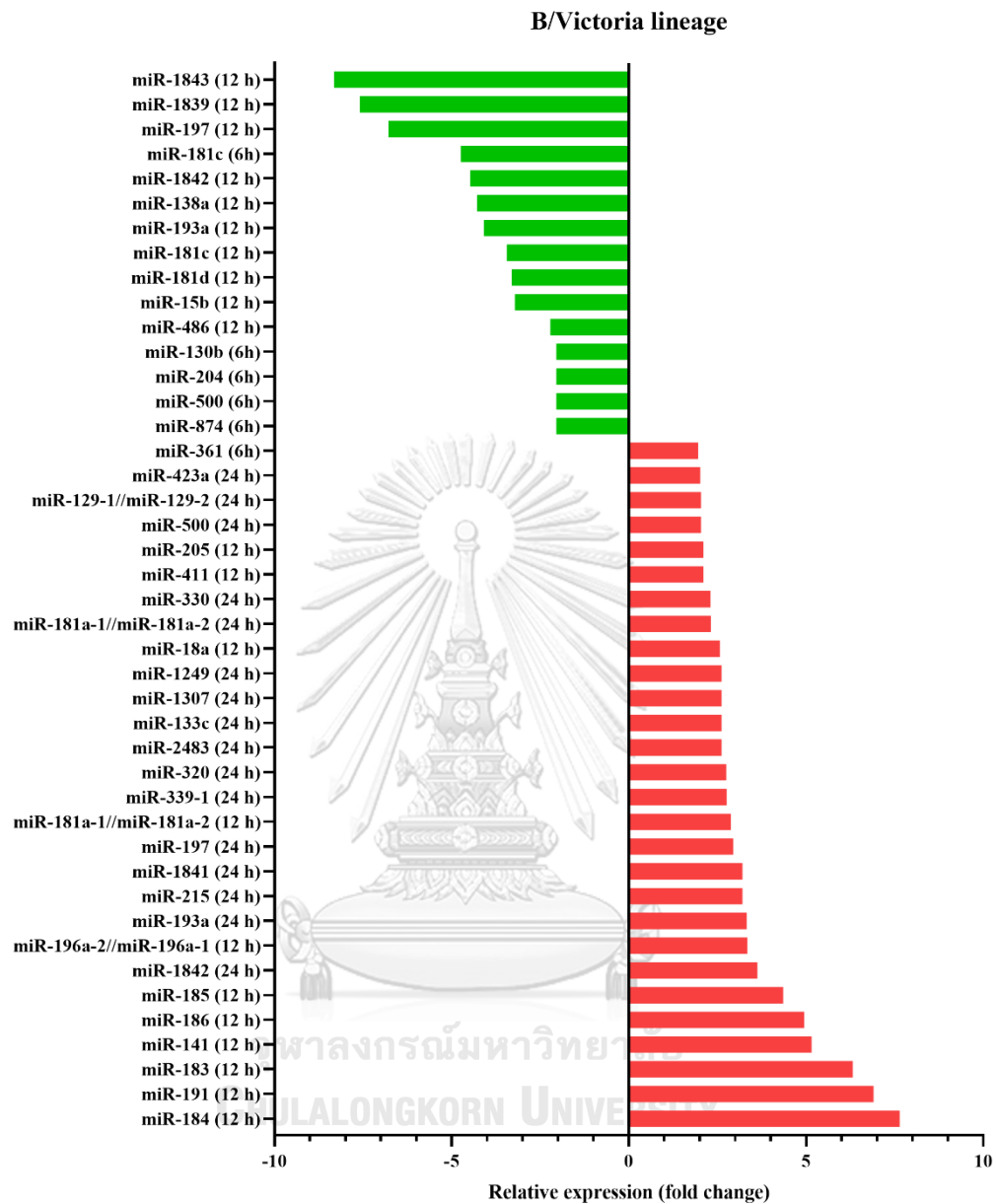


Figure 12 MicroRNA profile of MDCK cells in response to IBV Victoria infection.

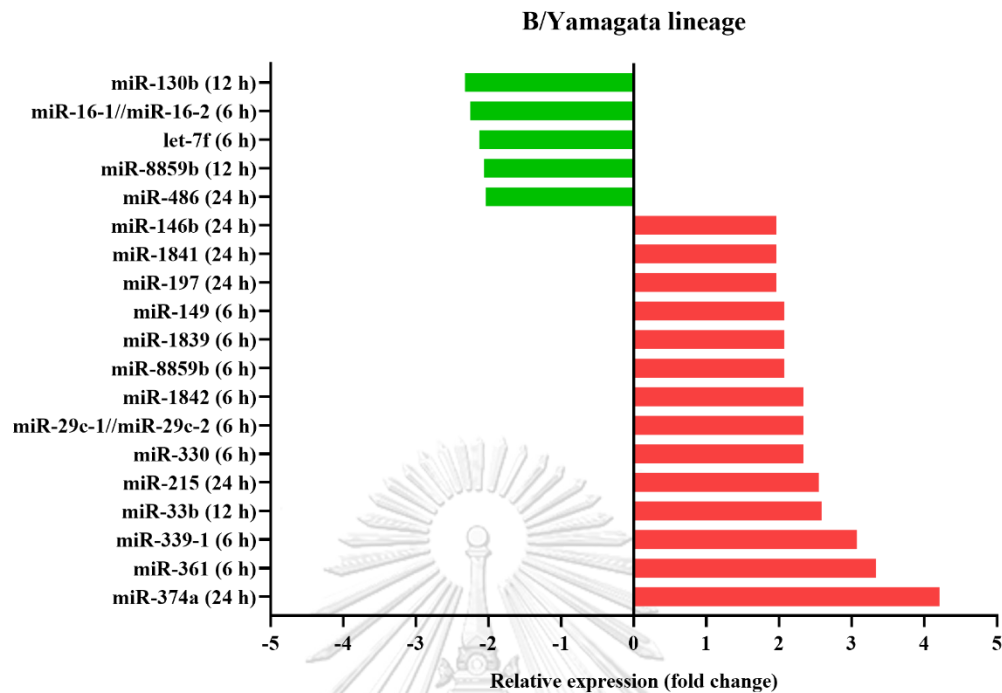
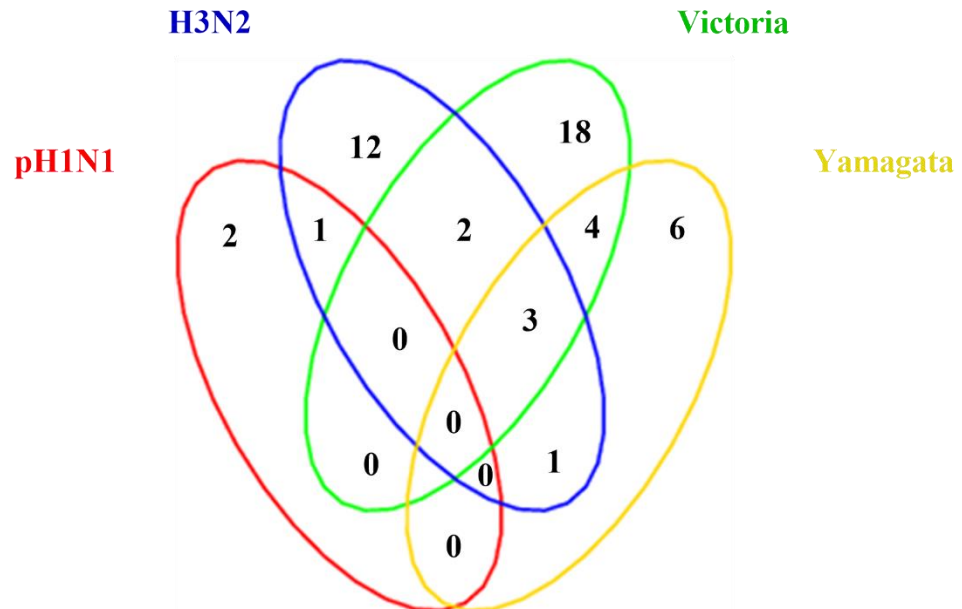


Figure 13 MicroRNA profile of MDCK cells in response to IBV Yamagata infection.

On the other hand, downregulation of some microRNAs was revealed in the cells infected with different influenza virus strains (Figure 14B). For instance, *cfa*-miR-181c was down-modulated upon infection of IAV pH1N1, H3N2, and IBV Victoria lineage. While *cfa*-miR-374a, *cfa*-miR-30e, *cfa*-miR-151, *cfa*-miR-18a, and *cfa*-miR-106b were down-expressed in the cells infected with different IAV subtypes, the expression level of *cfa*-miR-486 and *cfa*-miR-130b was decreased in the cells infected with different lineages of IBV. In addition, down-expression of *cfa*-miR-8859b was found upon infection of either IAV H3N2 or IBV Yamagata. The expression level of *cfa*-miR-15b was decreased in the cells infected with IAV pH1N1 or IBV Victoria lineage.

A. Up-regulation



B. Down-regulation

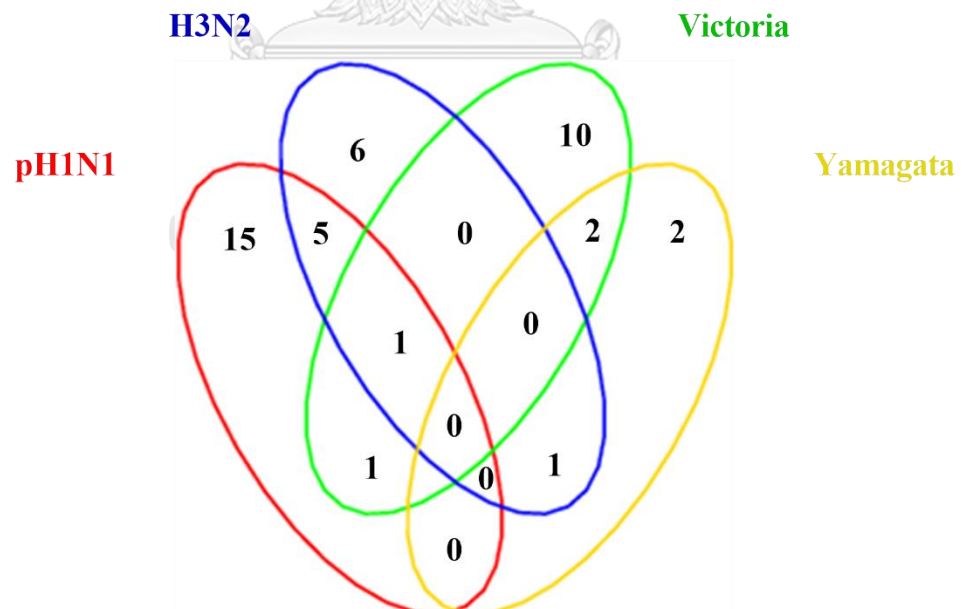


Figure 14 Venn Diagram shows (A) upregulated and (B) downregulated microRNAs of MDCK cells upon different strains of seasonal influenza infection.

4.2. Validation of MicroRNA Profiles

The alteration of expression patterns was further verified for a subset of the NGS-identified microRNAs. Prior to reverse transcription with stem-loop polyA, extracted microRNAs were tailed by polyU polymerase. Afterwards, cDNAs were analysed using SYBR[®] Green-based qPCR, and normalised expression levels of the influenza virus-infected groups were then differentially compared to those of mock-infected groups at each time point. *Cfa*-miR-543, miR-340, and miR-125b were all validated as highly expressed upon infection with pH1N1 viruses (Figure 15A). Notably, most of the tested microRNAs, except *cfa*-miR-125b, were upregulated, demonstrating a high correlation between microRNA expression levels detected by next-generation sequencing and by RT-qPCR analysis.

In H3N2-infected groups, some of the upregulated microRNAs identified by NGS were verified due to limitation of RT-qPCR condition (Figure 15B). The results showed that validated microRNAs were mostly overexpressed, with the exception of *cfa*-miR-339-1 at 12 hpi and *cfa*-miR-1249 at 24 hpi. *Cfa*-miR-340 showed the highest expression level, followed by *cfa*-miR-1249 (6 hpi), miR-122, miR-146b (6 hpi), and miR-132, respectively. In addition, two upregulated microRNAs were validated at more than one-time point. *Cfa*-miR-146b was over-expressed at 6 and 12 hpi, whereas *cfa*-miR-215 was upregulated at 12 and 24 hpi. Altogether, these results

indicated that data from the library sequencing analyses veraciously reflect microRNAs responded to the infection of pH1N1 and H3N2 viruses.

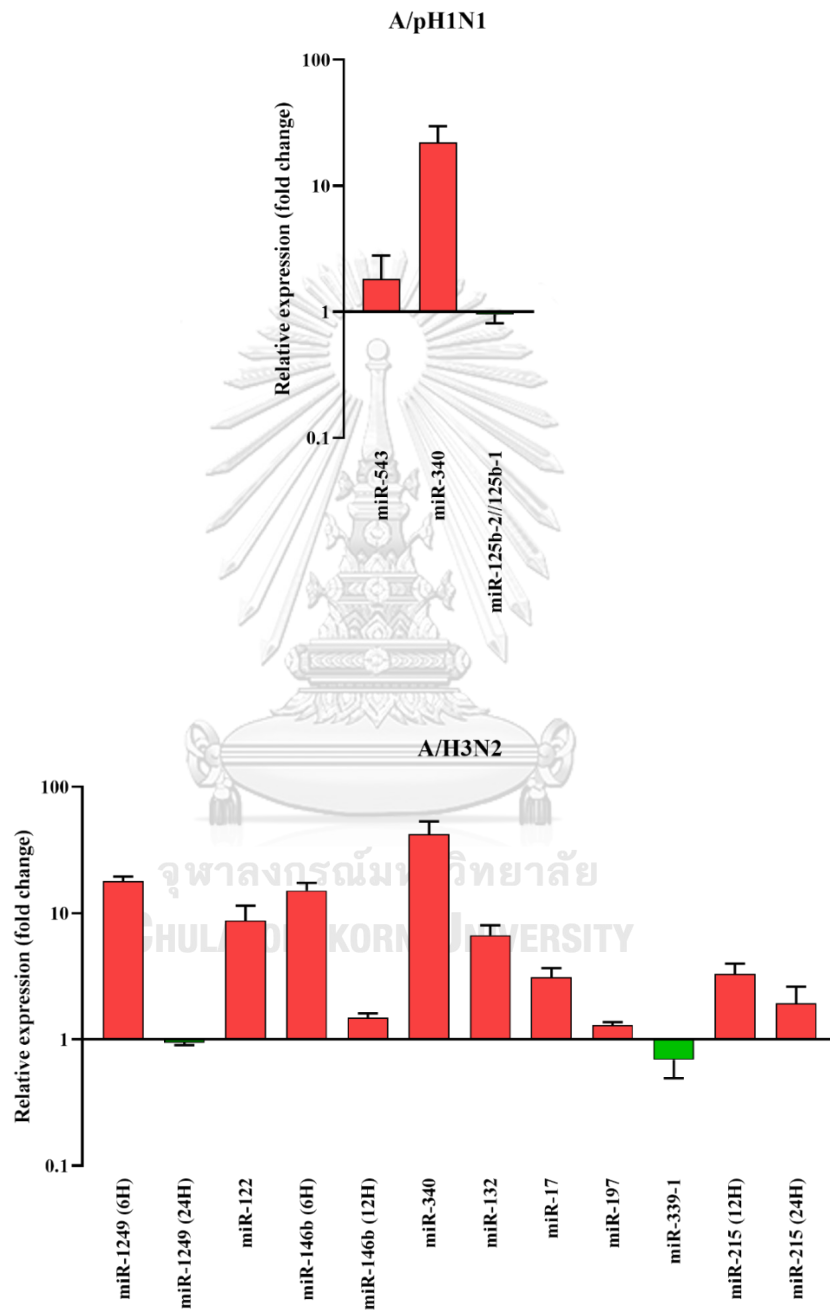


Figure 15 Validation of upregulated microRNAs during IAV infection

(A) pH1N1 and (B) H3N2.

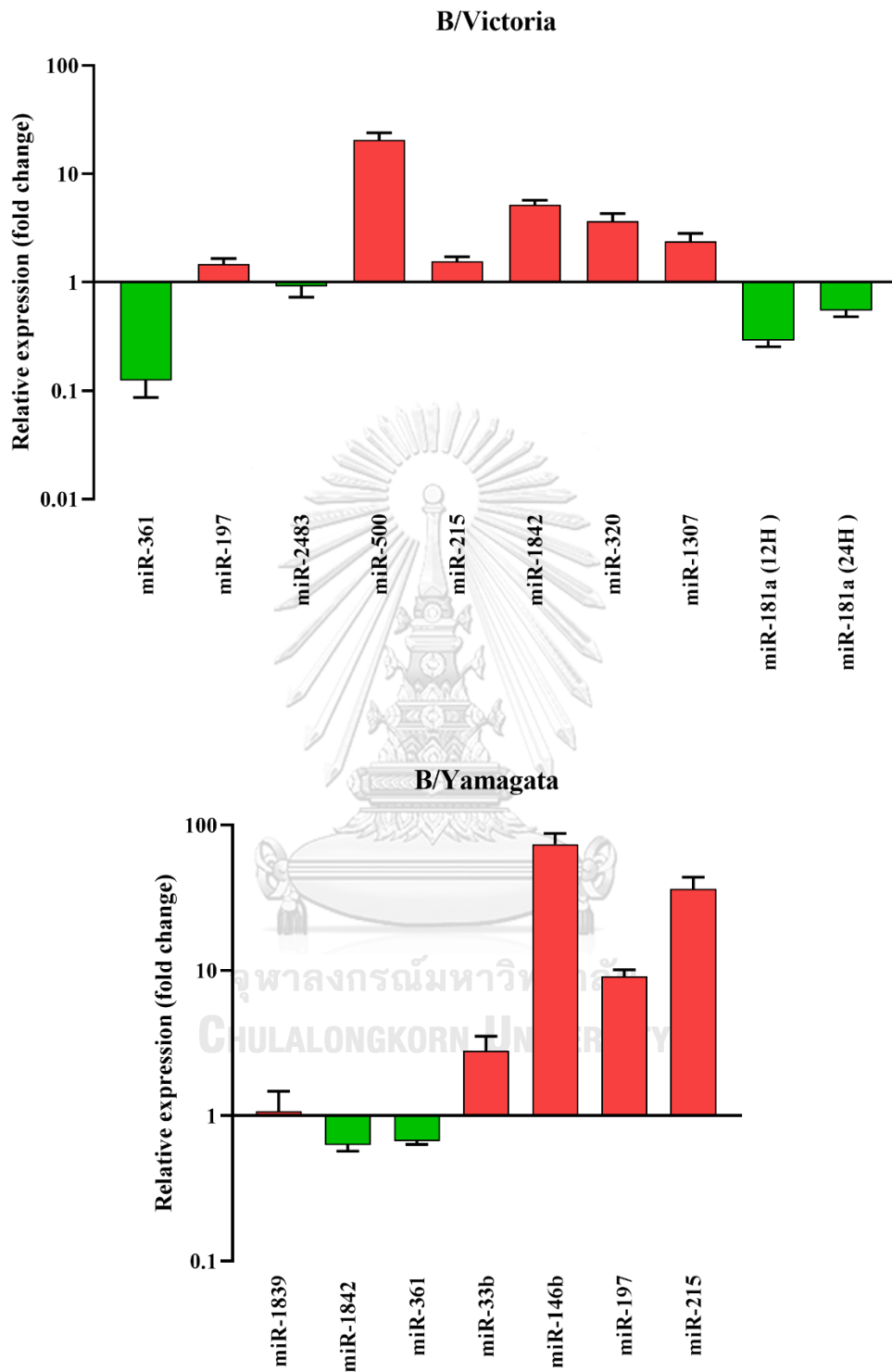


Figure 16 Validation of upregulated microRNAs during IBV infection.

(A) Vicotoria and (B) Yamagata.

For IBV Victoria infection (Figure 16A), nine microRNAs from NGS screening were validated by RT-qPCR. The result exhibited that *cfa*-miR-197, *cfa*-miR-215, *cfa*-miR-320, *cfa*-miR-500, *cfa*-miR-1307, and *cfa*-miR-1842 were overexpressed upon infection of Victoria lineage. However, *cfa*-miR-181a, *cfa*-miR-361 and *cfa*-miR-2483 were not validated. Furthermore, most of the validated microRNAs in B/Yamagata-infected groups, but not *cfa*-miR-361 and *cfa*-miR-1842, demonstrated an increasing trend (Figure 16B). The expressions of *cfa*-miR-146b, *cfa*-miR-215, and *cfa*-miR-197 were the three most upregulated genes in B/Yamagata groups. As a result, these data showed microRNA profiles gained from NGS was consistent with the expression validated by RT-qPCR.

Based on NGS screening and RT-qPCR validation, common canine microRNAs in response to the infection of seasonal influenza viruses were summarised in Table 11. Some microRNAs of our interest were reliant on most common overexpression upon infection with different subtypes. Unfortunately, there were no universal microRNAs which were overexpressed in all four strains of the seasonal influenza viruses. However, the results showed that four microRNAs including *cfa*-miR-146b, *cfa*-miR-197, *cfa*-miR-215, and *cfa*-miR-340 were most commonly upregulated during seasonal influenza infections. The expression of *cfa*-miR-340 was increased at 12 hpi upon different IAV infections. Moreover, *cfa*-miR-197 and *cfa*-miR-215 were upregulated when the MDCK cells infected with either

H3N2, Victoria, or Yamagata. Additionally, NGS screening demonstrated that the expression of *cfa*-miR-146b was increased by greater than 1.5-fold in pH1N1-infected cells as compared to the mock-infected group. Besides, the upregulated *cfa*-miR-146b could be found in H3N2 or B/Yamagata-infected cells.

Table 11 Summary of common microRNA validation.

MicroRNA	Time Points (Hours Post Infection)				Validation by RT-qPCR
	pH1N1	H3N2	Victoria	Yamagata	
mir-340	12	12			Valid
mir-146b	(24)	6, 12		24	Valid
mir-215		12, 24	24	24	Valid
miR-197		12	24	24	Valid
mir-1249		6, 24	24		Invalid (H3N2)
miR-339-1		12	24	6	Invalid (H3N2)
miR-1842			24	6	Invalid (Yamagata)
miR-361			6	6	Invalid
miR-129-1//miR-129-2		24	24		ND
miR-1841			24	24	ND
miR-330			24	6	ND

Note: ND – Not Determined due to limitation of RT-qPCR conditions.

4.3. Effect of Candidate MicroRNAs Expression on Viral Propagation Yield

When the validated microRNAs were considered among the groups infected with different influenza viruses (Table 11), *cfa*-miR-215 and *cfa*-miR-197 were over-

expressed in A/H3N2-, B/Victoria-, and B/Yamagata-infected groups. Moreover, *cfa*-miR-146b was upregulated in A/H3N2- and B/Yamagata-infected groups. In addition, the expression of *cfa*-miR-340 was increased in both A/pH1N1 and A/H3N2 infected groups. Taken together, *cfa*-miR-146b, *cfa*-miR-197, *cfa*-miR-215 were shown as promising microRNAs in the manipulation of IAV and IBV propagations. Moreover, *cfa*-miR-340 was shown as a candidate microRNA in IAV production. Mechanistically, these four microRNAs may target viral genomes. Therefore, microRNA inhibitors may antagonize the effect of candidate microRNAs, resulted in the enhancement of virus propagation. MDCK cells were transfected with either microRNA inhibitors or microRNA overexpressing plasmids, followed by infection of each influenza virus strain. The yield of each virus was determined by RT-qPCR and ELISA assay.

As seen in Figure 17, the effect of candidate microRNA inhibition and overexpression on IAV pH1N1 replication was determined. The results showed that *cfa*-miR-146b and *cfa*-miR-215 inhibitors significantly increased the copy number of pH1N1 M gene by around 3.3-fold and 1.7-fold, respectively (Figure 17A). In addition, the result gained from ELISA was consistent with RT-qPCR, confirming that *cfa*-miR-146b and *cfa*-miR-215 inhibitors enhanced the yield of pH1N1 (Figure 17B). In contrast, the amount of pH1N1 viral gene were dramatically decreased when the cells were treated with vectors overexpressing *cfa*-miR-146b and *cfa*-miR-215

(Figure 17C). Furthermore, overexpression of *cfa*-miR-146b and *cfa*-miR-215 reduced the viral titre (Figure 17D). Although *cfa*-miR-197 and *cfa*-miR-340 suppressed the yields of pH1N1 (Figure 17C and D), the enhancing effect was not exhibited in the cells treated with *cfa*-miR-197 and *cfa*-miR-340 inhibitors (Figure 17A and B). Therefore, the role of these two microRNAs in pH1N1 propagation was unclear. These results suggest that *cfa*-miR-146b and *cfa*-miR-215 could inhibit pH1N1 replication, and the suppressive effect may be resolved with microRNA inhibitors.



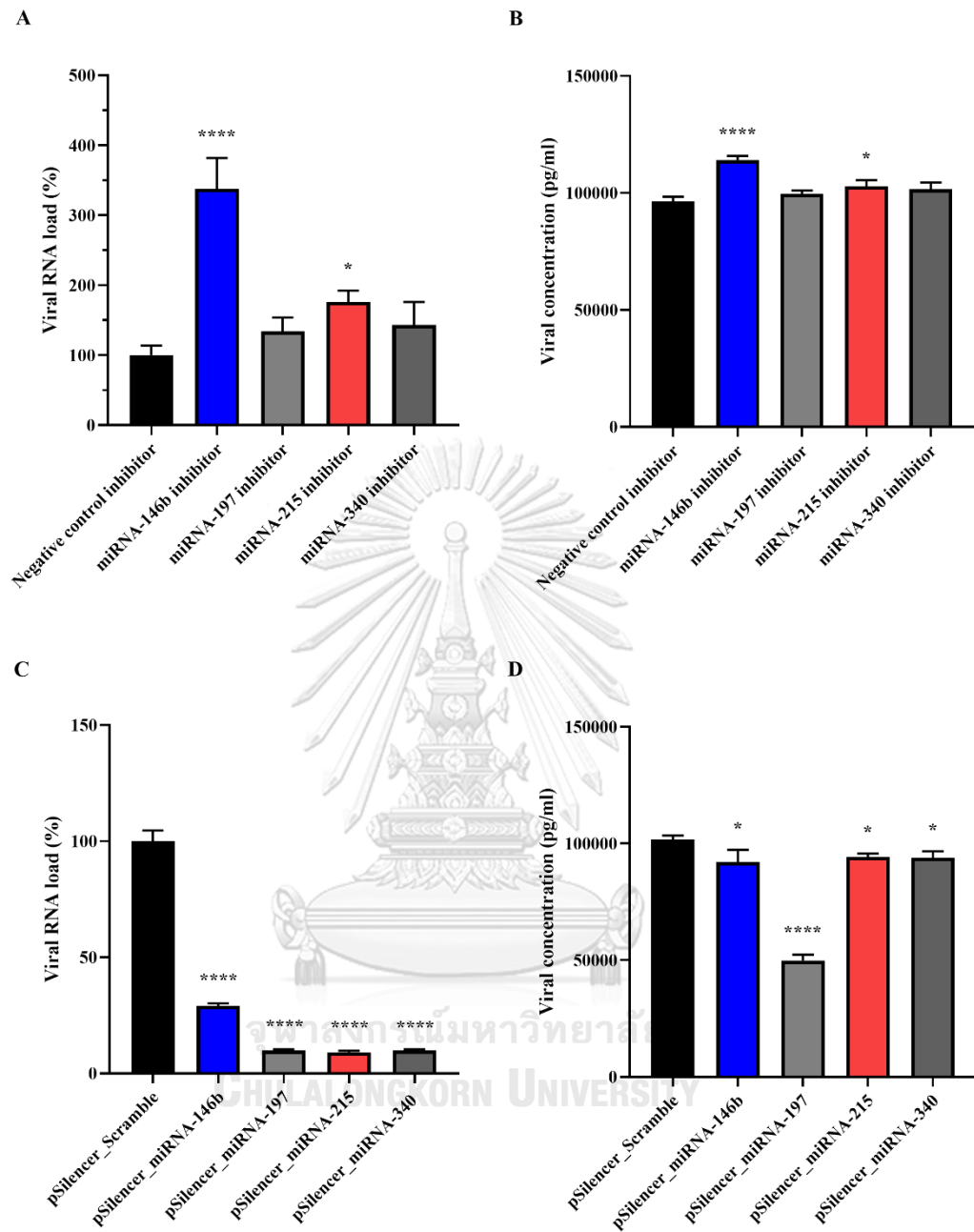


Figure 17 Effect of candidate microRNAs on the yield of IAV pH1N1 was determined by RT-qPCR (A and C) and ELISA assay (B and D) ($p \leq 0.05$ is designated as *; $p \leq 0.0001$ is designated as ****).

As shown in Figure 18, the efficiency of propagation of H3N2 virus in the modified MDCK cells was also investigated by RT-qPCR and ELISA assay. The amount of H3N2 viral gene from *cfa*-miR-197 inhibitor-treated group was significantly increased by approximately 2.5-fold (Figure 18A). Moreover, there was a 1.5-fold increase in viral titer after the cells had been treated with *cfa*-miR-197 inhibitor (Figure 18B). On the other hand, overexpression of *cfa*-miR-197 could markedly decrease the number of H3N2 gene by roughly 70% compared to the scramble control group (Figure 18C). Moreover, the ELISA result also exhibited decreasing trend in the cells treated with *cfa*-miR-197 (Figure 18D). Although *cfa*-miR-215 inhibitor increased the viral titer (Figure 18A), the suppressive effect was not demonstrated in the cells treated with vector overexpressing *cfa*-miR-215 (Figure 18C and D). Therefore, the function of *cfa*-miR-215 on H3N2 propagation was unclear. Altogether, the results suggest that the yield of H3N2 may be enhanced by the inhibition of *cfa*-miR-197.

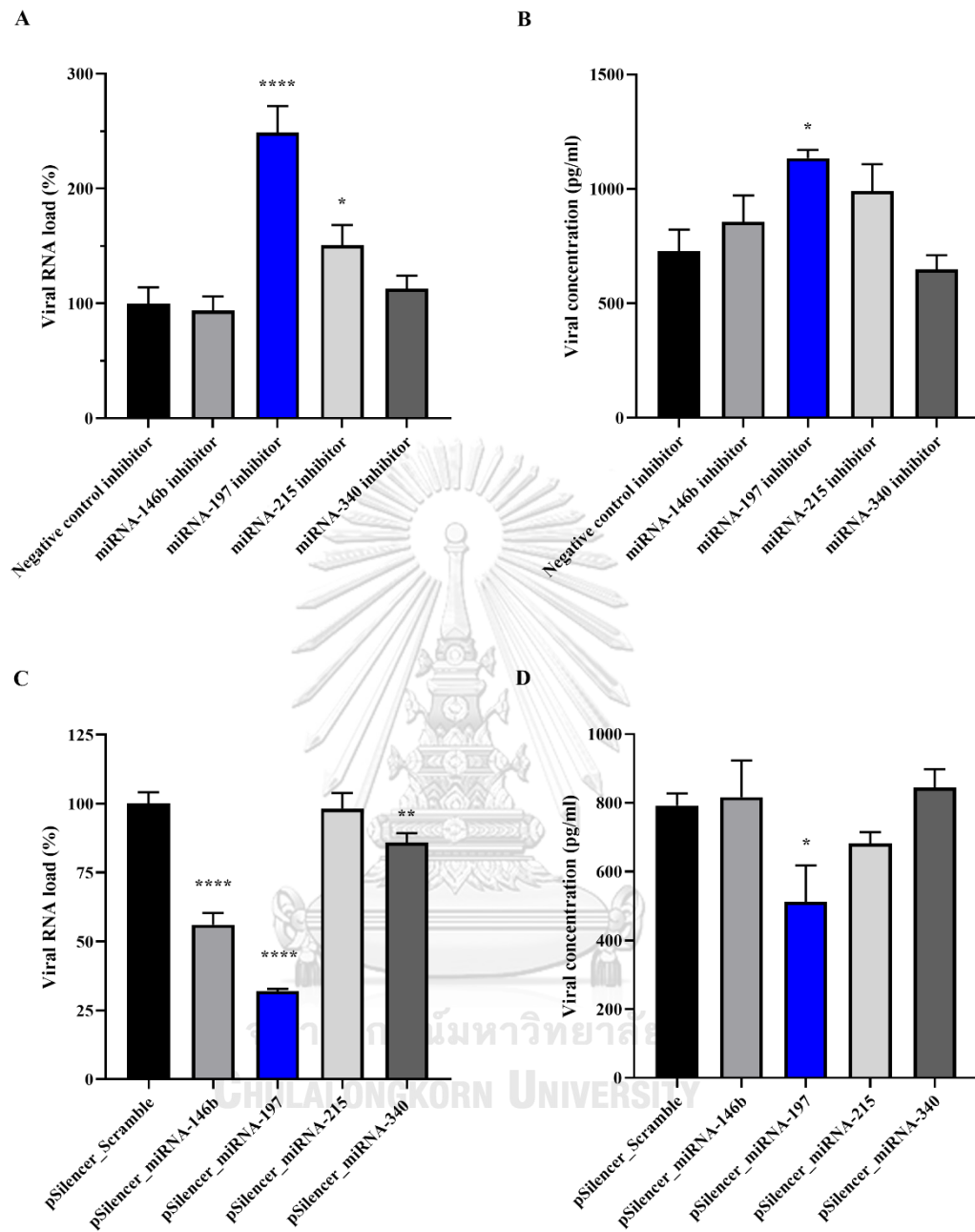


Figure 18 Effect of candidate microRNAs on the yield of IAV H3N2 was determined by RT-qPCR (A and C) and ELISA assay (B and D) ($p \leq 0.05$ is designated as *; $p \leq 0.01$ is designated as **; $p \leq 0.0001$ is designated as ****).

In addition to IAV propagation, the effect of microRNA on IBV production was investigated. It can be seen from Figure 19 that the amount of B/Victoria viral RNA increased by up to 1.5-fold after the cells had been treated with *cfa*-miR-215 inhibitor (Figure 19A). Moreover, the result obtained from ELISA analysis demonstrated that *cfa*-miR-215 inhibitor could significantly increase viral titre when compared to the negative control inhibitor (Figure 19B). Conversely, the copy number of the viral gene was reduced in the *cfa*-miR-215 over-expressing cells (Figure 19C). A significant decrease in viral titre was observed when the cells were overexpressed with *cfa*-miR-215 (Figure 19D). As a result, the antagonistic function of *cfa*-miR-215 inhibitor increased the viral yield of B/Victoria lineage.

To determine the effect of candidate microRNAs on replication of IBV Yamagata, RT-qPCR and ELISA were performed (Figure 20). The results showed that the amount of B/Yamagata viral RNA from *cfa*-miR-146b inhibitor-treated group increased by 1.45-fold as compared to that from the scramble control group (Figure 20A). In addition, *cfa*-miR-146b enhanced viral titre (Figure 20B). In contrast, overexpression of *cfa*-miR-146b significantly reduced viral titre when compared to the scramble control group (Figure 20D). Therefore, the results suggested that the yield of IBV Yamagata is increased by the suppression of *cfa*-miR-146b.

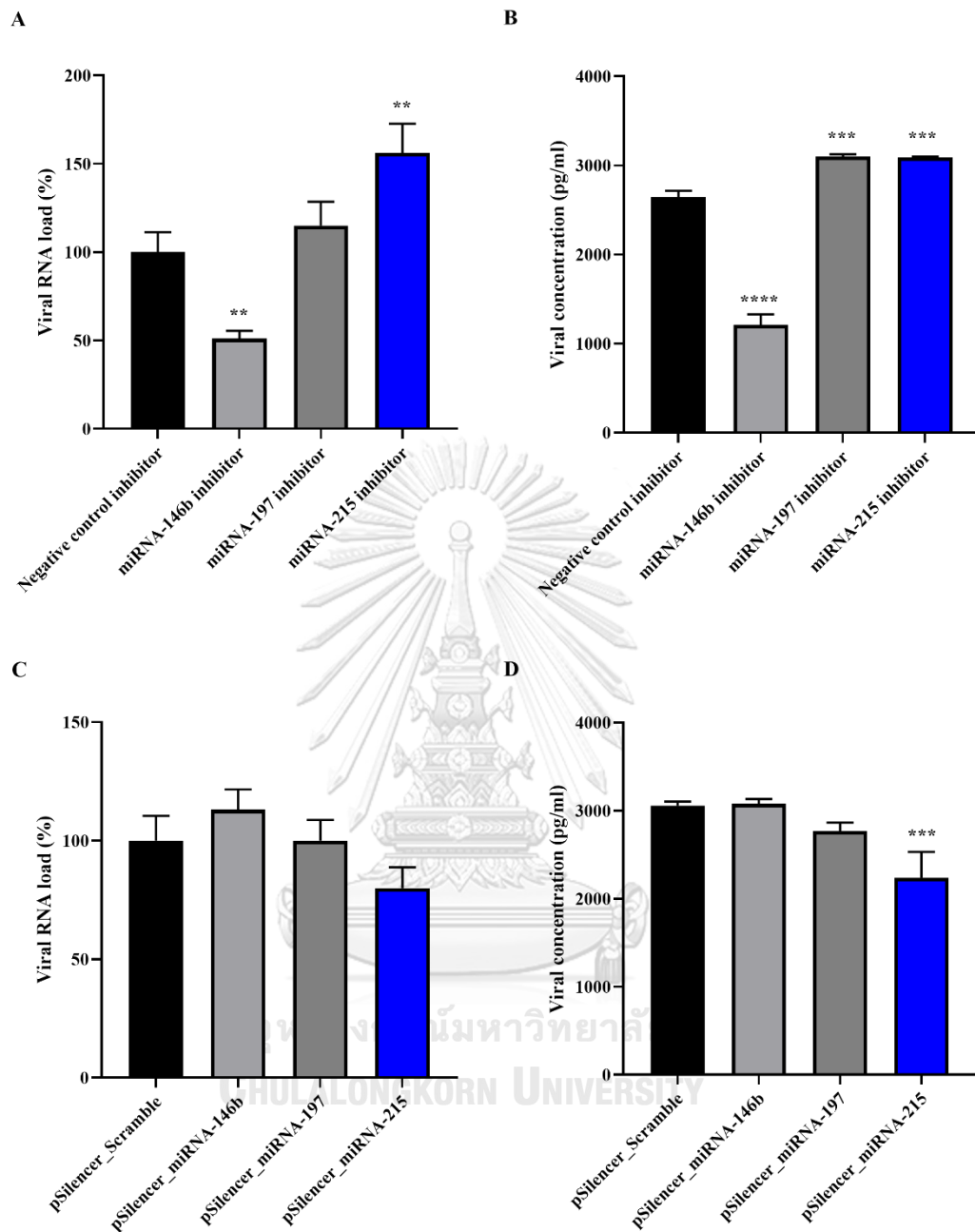


Figure 19 Effect of candidate microRNAs on the yield of IBV Victoria was determined by RT-qPCR (A and C) and ELISA assay (B and D) ($p \leq 0.01$ is designated as **; $p \leq 0.001$ is designated as ***; $p \leq 0.0001$ is designated as ****).

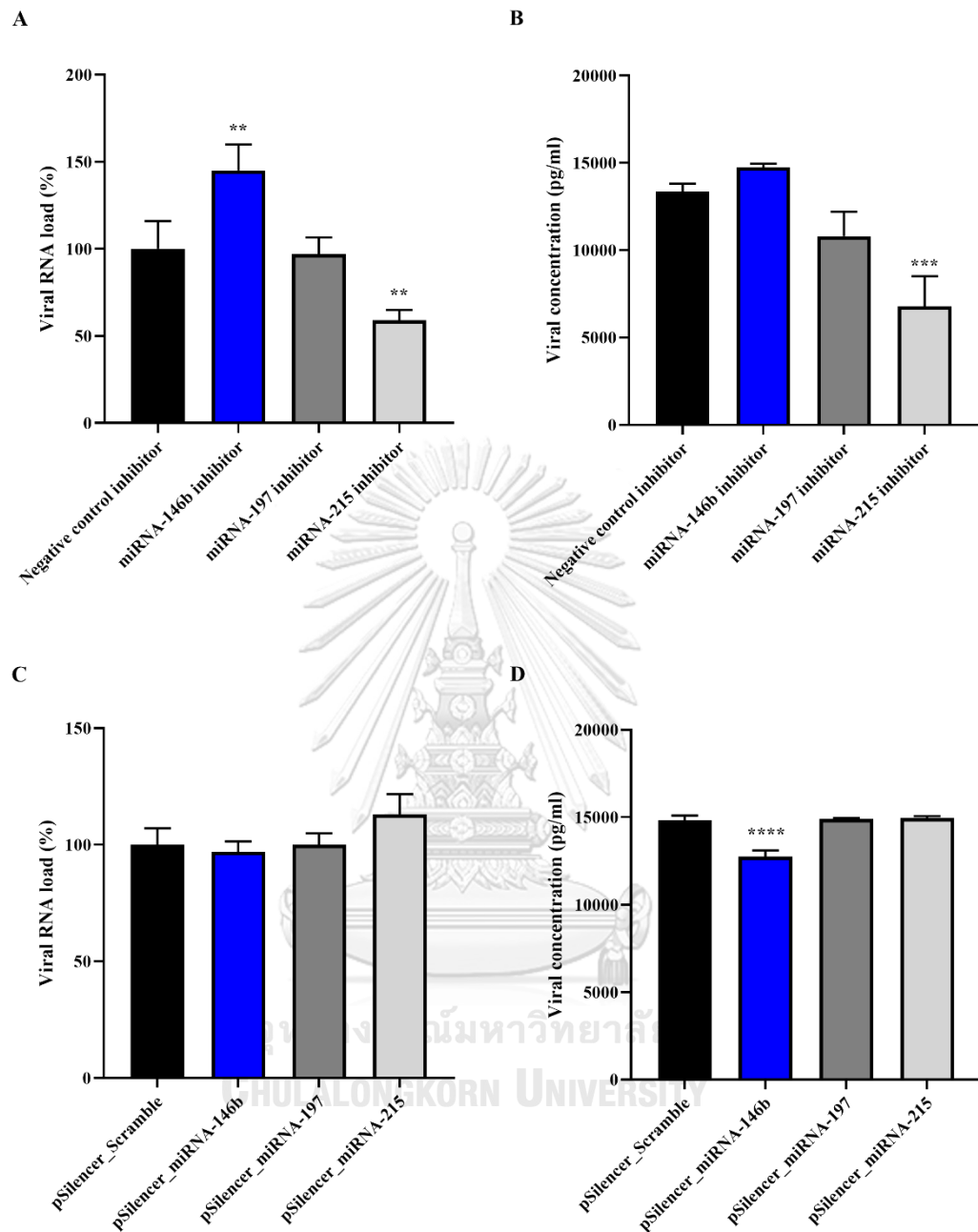


Figure 20 Effect of candidate microRNAs on the yield of IBV Yamagata was determined by RT-qPCR (A and C) and ELISA assay (B and D) ($p \leq 0.01$ is designated as **, $p \leq 0.001$ is designated as ***, $p \leq 0.0001$ is designated as ****).

It is suggested that to increase the production of pH1N1 and B/Yamagata viruses, *cfa*-miR-146b is a candidate target of microRNA inhibitor. *Cfa*-miR-215 could be another good candidate for enhancing pH1N1 and B/Victoria viral production. On the other hand, the microRNA inhibitor which targets *cfa*-miR-197 would be useful for the propagation of the H3N2 virus. Based on our results, microRNAs tended to target viral genes in a strain-specific manner, and the candidate microRNAs could target viral genomes, and result in suppression of viral replication.

4.4. Computational Prediction of Seasonal Influenza Viral Genomes Targeted by Canine MicroRNAs

According to viral quantification by RT-qPCR and ELISA, the treatments with *cfa*-miR-146b inhibitor enhanced the yields of IAV pH1N1 and IBV Yamagata. *Cfa*-miR-215 inhibitor increased the production of IAV pH1N1 and IBV Victoria. Moreover, *cfa*-miR-197 inhibitor facilitated the propagation of IAV H3N2. Therefore, it is suggested that these microRNA inhibitors may antagonise the inhibitory effect of such microRNAs on viral propagation. MicroRNA-binding sites on viral genomes remain to be investigated.

To predict the target sites, two web-based programs including miRBase, and RNAhybrid were used on the basis of hybridization patterns between the microRNAs and viral genomes. As shown in Table 12, *cfa*-miR-146b targeted three genes of IAV pH1N1 including PB2 (the position 1979), PB1 (the position 2191), and NA (the position 693). In addition, *cfa*-miR-146b inhibited the replication of IBV Yamagata

by targeting one site on the PA gene (the position 534) and two sites on the NP gene (the position of 973 and 1290).

Table 12 *In silico* analysis of microRNA target prediction.

Viruses	miRNAs	Target genes (position)	Hybridization pattern between miRNA (bottom strand) and target gene (top strand)	MPE kcal/mol
A/pH1N1	miR-146b	PB2 (1979)	5' A AACCAAAC C A G 3' GGC GA UU CAGUUCUU UCG CU AA GUCAAGAG 3' GAUAC U U 5'	-17.4
		PB1 (2191)	5' G GAC AAGAAAGAAG U 3' AGUCUG GGA UC AGUUCUC UCGGAU CCU AG UCAAGAG 3' A UA U 5'	-21.4
		NA (693)	5' U A UAAAU G 3' GC UGUG GGUUCUU CG AUAC UCAAGAG 3' U G CUUAAG U 5'	-16.3
	miR-215	PB2 (350)	5' C U AAA A 3' UUA UUCG AGGUCG AGU AAGC UCCAGU 3' ACAGAU U A A 5'	-16.7
		PB1 (2155)	5' G GGGCCCGGA GCCA A 3' UGUCUA UUGAU GGGUCG ACAGAU AGUUA UCCAGU 3' AGCA A 5'	-18.8
		miR-197	PB2 (865)	5' A C AC A C 3' UUGG GGA AAGG UGGUGGA GACC CCU UUCC ACCACUU 3' C CA C 5'
B/Victoria	miR-215	PB2 (1447)	5' A UGGAU AUACUCCAGUACAGA U 3' UGGGUG GA GAGGGUGGUGG ACCCAC CU CUUCCACCACU 3' CG U 5'	-29.8
		PB1 (2101)	5' A GC UACAGGAAGCCA A 3' GU AUCA GUGGGUCA CA UAGU CAUCCAGU 3' A GA UAAG A 5'	-19.8
		HA (98)	5' C C GGGG A 3' UG CUA UCAA AGGUCA AC GAU AGUU UCCAGU 3' A AAGCA A 5'	-19.2
B/Yamagata	miR-146b	NP (617)	5' A CAA A 3' UGUCUGUU UC AGGUCA ACAGAUAG AG UCCAGU 3' UUA CA A 5'	-22.4
		PA (534)	5' A CA U 3' CCUAUGG AGUUCUCA GGAUACC UCAAGAGU 3' UC UUAAG 5'	-26.2

Viruses	miRNAs	Target genes (position)	Hybridization pattern between miRNA (bottom strand) and target gene (top strand)	MPE kcal/mol
		NP (973)	<pre> 5' A CUC C GCAAAG C 3' GGCC UGUGG GA UGGUUCUU UCGG AUACC UU GUCAAGAG 3' U 5' </pre>	-21.0
		NP (1290)	<pre> 5' U C C U 3' CUU UGGAA UCGGUUUUC GGA ACCUU AGUCAAGAG 3' UC U A U 5' </pre>	-23.0

On the other hand, the computational analysis revealed that two positions on IAV pH1N1 such as PB2 gene (the position 350) and PB1 gene (the position 2155) were direct targets of *cfa*-miR-215. Furthermore, *cfa*-miR-215 could bind to three sites of IBV Victoria including PB1 (the position 2101), HA (the position 98), and NP (the position 617). For IAV subtype H3N2, *in silico* target prediction demonstrated that *cfa*-miR-197 could target two locations on the PB2 gene including the positions of 865 and 1447.

4.5. MicroRNA Target Sites Validation

To confirm whether the predicted sites on influenza viral genomes were putative targets of candidate microRNAs in MDCK cells, luciferase reporter assays were conducted at 48 hours after co-transfection of pmirGLO containing viral sequences and pSilencer encoding microRNA mimic (Figure 21). For silencing control, pSilencer_siLuc2 was constructed to inhibit the expression of *Luc2* gene which is the reporter gene in pmirGLO. On the other hand, pSilencer_Scramble was used as a non-targeting control. All constructed vectors were confirmed by Sanger sequencing.

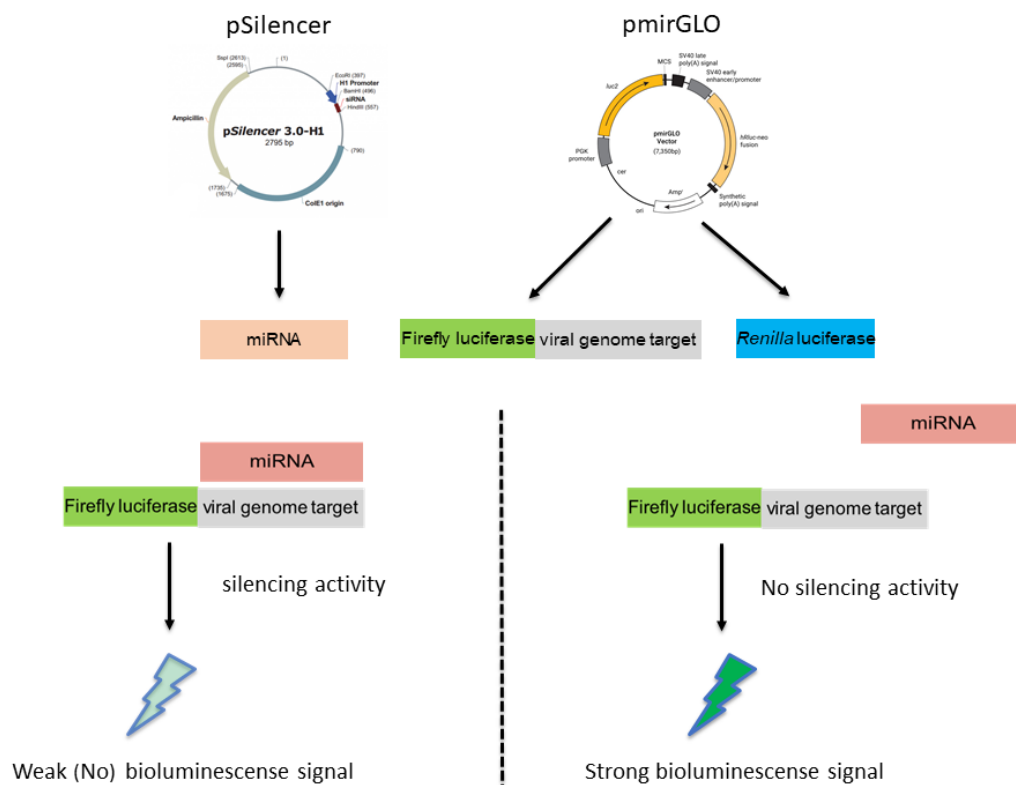
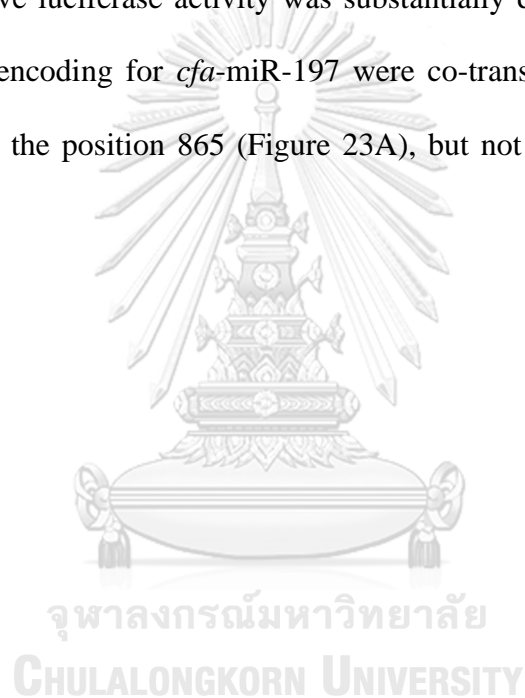


Figure 21 Schematic diagram of luciferase reporter assay for target site validation. pSilencer and pmirGLO were co-transfected into the cells for encoding microRNA and viral genome target tagged with firefly luciferase, respectively. Silencing luciferase activity indicates that microRNA could specifically bind to its target, and negatively control gene expression.

According to *in silico* analysis of microRNA targets, *cfa*-miR-146b had three target sites on IAV pH1N1 (Figure 22A-C). In addition, pH1N1 also contained two positions which could be targeted by *cfa*-miR-215 (Figure 22D-E). As can be seen in Figure 22B, relative luciferase activity was significantly decreased ($p \leq 0.05$) when the pmirGLO containing PB1 gene was co-transfected with silencing vectors encoding for *cfa*-miR-146b. Although luciferase activity involved in the other two target sites on PB2 (Figure 22A) and NA (Figure 22C) were also significantly reduced

, luciferase activity of pSilencer_SiLuc2 was not significantly decreased. As a result, PB1 gene of IAV pH1N1 was a putative target of *cfa*-miR-146b. Besides, *cfa*-miR-215 targeted the PB1 (Figure 22D), but not the NP gene (Figure 22E) of IAV pH1N1 since a significant decrease in luciferase activity was observed ($p \leq 0.01$).

For IAV subtype H3N2, the computational analysis showed that there were two binding sites on PB2 gene which might be targeted by *cfa*-miR-197. The results showed that relative luciferase activity was substantially decreased ($p \leq 0.01$) when silencing vectors encoding for *cfa*-miR-197 were co-transfected with the pmirGLO containing PB2 at the position 865 (Figure 23A), but not the position 1447 (Figure 23B).



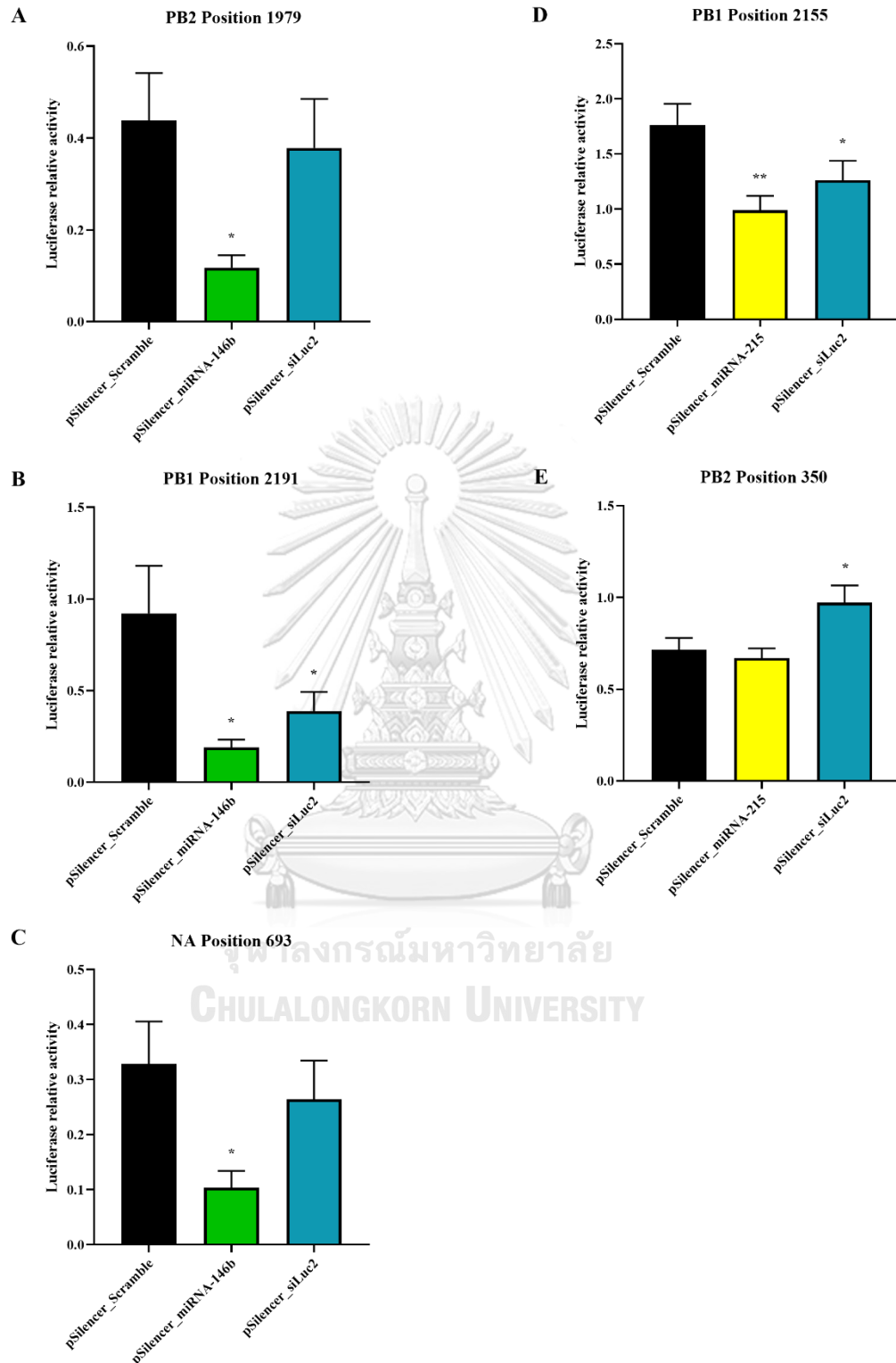


Figure 22 Luciferase assay was assessed for microRNA targets on IAV pH1N1

($p \leq 0.05$ is designated as *; $p \leq 0.01$ is designated as **).

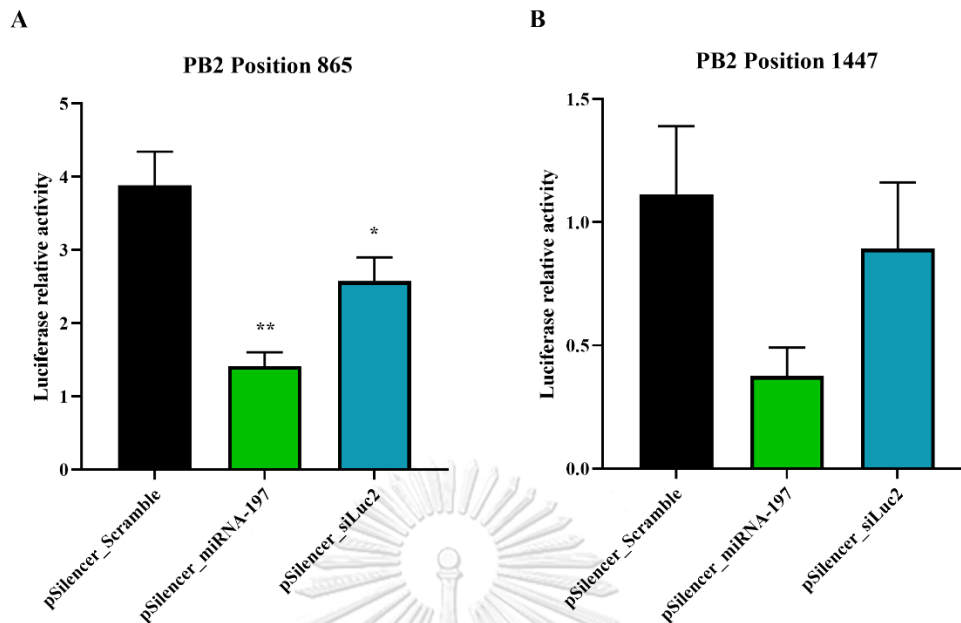


Figure 23 Luciferase assay was assessed for microRNA targets on IAV H3N2

($p \leq 0.05$ is designated as *; $p \leq 0.01$ is designated as **).

Furthermore, *cfa*-miR-215 and *cfa*-miR-146b were predicted to target different three positions on IBV Victoria (Figure 24A-C) and Yamagata (Figure 24A-C) lineages, respectively. More specifically, silencing vectors encoding for *cfa*-miR-215 significantly decreased the luciferase activity ($p \leq 0.001$) when co-transfected with pmirGLO containing PB1 gene of IBV Victoria lineage (Figure 24A). On the other hand, luciferase activities related to other predicted sites including HA (Figure 24B) and NP (Figure 24C) genes were not markedly declined.

On the other hand, a significant decrease ($p \leq 0.05$) in luciferase activity was revealed when pmirGLO containing PA gene of IBV Yamagata lineage (Figure 25A) was co-transfected with *cfa*-miR-146b. Even though the luciferase activity was significantly reduced ($p \leq 0.05$) in the reporter vectors containing the NP gene at the position 973 (Figure 25B), luciferase activity of pSilencer_SiLuc2 was not

significantly decreased. Moreover, there was no significant decrease in luciferase activity when pmirGLO containing the position 617 of NP gene (Figure 25C). Therefore, only PA gene of IBV Yamagata was the direct target of *cfa*-miR-146b.

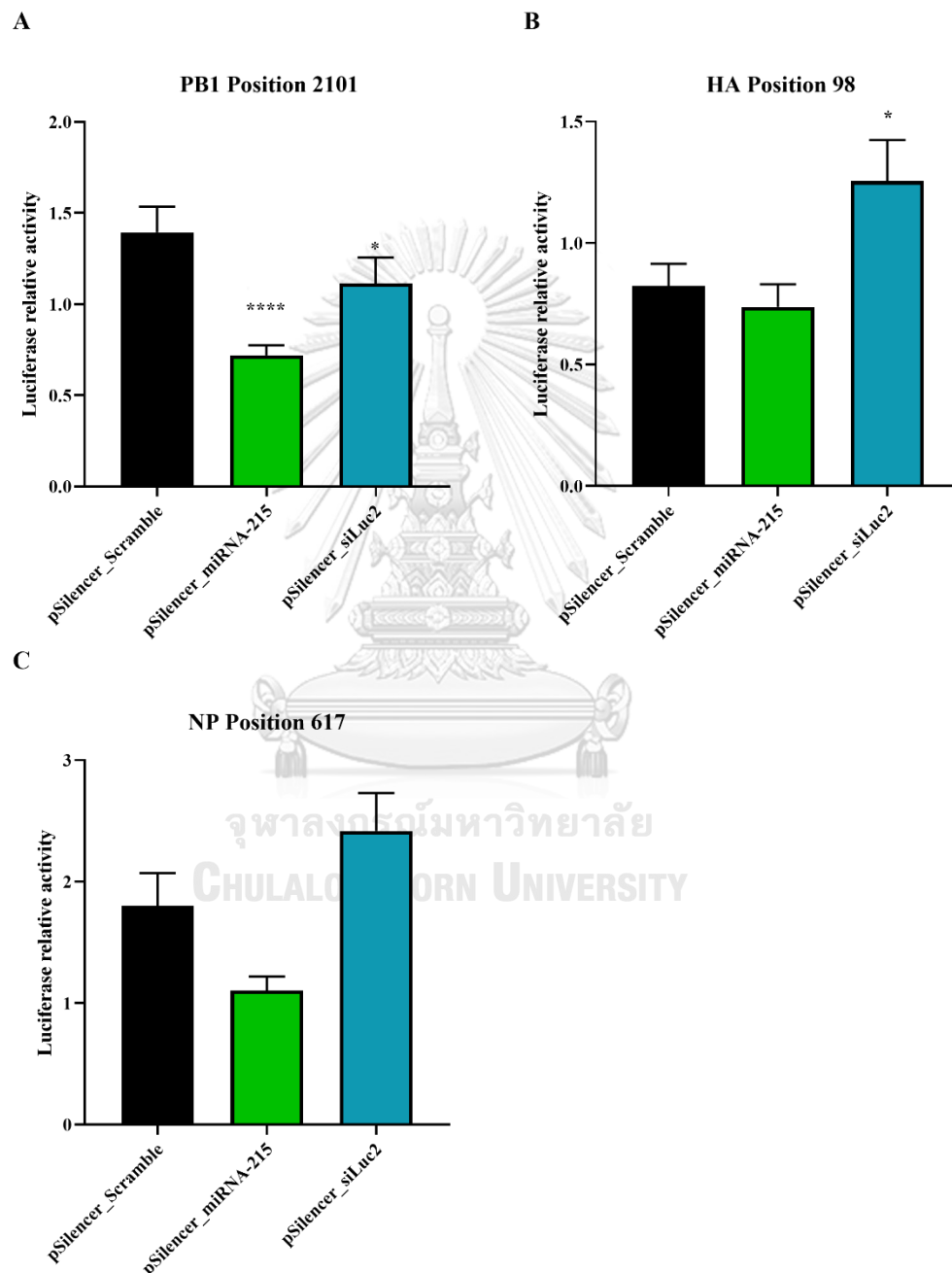


Figure 24 Luciferase assay was assessed for microRNA targets on IBV Victoria

($p \leq 0.05$ is designated as *; $p \leq 0.001$ is designated as ****).

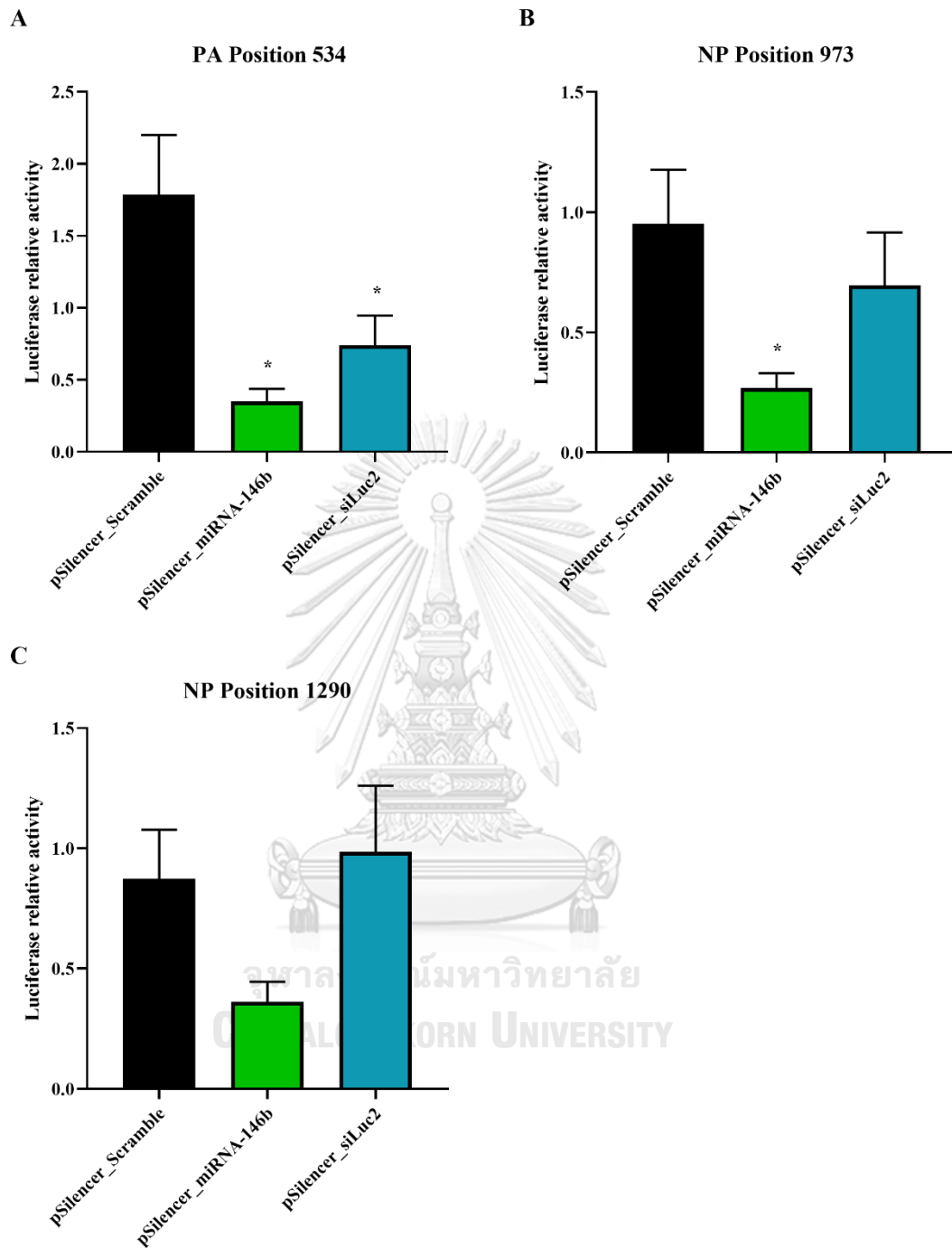


Figure 25 Luciferase assay was assessed for microRNA targets on IBV Yamagata

($p \leq 0.05$ is designated as *).

4.6. Effect of MicroRNA Inhibitor Manipulation on microRNA Binding Sites and Antigenic Sequences

Due to the unavailability of seed vaccine strains, the strains tested in this study, except Yamagata lineage, were not the same strains used in vaccine manufacturing. However, the sequences of viral seed strains retrieved from NCBI or GISAID were observed with respect to the sequences of the experimental strains. According to the luciferase results, *cfa*-miR-146b and *cfa*-miR-215 could target the PB1 gene of IAV pH1N1. As shown in Figure 26A, the seed region of *cfa*-miR-146b could bind with the PB1 of other pH1N1 seed strains. However, a nucleotide change from G to A was found in the seed strains A/Michigan/45/2015 and A/Brisbane/02/2018 (Figure 26B). As a result, this mutation interfered with the binding between the seed sequence of *cfa*-miR-215 and the PB1 of the pH1N1 seed strains. In addition, microRNA binding sites of IAV H3N2 and IBV Victoria were observed. The results showed that *cfa*-miR-197 could bind to the PB2 gene of other H3N2 seed strains (Figure 26C), while *cfa*-miR-215 could target the PB1 gene of Victoria seed viral strains (Figure 26D). For microRNA binding site of the IBV Yamagata lineage, a nucleotide alteration from C to T was exhibited in the PA gene of the seed strain B/Phuket/3073/2013 (Figure 26E). Although this mutation resided in the microRNA-binding site, it was located outside the positions which the seed sequence of *cfa*-miR-146b bound with. Therefore, this mutation might not influence the pairing between the seed region of *cfa*-miR-146b and the PA of the Yamagata seed strain. As a result, the manipulation of microRNA inhibitor might be affected when viral mutation occurred in microRNA-binding sites, particularly the positions which bound to the seed region of microRNAs.

Besides microRNA-binding sites, antigenic changes are crucial for vaccine production. Previous studies demonstrated that MDCK cells-based production could reduce the occurrence of HA mutations from the selective pressures found in egg-based manufacturing (137). For vaccine production, candidate vaccine viruses (CVVs) are inoculated into the cells and incubated for a few days to allow virus to replicate. Therefore, different strains of influenza viruses were propagated for two days in MDCK cells transfected with microRNA inhibitors or negative control inhibitor. To determine the effect of microRNA inhibitors on antigenic alterations, the nucleotides of HA and NA genes were sequenced with respect to parental strains. The sequences of HA and NA were obtained from IAV pH1N1, IBV Victoria, and IBV Yamagata viruses. Unfortunately, those of IAV H3N2 could not be retrieved from gel electrophoresis. This might be because of the low amount and quality of the viruses. However, there were no nucleotide changes in both HA and NA genes found in the IAV pH1N1 viruses in the presence of *cfa*-miR-146b and *cfa*-miR-215 inhibitors (Figure 27). In addition, no antigenic alterations of HA and NA genes were shown in the IBV Victoria viruses grown in the cells treated with *cfa*-miR-215 inhibitor (Figure 28). For IBV Yamagata propagated in the cells treated with *cfa*-miR-146b inhibitor, HA and NA sequence changes were not found as can be seen in Figure 29.

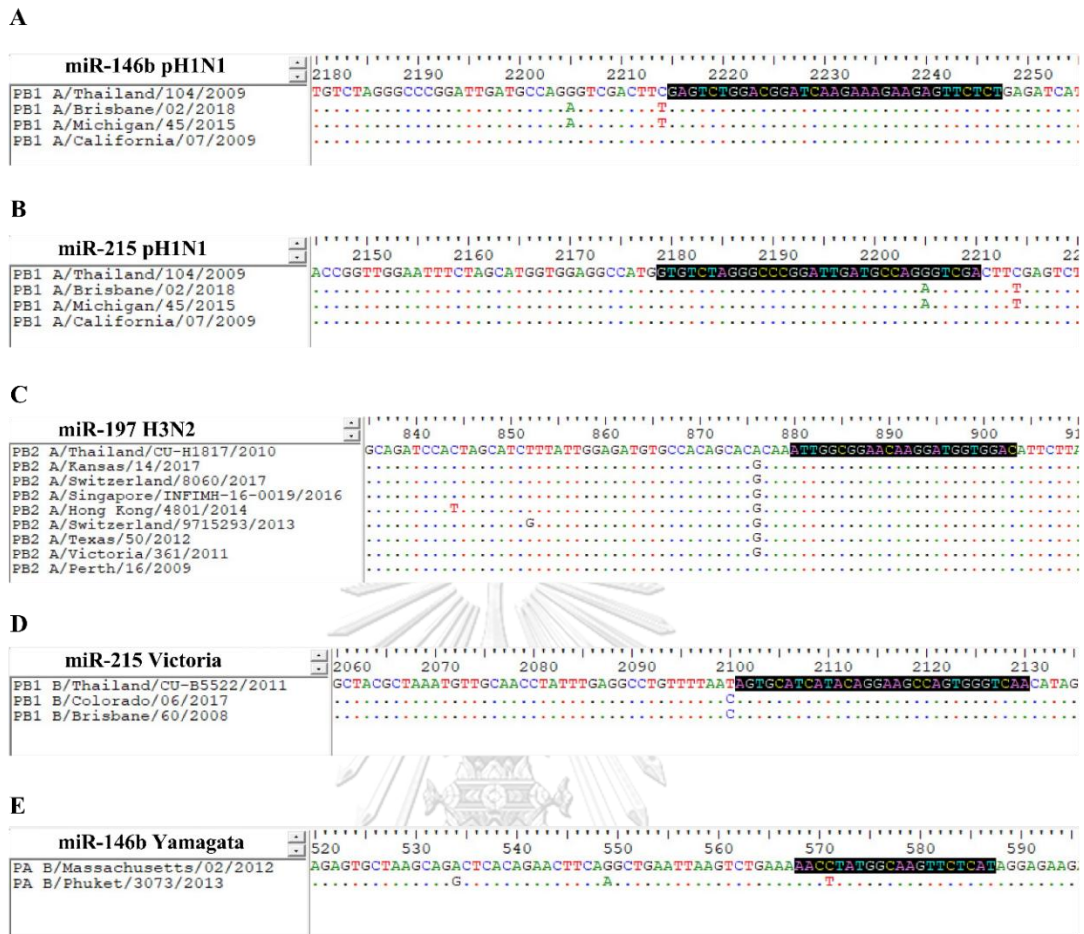


Figure 26 MicroRNA binding sites of the experimental strains (top sequences) and other seed viral strains (lower sequences) used for influenza vaccine manufacturing during 2011-2019.

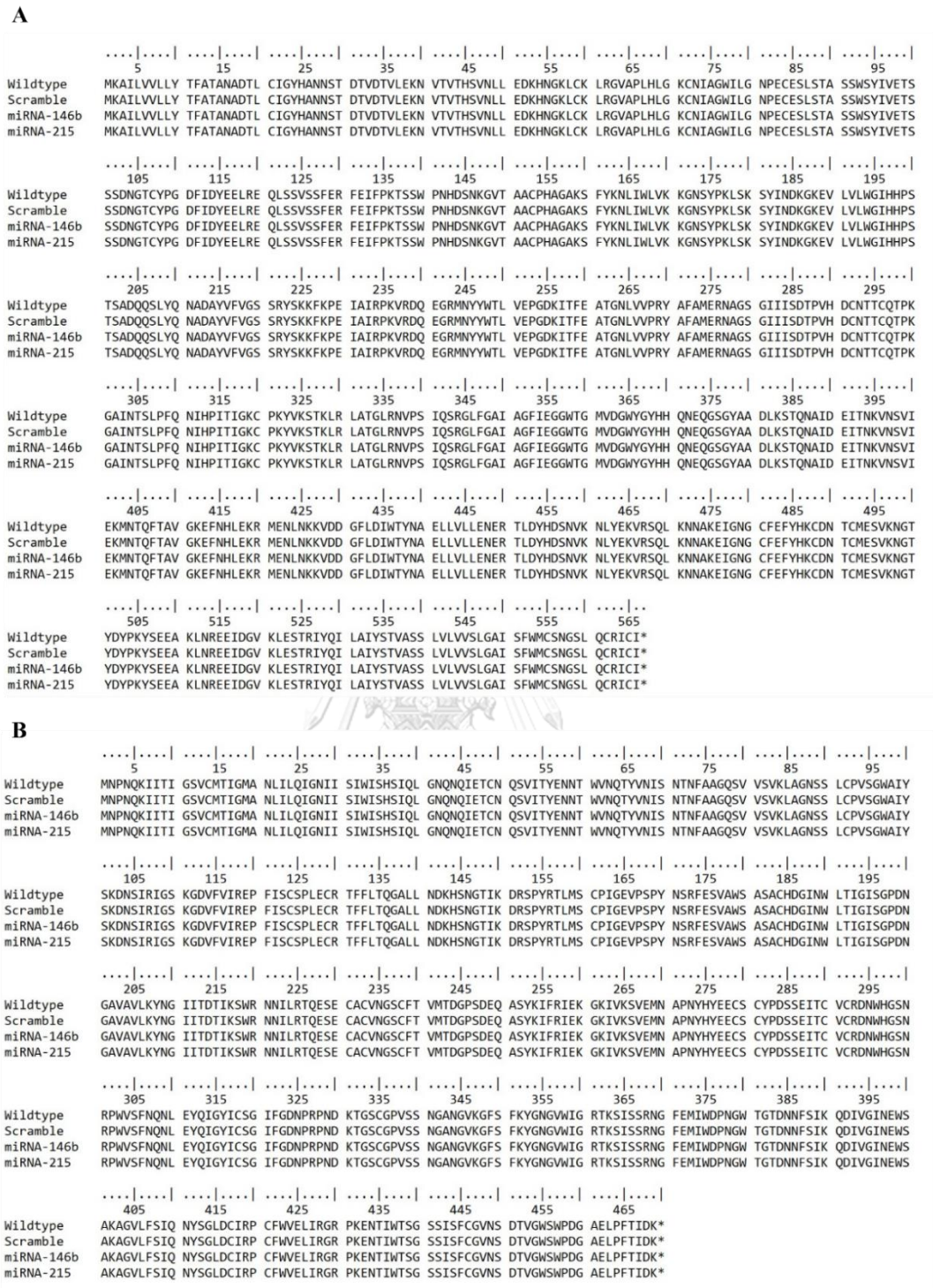


Figure 27 (A) HA and (B) NA sequences of the IAV pH1N1 viruses in the presence of microRNA inhibitors (compared with the parental strain shown in the first row).

A

	5 15 25 35 45 55 65 75 85 95
Wildtype	MKAIIVLLMV VTSNADRICT GITSSNSPHV VKTATQGEVN VTGVIPLTTT PTKSHFANKL GTETRGLKCP KCLNCTDLVD ALGRPCKTGK IPSARVSILH
Scramble	MKAIIVLLMV VTSNADRICT GITSSNSPHV VKTATQGEVN VTGVIPLTTT PTKSHFANKL GTETRGLKCP KCLNCTDLVD ALGRPCKTGK IPSARVSILH
miRNA-215	MKAIIVLLMV VTSNADRICT GITSSNSPHV VKTATQGEVN VTGVIPLTTT PTKSHFANKL GTETRGLKCP KCLNCTDLVD ALGRPCKTGK IPSARVSILH

	105 115 125 135 145 155 165 175 185 195
Wildtype	EVRPVTSGCF PIMHRTKIR QLPNLLRGYE HIRLSTHNVI NAENAPGGPY KIGTSGSCPVT VTNNGFFET MAWAVPKNDK NKTATNPLTI EVPYICTEGE
Scramble	EVRPVTSGCF PIMHRTKIR QLPNLLRGYE HIRLSTHNVI NAENAPGGPY KIGTSGSCPVT VTNNGFFET MAWAVPKNDK NKTATNPLTI EVPYICTEGE
miRNA-215	EVRPVTSGCF PIMHRTKIR QLPNLLRGYE HIRLSTHNVI NAENAPGGPY KIGTSGSCPVT VTNNGFFET MAWAVPKNDK NKTATNPLTI EVPYICTEGE

	205 215 225 235 245 255 265 275 285 295
Wildtype	DQITVWGFHS DDETMQAKLY GDSKPQKFTS SANGVTTHYV SQTGGFPNQT EDGGLPQSQR IVVDYMQKS GKTGTIYQR GILLPQKVMC ASGRSKVIKG
Scramble	DQITVWGFHS DDETMQAKLY GDSKPQKFTS SANGVTTHYV SQTGGFPNQT EDGGLPQSQR IVVDYMQKS GKTGTIYQR GILLPQKVMC ASGRSKVIKG
miRNA-215	DQITVWGFHS DDETMQAKLY GDSKPQKFTS SANGVTTHYV SQTGGFPNQT EDGGLPQSQR IVVDYMQKS GKTGTIYQR GILLPQKVMC ASGRSKVIKG

	305 315 325 335 345 355 365 375 385 395
Wildtype	SLPLIGEADC LHEKYGGLNK SKPYTGEHA KAIGNCPYW KTPLKLANGT KYRPPAKLLK ERGFFGAIAG FLEGGWEGMI AGWHGYTSHG AHGVAAADL
Scramble	SLPLIGEADC LHEKYGGLNK SKPYTGEHA KAIGNCPYW KTPLKLANGT KYRPPAKLLK ERGFFGAIAG FLEGGWEGMI AGWHGYTSHG AHGVAAADL
miRNA-215	SLPLIGEADC LHEKYGGLNK SKPYTGEHA KAIGNCPYW KTPLKLANGT KYRPPAKLLK ERGFFGAIAG FLEGGWEGMI AGWHGYTSHG AHGVAAADL

	405 415 425 435 445 455 465 475 485 495
Wildtype	KSTQEAINKI TKNLNSLSEL EVKNLQRLSG AMDELHNEIL ELDEKVDLDR ADTISSQIEL AVLLSNEGII NSEDEHLLAL ERKLLKMLGP SAVEIGNGCF
Scramble	KSTQEAINKI TKNLNSLSEL EVKNLQRLSG AMDELHNEIL ELDEKVDLDR ADTISSQIEL AVLLSNEGII NSEDEHLLAL ERKLLKMLGP SAVEIGNGCF
miRNA-215	KSTQEAINKI TKNLNSLSEL EVKNLQRLSG AMDELHNEIL ELDEKVDLDR ADTISSQIEL AVLLSNEGII NSEDEHLLAL ERKLLKMLGP SAVEIGNGCF

	505 515 525 535 545 555 565 575 585
Wildtype	ETKHKCNQTC LDRIAAGTFD AGEFSLPTFD SLNITAAASLN DDGLDNHTIL LYYSTAASSL AVTLMIAIFV VYMISRDNVMS CSICL*
Scramble	ETKHKCNQTC LDRIAAGTFD AGEFSLPTFD SLNITAAASLN DDGLDNHTIL LYYSTAASSL AVTLMIAIFV VYMISRDNVMS CSICL*
miRNA-215	ETKHKCNQTC LDRIAAGTFD AGEFSLPTFD SLNITAAASLN DDGLDNHTIL LYYSTAASSL AVTLMIAIFV VYMISRDNVMS CSICL*

B

	5 15 25 35 45 55 65 75 85 95
Wildtype	MLPSTIQTLT LFLTSGGVLL SLYVSASLSY LLYSDILLKF SPTIEITAPTML PLDCANASNV QAVNRSATKG VTLTLLPEPEW TYPRLSPCPGS TFQKALLISP
Scramble	MLPSTIQTLT LFLTSGGVLL SLYVSASLSY LLYSDILLKF SPTIEITAPTML PLDCANASNV QAVNRSATKG VTLTLLPEPEW TYPRLSPCPGS TFQKALLISP
miRNA-215	MLPSTIQTLT LFLTSGGVLL SLYVSASLSY LLYSDILLKF SPTIEITAPTML PLDCANASNV QAVNRSATKG VTLTLLPEPEW TYPRLSPCPGS TFQKALLISP

	105 115 125 135 145 155 165 175 185 195
Wildtype	HRFGETKGNSS APLIIREPFI ACPGNECKHF ALTHYAAQPG GYNGTRGDR NKLRLHLSVK LGKIPTVENS IFHMAAWSGS ACHDGKENTY IGVDPDNNA
Scramble	HRFGETKGNSS APLIIREPFI ACPGNECKHF ALTHYAAQPG GYNGTRGDR NKLRLHLSVK LGKIPTVENS IFHMAAWSGS ACHDGKENTY IGVDPDNNA
miRNA-215	HRFGETKGNSS APLIIREPFI ACPGNECKHF ALTHYAAQPG GYNGTRGDR NKLRLHLSVK LGKIPTVENS IFHMAAWSGS ACHDGKENTY IGVDPDNNA

	205 215 225 235 245 255 265 275 285 295
Wildtype	LLKVKYGEAY TDTYHSYANK ILRTQESACN CIGGNCYLMI TDGASGVSE CRFLKIREGR IIKEIFPTGR VKHTEECTCG FASNKTIECA CRDNSYTAKR
Scramble	LLKVKYGEAY TDTYHSYANK ILRTQESACN CIGGNCYLMI TDGASGVSE CRFLKIREGR IIKEIFPTGR VKHTEECTCG FASNKTIECA CRDNSYTAKR
miRNA-215	LLKVKYGEAY TDTYHSYANK ILRTQESACN CIGGNCYLMI TDGASGVSE CRFLKIREGR IIKEIFPTGR VKHTEECTCG FASNKTIECA CRDNSYTAKR

	305 315 325 335 345 355 365 375 385 395
Wildtype	PFVKLNVEDT TAEIRLMCTD TYLDTPRPND GSRSRHCESN GDKGSGGIGK GFVHQRMESK IGRWYSRTMS KTERMGMELY VKYDGDWPAD SDALDFSGVM
Scramble	PFVKLNVEDT TAEIRLMCTD TYLDTPRPND GSRSRHCESN GDKGSGGIGK GFVHQRMESK IGRWYSRTMS KTERMGMELY VKYDGDWPAD SDALDFSGVM
miRNA-215	PFVKLNVEDT TAEIRLMCTD TYLDTPRPND GSRSRHCESN GDKGSGGIGK GFVHQRMESK IGRWYSRTMS KTERMGMELY VKYDGDWPAD SDALDFSGVM

	405 415 425 435 445 455 465
Wildtype	VSMKEPQWYS FGFEIKDKKC DVPCIGIEMV HDGGKETWHS AATAIYCLMG SGQLLNDTVT GVNMMAL*
Scramble	VSMKEPQWYS FGFEIKDKKC DVPCIGIEMV HDGGKETWHS AATAIYCLMG SGQLLNDTVT GVNMMAL*
miRNA-215	VSMKEPQWYS FGFEIKDKKC DVPCIGIEMV HDGGKETWHS AATAIYCLMG SGQLLNDTVT GVNMMAL*

Figure 28 (A) HA and (B) NA sequences of the IBV Victoria viruses in the presence of microRNA inhibitors (compared with the parental strain shown in the first row).

A

	5	15	25	35	45	55	65	75	85	95
Wildtype	MKAIIVLLMV	VTSNADRICT	GITSSNSPHV	VKTATQGEVN	VTGVIPLTTT	PTKSYFANLK	GTKTRGKLC	DCLNCTDLV	ALGRPMC	TPSAKASILH
Scramble	MKAIIVLLMV	VTSNADRICT	GITSSNSPHV	VKTATQGEVN	VTGVIPLTTT	PTKSYFANLK	GTKTRGKLC	DCLNCTDLV	ALGRPMC	TPSAKASILH
miRNA-146b	MKAIIVLLMV	VTSNADRICT	GITSSNSPHV	VKTATQGEVN	VTGVIPLTTT	PTKSYFANLK	GTKTRGKLC	DCLNCTDLV	ALGRPMC	TPSAKASILH
	105	115	125	135	145	155	165	175	185	195
Wildtype	EVPRVTS	PIMHRTKIR	QLANLLRGYE	NIRLSTQ	DAEKAPGGPY	RLGTSGSCP	ATSKSGFFAT	MAWAVPKD	KNATNPLT	VPYICAE
Scramble	EVPRVTS	PIMHRTKIR	QLANLLRGYE	NIRLSTQ	DAEKAPGGPY	RLGTSGSCP	ATSKSGFFAT	MAWAVPKD	KNATNPLT	VPYICAE
miRNA-146b	EVPRVTS	PIMHRTKIR	QLANLLRGYE	NIRLSTQ	DAEKAPGGPY	RLGTSGSCP	ATSKSGFFAT	MAWAVPKD	KNATNPLT	VPYICAE
	205	215	225	235	245	255	265	275	285	295
Wildtype	QITVWGF	DKTQMK	DSNPQKF	ANGVTTH	QIGGFPD	DGGLPQSG	VVDYMMQ	KTGTIVY	VLLPQKV	SGRSKVI
Scramble	QITVWGF	DKTQMK	DSNPQKF	ANGVTTH	QIGGFPD	DGGLPQSG	VVDYMMQ	KTGTIVY	VLLPQKV	SGRSKVI
miRNA-146b	QITVWGF	DKTQMK	DSNPQKF	ANGVTTH	QIGGFPD	DGGLPQSG	VVDYMMQ	KTGTIVY	VLLPQKV	SGRSKVI
	305	315	325	335	345	355	365	375	385	395
Wildtype	LPLIGEAD	HEKYGLN	KPYTGEH	AIGNCPI	TPCLKANG	YRPPAKL	RGFFGAI	LEGGWEG	GMHGYTS	HGVAVAAD
Scramble	LPLIGEAD	HEKYGLN	KPYTGEH	AIGNCPI	TPCLKANG	YRPPAKL	RGFFGAI	LEGGWEG	GMHGYTS	HGVAVAAD
miRNA-146b	LPLIGEAD	HEKYGLN	KPYTGEH	AIGNCPI	TPCLKANG	YRPPAKL	RGFFGAI	LEGGWEG	GMHGYTS	HGVAVAAD
	405	415	425	435	445	455	465	475	485	495
Wildtype	STQEAIN	KNLNSL	VKNLQRL	MDELHNE	LDEKVDL	DTISSQI	VLLSNEG	SEDEHLL	RKLLKML	AVDIGNG
Scramble	STQEAIN	KNLNSL	VKNLQRL	MDELHNE	LDEKVDL	DTISSQI	VLLSNEG	SEDEHLL	RKLLKML	AVDIGNG
miRNA-146b	STQEAIN	KNLNSL	VKNLQRL	MDELHNE	LDEKVDL	DTISSQI	VLLSNEG	SEDEHLL	RKLLKML	AVDIGNG
	505	515	525	535	545	555	565	575	585	
Wildtype	TKHKCNQ	DRIAAGT	GEFSLPT	LNITAAS	DGLDNHT	YVSTAAS	VTLMLAI	YVMSRDN	SICL*	
Scramble	TKHKCNQ	DRIAAGT	GEFSLPT	LNITAAS	DGLDNHT	YVSTAAS	VTLMLAI	YVMSRDN	SICL*	
miRNA-146b	TKHKCNQ	DRIAAGT	GEFSLPT	LNITAAS	DGLDNHT	YVSTAAS	VTLMLAI	YVMSRDN	SICL*	



B

	5	15	25	35	45	55	65	75	85	95
Wildtype	MLPSTIQ	LFLTSGG	SLYVSAS	LLYSDIL	SQTEITAP	PLDCANAS	QAVNHSAA	VTLLLPE	TYPRLS	TFQKALL
Scramble	MLPSTIQ	LFLTSGG	SLYVSAS	LLYSDIL	SQTEITAP	PLDCANAS	QAVNHSAA	VTLLLPE	TYPRLS	TFQKALL
miRNA-146b	MLPSTIQ	LFLTSGG	SLYVSAS	LLYSDIL	SQTEITAP	PLDCANAS	QAVNHSAA	VTLLLPE	TYPRLS	TFQKALL
	105	115	125	135	145	155	165	175	185	195
Wildtype	HRFGEIK	APLIIRE	ACGPTCK	ALTHYAA	GYNGTRE	NKLRHLIS	LGKIPTV	IFHMAAW	ACHDGKE	IGVDGPD
Scramble	HRFGEIK	APLIIRE	ACGPTCK	ALTHYAA	GYNGTRE	NKLRHLIS	LGKIPTV	IFHMAAW	ACHDGKE	IGVDGPD
miRNA-146b	HRFGEIK	APLIIRE	ACGPTCK	ALTHYAA	GYNGTRE	NKLRHLIS	LGKIPTV	IFHMAAW	ACHDGKE	IGVDGPD
	205	215	225	235	245	255	265	275	285	295
Wildtype	LLKIKYGE	TDYHSYA	ILRTQES	CIGGDCY	TDGPASG	CRFLKIRE	IIKEIFPT	VKHTEEC	FASNKTIE	CRDNRYT
Scramble	LLKIKYGE	TDYHSYA	ILRTQES	CIGGDCY	TDGPASG	CRFLKIRE	IIKEIFPT	VKHTEEC	FASNKTIE	CRDNRYT
miRNA-146b	LLKIKYGE	TDYHSYA	ILRTQES	CIGGDCY	TDGPASG	CRFLKIRE	IIKEIFPT	VKHTEEC	FASNKTIE	CRDNRYT
	305	315	325	335	345	355	365	375	385	395
Wildtype	PFVKLVET	TAEIRLM	TYLDTPR	GSITGPC	GDGSGGI	GFVHQRM	IGRWYSR	KTKRMGM	VKYDGP	SEALALS
Scramble	PFVKLVET	TAEIRLM	TYLDTPR	GSITGPC	GDGSGGI	GFVHQRM	IGRWYSR	KTKRMGM	VKYDGP	SEALALS
miRNA-146b	PFVKLVET	TAEIRLM	TYLDTPR	GSITGPC	GDGSGGI	GFVHQRM	IGRWYSR	KTKRMGM	VKYDGP	SEALALS
	405	415	425	435	445	455	465			
Wildtype	VSMEEPGW	FGFEIKD	DVPCIGI	HDGGKTT	AATAIYCL	SGQLLND	TVT	GVDMAL*		
Scramble	VSMEEPGW	FGFEIKD	DVPCIGI	HDGGKTT	AATAIYCL	SGQLLND	TVT	GVDMAL*		
miRNA-146b	VSMEEPGW	FGFEIKD	DVPCIGI	HDGGKTT	AATAIYCL	SGQLLND	TVT	GVDMAL*		

Figure 29 (A) HA and (B) NA sequences of the IBV Yamagata viruses in the presence of microRNA inhibitors (compared with the parental strain shown in the first row).

CHAPTER V

DISCUSSION AND CONCLUSIONS

Influenza A and B viruses cause seasonal epidemics which affect millions of people each year. Vaccination is the most effective intervention for reduction of mortality and morbidity associated with seasonal influenza. Currently, the majority of influenza vaccines are manufactured using embryonated chicken eggs, and this method of vaccine virus production has remained the major vaccine production strategy over decades (122, 123). Although egg-based vaccine production confers many advantages, there are several disadvantages. This manufacturing method, for instance, requires the antigenicity screening of isolated virus strains, thereby increasing the production time (124). In addition, not all influenza strains recommended for seasonal vaccines grow equally well in eggs (79, 125). Moreover, egg-adapted strains could have a negative impact on vaccine effectiveness (79, 126, 127). Differences in sialic acids from human cells, avian cells exhibit different conformation for recognition by the viral HA protein (128, 129). As a result, poor binding between human influenza viruses and avian receptor leads to lower viral growth in eggs, resulting in a selective pressure on these viruses to adapt their HA proteins.

To address these issues related to the egg-based vaccine production, novel methods have been developed to improve seasonal influenza vaccine production. Since Madin-Darby Canine Kidney (MDCK) cells are known to be permissive to influenza virus infection and replication, this cell line has been widely used for identification and diagnosis of influenza viruses from clinical specimens (130). In

November 2012, the approval of Flucelvax[®], the first non-egg based influenza vaccine alternative in the US, was announced by the FDA (131). More recently, this cell-based vaccine was also approved by the European Medicines Agency in December 2018 (132). Flucelvax[®] is developed by Novartis and now owned by Seqirus, wherein influenza viruses are grown in Madin-Darby Canine Kidney (MDCK) cells (133). This strategy has several benefits over the egg-based counterpart. Principally, the possible constraints of shortages in egg supply could be minimized by the utilization of cell-based manufacturing method. Sometimes egg-based production time is slow, dependent on their availability. By contrast, cell-based production is reliant on the capacity of bioreactors, offering a more flexible lead time (134). Additionally, recent evidence showed that viruses propagated in avian cells exhibit a significant difference in glycosylation profiles, which dramatically affect immunogenicity (126, 135, 136). Another advantage is that there is no special consideration regarding egg allergy in cell-based production strategy. FDA approved the use of cell-isolated candidate vaccine viruses in the production of Flucelvax[®] in August 2016 (131). An attractive benefit is that this strategy could reduce the occurrence of HA mutations from the selective pressures found in egg-based production (137). As a result, this cell-based strategy has been used to produce quadrivalent influenza vaccines, composed of two subtypes of influenza A viruses (H1N1 and H3N2) and two lineages of influenza B viruses (Yamagata and Victoria).

The knowledge that host factors are essential for viral replication has provided targets for disease intervention. Among the host components, it has been shown that virus infection can mediate alterations in cellular microRNA expression, thus leading to the regulation of various biological processes within an infected cell. As a result,

microRNAs could be utilized for studies on infectious disease treatments (138, 139), biomarkers (140-142), and vaccine developments (143, 144). Thus far, investigations of influenza viruses, particularly influenza A viruses, have used human cell lines as a study model. Nonetheless, studies of microRNAs in MDCK infected with seasonal influenza A and B viruses are still limited. This study has investigated microRNA profiles of MDCK cells in response to seasonal influenza virus infection. To date, 453 mature microRNAs have been predicted throughout the canine genome (145). Based on our microRNA profile data, dysregulated microRNAs were considered when changes in microRNA expression were greater than 2-fold as compared to mock-infected groups. In this study, 3 upregulated microRNAs and 22 down-regulated microRNAs were found in MDCK cells infected with A/pH1N1. Moreover, 19 microRNAs were overexpressed and 13 microRNAs were down-regulated upon infection of A/H3N2. On the other hand, upregulation of 27 microRNAs and downregulation of 14 microRNAs were expressed in the B/Victoria-infected cells. Lastly, 14 overexpressed microRNAs and 5 downregulated microRNAs were found in the B/Yamagata-infected cells. After the profiles were validated by RT-qPCR, some microRNAs of our interest were reliant on common overexpression upon infection with different subtypes. Although no microRNAs were universally upregulated among four strains, the four most common microRNAs including *cfa*-miR-146b, *cfa*-miR-197, *cfa*-miR-215, *cfa*-miR-340 were upregulated in this study. In agreement with our study, *cfa*-miR-146b were overexpressed in canine lung and tracheal cells infected with canine influenza H3N2 virus (146).

In addition to those four microRNAs which were commonly upregulated by different strains of seasonal influenza viruses, other microRNA expressions obtained

from this study were compared to previous studies which were performed in various subtypes of influenza viruses and cellular models. For instance, the current investigation demonstrated overexpression of *cfa*-miR-17, *cfa*-miR-122, *cfa*-miR-132 in H3N2-infected cells. The finding of upregulated *cfa*-miR-17 is consistent with previous studies using pH1N1-infected human lung epithelial cells (112), and serum of H7N9-infected patients (147). However, some studies showed downregulation of *hsa*-miR-17-3p in H1N1 (PR8)-infected lung epithelial cells (148). Moreover, *cfa*-miR-122 was over-expressed, which is in line with the study of avian influenza infection in the lungs of broiler chickens (149). Additionally, upregulation of *cfa*-miR-132 were revealed in this study, which concurs well with the previous results shown in human lung and bronchial epithelial cells infected with H1N1 (PR8) (150) and H3N2 (112). On the other hand, this study found overexpression of *cfa*-miR-320 in influenza B/Victoria-infected cells, which is in agreement with a previous result of H7N9-infected serum (151). Conversely, the microRNA profiles in this study demonstrated down-expression of *cfa*-miR-30e, *cfa*-miR-18a, and *cfa*-miR-374a in pH1N1- and H3N2-infected cells. It is controversial whether *hsa*-miR-30e is downregulated (152) or upregulated (112) upon infection of influenza A viruses. However, previous investigations also revealed the down-expression of *hsa*-miR-18a (27, 153) and *hsa*-miR-374a (27, 152). Moreover, this study showed that the expression of *cfa*-miR-15b was decreased in the cells infected with A/pH1N1 or B/Victoria virus. This finding corroborates with a recent study of human cells infected with influenza A viruses (27).

Interestingly, direct binding between host microRNAs and viral RNAs appeared to take place, leading to changes in the pathogenesis or in their translation

and replication processes. Accumulating evidence demonstrates that microRNAs could directly bind to a wide range of viruses such as eastern equine encephalitis virus (EEEV), human T cell leukemia virus type I (HTLV-1), primate foamy retrovirus type 1 (PFV-1), enterovirus 71 (EV71), porcine reproductive and respiratory syndrome virus (PRRSV), hepatitis C virus (HCV) (103, 154-158). The scope of this investigation was focused on microRNA targets on seasonal influenza genomes. Recently, it has been shown that microRNAs could directly interact with influenza A viruses. For instance, *hsa-miR-584-5p* and *hsa-miR-1249* dramatically inhibited replication of H5N1 and pH1N1 (A/Beijing/501/2009) IAVs in A549 cells through matched with the PB2 binding sequence (159). Among the eight segments of influenza A viruses, PB1 was reported most frequently. Our previous study demonstrated that *hsa-miR-3145* could also trigger silencing of viral PB1 genes of influenza A viruses (pH1N1, H3N2, H5N1), resulted in inhibition of influenza viral replication in human lung epithelial cell line A549 (26). Upon infection of highly pathogenic avian influenza H5N1 in human cells, *hsa-miR-324-5p* and *hsa-miR-485* inhibited viral replication by targeting the PB gene (160, 161). In addition to viral polymerases PB2 and PB1, *hsa-let-7c* bound to the 3' UTR of the H1N1 M1 gene, resulted in the regulation of viral replication in A549 cell lines (25). However, these previous studies demonstrated the effect of human microRNAs in human cells infected with influenza A viruses. So far there have been only a few studies reporting canine microRNAs targeting viral genomes in response to infection of influenza A viruses (24). Song and colleagues indicated that *cfa-miRNA-323*, *cfa-miRNA-491*, and *cfa-miRNA-654* inhibited replication of the H1N1 (A/WSN/33) viruses in MDCK cells through binding to the viral PB1 gene (24).

Unlike the earlier investigation of Song *et al.* (24), the present study demonstrated canine microRNAs profiles in MDCK cells infected with the current subtypes of seasonal influenza A viruses. This study found that *cfa*-miR-146b and *cfa*-miR-215 could directly bind to the pH1N1 PB1 gene, whilst *cfa*-miR-197 could interact with H3N2. Moreover, this study also investigated canine microRNAs targeting influenza B viruses, which have not been reported previously. The investigation found that the PB1 of B/Victoria virus could be targeted by *cfa*-miR-215, while *cfa*-miR-146b could bind to the PA of the B/Yamagata virus. Interestingly, our microRNA profile data demonstrated that *cfa*-miR-1249 was down-regulated upon influenza A/pH1N1 virus infection, which is consistent with previous findings (159). Wang and colleagues revealed that *hsa*-miR-1249-3p which bound to the PB2 binding sequence dramatically inhibited replication of influenza H5N1 and pH1N1 viruses in A549 cells (159). While the current study demonstrated overexpression of *cfa*-miR-1307 and down-expression of *cfa*-miR-486 in the B/Victoria-infected cells, other previous studies found that both microRNAs targeted viral genomes in human cells. Specifically, *hsa*-miR-1307 could target the NS1 gene of pH1N1 (162), while *hsa*-miR-486-5p bound to several segments of H1N1 (PR8) or H3N2 (163).

Naturally, microRNA-binding sites are located in the 3'-untranslated regions (UTR) of mRNAs. However, cellular microRNAs could bind to various regions of viral RNAs including the 3'-UTR (154), 5'-UTR (103), and the coding regions of viral proteins (24, 157). Generally, the interactions between microRNA and viral genome lead to inhibition of translation of the viral genome, preventing viral replication. In some circumstances, however, the direct binding could stabilise the virus RNA, thereby enhancing replication (103, 104, 164). It is intriguing that synergistic effort

between two or more miRNA-binding sites within the gene enhanced repression of mRNA translation (165). Therefore, the location and number of miRNA-binding sites within a viral genome can influence the function of microRNAs. Although individual microRNA mimics/ inhibitors were treated in the present study, we found that *cfa*-miR-146b and *cfa*-miR-215 could bind to the same PB1 gene of pH1N1 virus at the position of 2191 and 2155, respectively. Furthermore, some investigations reported that the combined effort of multiple microRNAs targeting different gene segments had a higher suppressive effect on some strains of influenza A viruses than that of individual microRNA treatment (163). However, the synergistic effect of microRNA mixtures has yet to be experimentally validated. Returning to the hypothesis posed at the beginning of this study, it is now possible to state that canine microRNAs could inhibit the replication of seasonal influenza viruses through direct binding to viral RNAs. Conversely, treatment of microRNA inhibitors could antagonize the suppressive effect of the microRNAs, resulting in enhanced propagation yields of the viruses.

In addition to direct binding with viral RNAs, the alteration of host microRNA expression could affect downstream transcriptomic profiles which can be either beneficial or deleterious to influenza viruses (110, 166-170). However, the effect of influenza virus-mediated microRNAs has been largely investigated in human cells as shown in most of the previous studies. Although Zhou *et al.* demonstrated that *cfa*-miR-143 promoted apoptosis via the p53 pathway in canine influenza virus H3N2-infected MDCK cells (166), investigations of canine cells infected with seasonal human influenza viruses are still limited. According to our validated microRNAs expression, *cfa*-miR-146b, *cfa*-miR-197, *cfa*-miR-215, and *cfa*-miR-340 were most

commonly upregulated microRNAs upon infection of seasonal influenza A and B viruses. *Cfa*-miR-340 was overexpressed during infection of influenza viruses A/pH1N1 and A/H3N2. Previous studies found that the 3'-UTR of Rho-associated, coiled-coil containing protein kinase 1 (ROCK1) and Janus Kinase 1 (JAK1) was identified as a target of *hsa*-miR-340 (171, 172). ROCK1 participates in the internalization of influenza A virus via RhoA-PIP5K signalling (173), while inhibition of JAK1/STAT3 leads to apoptosis in H5N1 infection (174). To predict whether dog ROCK1 and JAK1 could be a target of *cfa*-miR-340, TargetScan was utilised (175). As can be shown in Table 13, *cfa*-miR-340 might bind to the 3'-UTR of dog ROCK1 as well as that of JAK1. Most recently, *hsa*-miR-340-5p was found to target retinoic acid-inducible gene I (RIG-I) and 2'-5'-Oligoadenylate Synthetase 2 (OAS2), thus inhibiting replication of influenza A viruses (176). However, the target site of *cfa*-miRNA-340 on dog RIG-I and OAS2 could not be found by TargetScan and miRDB.

The present study showed that infections of A/H3N2 and B/Yamagata mediated the upregulation of *cfa*-miR-146b. It has been documented previously that *hsa*-miR-146b could target TNF receptor associated factor 6 (TRAF6) proteins, resulted in the regulation of cell apoptosis and cytokine production (177). Interestingly, *hsa*-miR-146a was also shown to regulate TRAF6 levels during infection of various viruses including influenza A/H3N2 virus (178), enterovirus 71 (179), dengue virus (180), and Japanese encephalitis virus (181). According to *in silico* target prediction (Table 13), the seed region of *cfa*-miR-146b is similar to that of *hsa*-miR-146b. Therefore, it is possible that *cfa*-miR-146b may interact with dog TRAF6, related to interferon production during seasonal influenza virus infection.

Furthermore, this investigation demonstrated that the over-expressions of *cfa*-miR-197 and *cfa*-miR-215 were present in the cells infected with A/H3N2, B/Victoria and B/Yamagata influenza viruses. Previously, *hsa*-miR-197 and *hsa*-miR-215 were altered upon virus infection, influencing gene expressions in their host organisms. For instance, *hsa*-miR-197 was downregulated by Enterovirus 71 (EV71) to maintain Ras-related Nuclear protein (RAN), leading to nuclear transport of viral proteins (182). Besides, RAN-GTP also involves in transport of influenza genome (183). Additionally, microRNA-197 was reported to suppress the expression of lysine 63 deubiquitinase (CYLD) (184). Interestingly, this tumour suppressor CYLD is a negative regulator of RIG-I-mediated antiviral response. Viral RNAs are detected in cytoplasm by RIG-1, leading to the activation of tank-binding kinase-1 (TBK1) and I κ B kinase- ϵ (IKK ϵ). These protein kinases activate IFN regulatory factor 3 (IRF3) and IRF7, thereby inducing interferon expression (185). Recently, it has been demonstrated that CYLD removed polyubiquitin chains from RIG-I and TBK1, concomitant with an inhibition of the IRF3 signalling pathway (186, 187). Like hybridisation found in human genes, TargenScan showed that *cfa*-miR-197 could bind to the 3'-UTRs of dog RAN and CYLD (Table 13).

Besides, X-chromosome-linked inhibitor of apoptosis (XIAP) could be targeted by microRNA-215 (188, 189). Therefore, it is possible that both microRNAs may involve in influenza virus-mediated apoptosis. XIAP is known to be an anti-apoptotic protein, which directly inhibits the proteolytic activity of caspases through binding with caspase-3 (190). It is intriguing that activation of caspase 3 during the onset of apoptosis is an essential event for efficient influenza virus propagation (191, 192). Mechanistically, retention of the viral RNP complexes in the nucleus appears

due to the inhibition of caspase-3, impeding virus progeny formation (191, 193). Similar to the complementary pairing in human genes, computational prediction demonstrated that the seed region of *cfa*-miR-215 might interact with the 3'-UTRs of dog XIAP (Table 13).

Table 13 Predicted host genes targeted by candidate microRNAs.

MicroRNAs	3'UTR position of dog genes	Hybridization pattern between miRNA (bottom strand) and target gene (top strand)	Seed type
<i>Cfa</i> -miR-197	111-117 of CYLD	5' ...AUGGAUGUCUUUGUGGUGGUGAU... 3' CGACCCACCUCUUCACCACUU 	7mer-m8
<i>Cfa</i> -miR-197	279-286 of RAN	5' ...CCAUCACAUAUCCAGUGGUGAA... 3' CGACCCACCUCUUCACCACUU 	8mer
<i>Cfa</i> -miR-215	3270-3276 of XIAP	5' ...UGUAAACUAAAGAAAUAGGUCAG... 3' ACAGAUAGUUAAGCAUCCAGUA 	7mer-m8
<i>Cfa</i> -miR-146b	478-485 of TRAF6	5' ...AUUAUUCUGGAGCUGAGUUCUCA... 3' UCGGAUACCUUAAGUCAAGAGU 	8mer
<i>Cfa</i> -miR-146b	39-46 of IRAK1	5' ...AAACCGGAAGUCAAGUUCUCA... 3' UCGGAUACCUUAAG--UCAAGAGU 	8mer
<i>Cfa</i> -miR-146b	55-62 of IRAK1	5' ...GUUCUCAUAGUCGGAAGUUCUCA... 3' UCGGAUACCUUAAGUCAAGAGU 	8mer
<i>Cfa</i> -miR-146b	1073-1079 of JAK1	5' ...UGCACUUUGUUACUCUUUAUAC... 3' UUAGUCAGAGUAACGAAUAUU 	7mer-m8
<i>Cfa</i> -miR-340	1153-1160 of ROCK1	5' ...UACAAUAAUGAAUGACUUUAUAA... 3' UUAGUCAGAGUAACGAAUAUU 	8mer
<i>Cfa</i> -miR-340	1347-1353 of ROCK1	5' ...AUACCUCUCAGUAAUUUAUAAU... 3' UUAGUCAGAGUAACGAAUAUU 	7mer-A1

MicroRNAs	3'UTR position of dog genes	Hybridization pattern between miRNA (bottom strand) and target gene (top strand)	Seed type
<i>Cfa</i> -miR-340	1073-1079 of JAK1	<pre> 5' ...UGCACUUUGUUUACUCUUUAUAC... 3' UUAGUCAGAGUAACGAAAUUU </pre>	7mer-m8

As stated earlier, viral genomes of influenza viruses are the main target of candidate microRNAs in this study. Although other previous studies in the human model together with *in silico* prediction (Table 13) lend support to possible targets on canine transcripts, the indirect effect of such microRNAs on phenotypic outcomes awaits further elucidation in canine cell lines. Regarding microRNAs targeting viral RNAs, the following points deserve particular attention. Firstly, maintenance of microRNA-binding sites within the viral genome could pose a challenging issue. It is well documented that the RNA polymerase of influenza viruses lacks the function of proofreading. Therefore, the incorporation of incorrect nucleotides usually happens during the influenza viral replication (194-196). Since viral seed strains were not available, most of the strains represented in this experiment were derived from clinical specimens obtained from the Centre of Excellence in Clinical Virology, Faculty of Medicine, Chulalongkorn University, Thailand. Nevertheless, the microRNA-binding sites of several viral seed strains obtained from NCBI or GISAID were observed with respect to the sequences of the experimental strains. Unfortunately, this study found that some microRNA-binding sites of vaccine strains, particularly the PB1 gene of pH1N1 viruses A/Michigan/45/2015 and A/Brisbane/02/2018, could not be targeted by *cfa*-miR-215. This observation is in agreement with most recent investigation by Bavagnoli and team, which demonstrated

that a mutation in the NS1 gene of A/pH1N1 strains present in Italy during 2010-2011 enabled the virus to escape the inhibitory effect of *hsa*-miR-1307-3p (162). Another example is that the expeditious loss of RISC-binding sites was found in the *in vitro* treatment of human immunodeficiency virus with siRNAs, which function similarly to microRNAs when they perfectly complementary bind to RNAs (197, 198). Whilst this investigation suggests negative regulation of influenza virus replication through host microRNAs, the ability of RNA viruses to evolve away from repression by specific microRNAs should be a concern.

Secondly, the effect of such microRNA inhibitor treatments on antigenic sequence changes should be taken into consideration. To our knowledge, acquired mutations in influenza virus HA and NA surface glycoproteins leads to immune evasion of viruses from protective neutralising antibody responses (199). In addition, influenza viruses could develop mutations in the HA and NA proteins after serial passaging in cell culture, eventually impacting vaccine efficacy (200). Some studies demonstrated that viral isolates spontaneously developed antigenic HA mutations after three passages in MDCK cells without any treatments (201). However, vaccine production does not require a longer period of culture or passage. In general, candidate vaccine viruses (CVVs) are inoculated into MDCK cells and incubated for two or three days to allow virus to replicate. To investigate the effect of microRNA inhibitor treatments on antigenic changes, different strains of seasonal influenza viruses were propagated for two days in MDCK cells transfected with microRNA inhibitors or negative control inhibitor. In this study the sequences of HA and NA obtained from the microRNA inhibitor-treated groups were determined, as compared with their parental populations. Fortunately, the results showed that there were no

mutations found in both HA and NA even though the viruses were grown in the cells treated with microRNA inhibitors. This may be inferred that the manipulation of microRNA inhibitors may not be a selection pressure on influenza viruses. Thirdly, this strategy might be concerned with production costs. Due to transient effect, the utilisation of microRNA inhibitors may be an impractical strategy for mass manufacturing. A recent breakthrough in CRISPR/Cas technology has paved the way for genetic engineering. This gene-editing technique has been proved to knockout or knockdown microRNAs *in vitro* (202-204) and *in vivo* (205). Moreover, this notion has been supported by a recent study of Waring and colleagues, identifying that microRNA-21 targets various regions of viral H1N1 (PR8) genome. The microRNA-21 deficient MDCK cells have the potential to be used as a vaccine platform to propagate viruses targeted by microRNA-21 and replace the conventional egg-based vaccine manufacturing (206).

In conclusion, this study provides the feasibility of host microRNA manipulation to enhance viral replication in MDCK cell-based production system. It is the first study to report canine microRNA profiles in response to seasonal influenza A and B viruses. According to the results, microRNAs tend to target viral genes in a strain-specific manner. Therefore, the candidate microRNAs might target viral genomes, resulted in suppression of viral replication. Conversely, the utilisation of microRNA inhibitors may antagonise the effect of candidate microRNAs, leading to an increase in viral yields. However, the strategy of microRNA targeting viral genomes might have some points to consider such as maintenance of microRNA-binding sites within the viral genome and transient effect of microRNA inhibitor transfection.

APPENDIX A

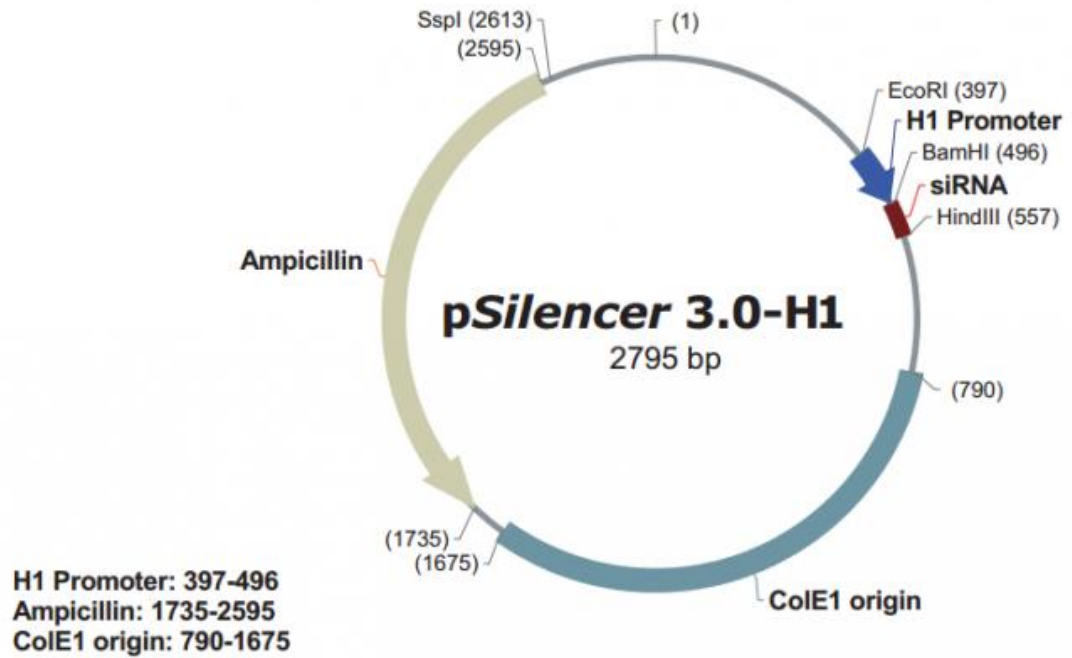
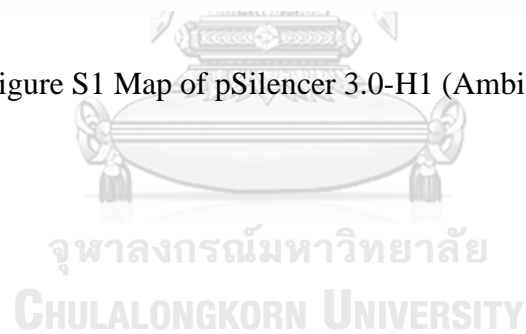


Figure S1 Map of pSilencer 3.0-H1 (Ambion) (207).



APPENDIX B

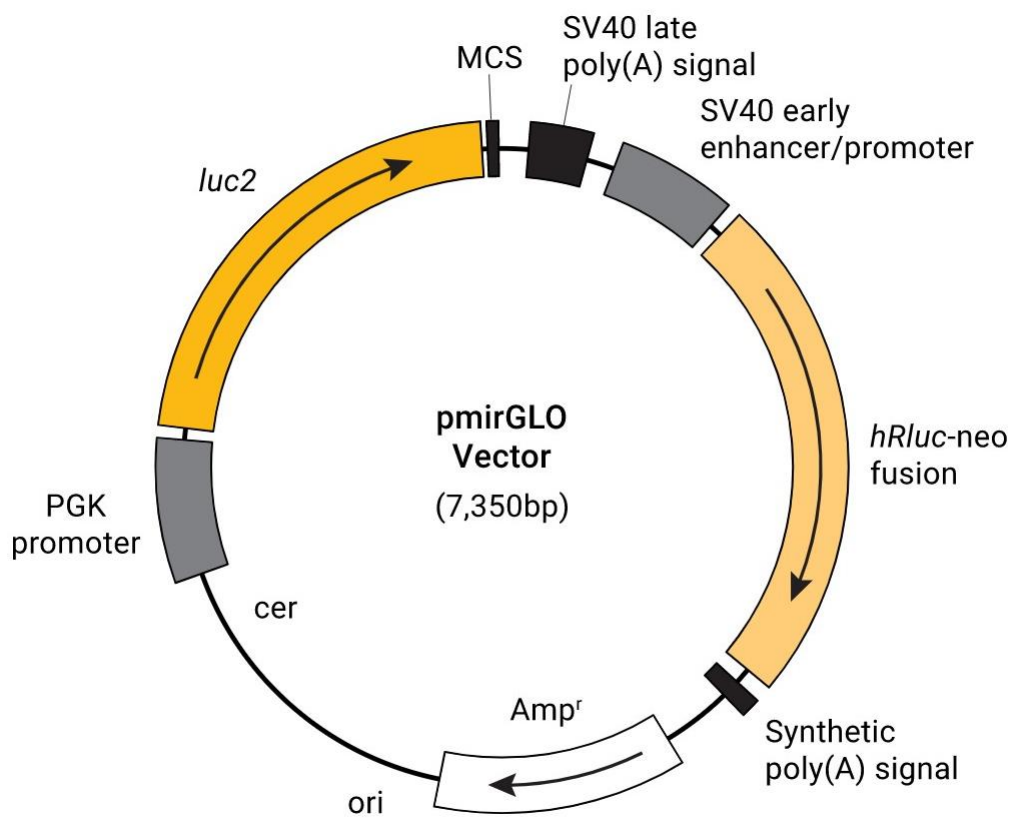


Figure S2 Map of pmirGLO (Promega) (208).

REFERENCES

1. Taubenberger JK, Morens DM. The pathology of influenza virus infections. *Annu Rev Pathol.* 2008;3:499-522.
2. Valkenburg SA, Rutigliano JA, Ellebedy AH, Doherty PC, Thomas PG, Kedzierska K. Immunity to seasonal and pandemic influenza A viruses. *Microbes Infect.* 2011;13(5):489-501.
3. World Health Organization. Influenza (Seasonal) Fact Sheet No. 211 2014a [Available from: [http:// www.who.int/mediacentre/factsheets/fs211/en/](http://www.who.int/mediacentre/factsheets/fs211/en/)]
4. Molinari NA, Ortega-Sanchez IR, Messonnier ML, Thompson WW, Wortley PM, Weintraub E, et al. The annual impact of seasonal influenza in the US: measuring disease burden and costs. *Vaccine.* 2007;25(27):5086-96.
5. Kawaoka Y, Neumann G. Influenza viruses: an introduction. *Methods Mol Biol.* 2012;865:1-9.
6. Tong S, Li Y, Rivaitter P, Conrardy C, Castillo DA, Chen LM, et al. A distinct lineage of influenza A virus from bats. *Proc Natl Acad Sci U S A.* 2012;109(11):4269-74.
7. Tong S, Zhu X, Li Y, Shi M, Zhang J, Bourgeois M, et al. New world bats harbor diverse influenza A viruses. *PLoS Pathog.* 2013;9(10):e1003657.
8. Krug RM, Yuan W, Noah DL, Latham AG. Intracellular warfare between human influenza viruses and human cells: the roles of the viral NS1 protein. *Virology.* 2003;309(2):181-9.
9. World Health Organization. Influenza virus infections in humans 2014b [Available from: http://www.who.int/influenza/human_animal_interface/virology_laboratories_and_vaccines/influenza_virus_infections_humans_feb14.pdf?ua=1]
10. Medina RA, Garcia-Sastre A. Influenza A viruses: new research developments. *Nat Rev Microbiol.* 2011;9(8):590-603.
11. Tscherne DM, Garcia-Sastre A. Virulence determinants of pandemic influenza viruses. *J Clin Invest.* 2011;121(1):6-13.
12. Brauer R, Chen P. Influenza virus propagation in embryonated chicken eggs. *J Vis Exp.* 2015(97).

13. Sabbaghi A, Miri SM, Keshavarz M, Zargar M, Ghaemi A. Inactivation methods for whole influenza vaccine production. *Rev Med Virol*. 2019;29(6):e2074.
14. Genzel Y, Reichl U. Continuous cell lines as a production system for influenza vaccines. *Expert Rev Vaccines*. 2009;8(12):1681-92.
15. Vlecken DH, Pelgrim RP, Ruminski S, Bakker WA, van der Pol LA. Comparison of initial feasibility of host cell lines for viral vaccine production. *J Virol Methods*. 2013;193(1):28-41.
16. Carvajal-Yepes M, Sporer KR, Carter JL, Colvin CJ, Coussens PM. Enhanced production of human influenza virus in PBS-12SF cells with a reduced interferon response. *Hum Vaccin Immunother*. 2015;11(9):2296-304.
17. Li IW, Chan KH, To KW, Wong SS, Ho PL, Lau SK, et al. Differential susceptibility of different cell lines to swine-origin influenza A H1N1, seasonal human influenza A H1N1, and avian influenza A H5N1 viruses. *J Clin Virol*. 2009;46(4):325-30.
18. Doroshenko A, Halperin SA. Trivalent MDCK cell culture-derived influenza vaccine Optaflu (Novartis Vaccines). *Expert Rev Vaccines*. 2009;8(6):679-88.
19. Krol J, Loedige I, Filipowicz W. The widespread regulation of microRNA biogenesis, function and decay. *Nat Rev Genet*. 2010;11(9):597-610.
20. Walters RW, Bradrick SS, Gromeier M. Poly(A)-binding protein modulates mRNA susceptibility to cap-dependent miRNA-mediated repression. *Rna*. 2010;16(1):239-50.
21. Wang X, Liu XS. Systematic Curation of miRBase Annotation Using Integrated Small RNA High-Throughput Sequencing Data for *C. elegans* and *Drosophila*. *Front Genet*. 2011;2:25.
22. Tomankova T, Petrek M, Kriegova E. Involvement of microRNAs in physiological and pathological processes in the lung. *Respir Res*. 2010;11:159.
23. tenOever BR. RNA viruses and the host microRNA machinery. *Nat Rev Microbiol*. 2013;11(3):169-80.
24. Song L, Liu H, Gao S, Jiang W, Huang W. Cellular microRNAs inhibit replication of the H1N1 influenza A virus in infected cells. *J Virol*. 2010;84(17):8849-60.

25. Ma YJ, Yang J, Fan XL, Zhao HB, Hu W, Li ZP, et al. Cellular microRNA let-7c inhibits M1 protein expression of the H1N1 influenza A virus in infected human lung epithelial cells. *J Cell Mol Med.* 2012;16(10):2539-46.
26. Khongnomnan K, Makkoch J, Poomipak W, Poovorawan Y, Payungporn S. Human miR-3145 inhibits influenza A viruses replication by targeting and silencing viral PB1 gene. *Exp Biol Med (Maywood).* 2015;240(12):1630-9.
27. Terrier O, Textoris J, Carron C, Marcel V, Bourdon JC, Rosa-Calatrava M. Host microRNA molecular signatures associated with human H1N1 and H3N2 influenza A viruses reveal an unanticipated antiviral activity for miR-146a. *J Gen Virol.* 2013;94(Pt 5):985-95.
28. Harper SA, Bradley JS, Englund JA, File TM, Gravenstein S, Hayden FG, et al. Seasonal influenza in adults and children--diagnosis, treatment, chemoprophylaxis, and institutional outbreak management: clinical practice guidelines of the Infectious Diseases Society of America. *Clin Infect Dis.* 2009;48(8):1003-32.
29. International Committee on Taxonomy of Viruses. *Virus Taxonomy: 2018b Release 2018* [Available from: <https://talk.ictvonline.org/taxonomy/>].
30. Shaw ML, Palese P. Orthomyxoviridae. Knipe DM, Howley PM, Cohen JI, Griffin DE, Lamb RA, Martin MA, et al., editors. Philadelphia: Wolters Kluwer, Lippincott Williams & Wilkins; 2013. 1151–85 p.
31. Wright PF, Neumann G, Kawaoka Y. Orthomyxoviruses. Knipe DM, Howley PM, Cohen JI, Griffin DE, Lamb RA, Martin MA, et al., editors: Philadelphia; 2013. 1186–243 p.
32. Osterhaus AD, Rimmelzwaan GF, Martina BE, Bestebroer TM, Fouchier RA. Influenza B virus in seals. *Science.* 2000;288(5468):1051-3.
33. Ran Z, Shen H, Lang Y, Kolb EA, Turan N, Zhu L, et al. Domestic pigs are susceptible to infection with influenza B viruses. *J Virol.* 2015;89(9):4818-26.
34. Schrauwen EJ, Fouchier RA. Host adaptation and transmission of influenza A viruses in mammals. *Emerg Microbes Infect.* 2014;3(2):e9.
35. Wu Y, Wu Y, Tefsen B, Shi Y, Gao GF. Bat-derived influenza-like viruses H17N10 and H18N11. *Trends Microbiol.* 2014;22(4):183-91.
36. van de Sandt CE, Bodewes R, Rimmelzwaan GF, de Vries RD. Influenza B

viruses: not to be discounted. *Future Microbiol.* 2015;10(9):1447-65.

37. Chen R, Holmes EC. The evolutionary dynamics of human influenza B virus. *J Mol Evol.* 2008;66(6):655-63.
38. Rota PA, Wallis TR, Harmon MW, Rota JS, Kendal AP, Nerome K. Cocirculation of two distinct evolutionary lineages of influenza type B virus since 1983. *Virology.* 1990;175(1):59-68.
39. Chen JM, Guo YJ, Wu KY, Guo JF, Wang M, Dong J, et al. Exploration of the emergence of the Victoria lineage of influenza B virus. *Archives of virology.* 2007;152(2):415-22.
40. Burleigh LM, Calder LJ, Skehel JJ, Steinhauer DA. Influenza A viruses with mutations in the M1 helix six domain display a wide variety of morphological phenotypes. *J Virol.* 2005;79(2):1262-70.
41. Elleman CJ, Barclay WS. The M1 matrix protein controls the filamentous phenotype of influenza A virus. *Virology.* 2004;321(1):144-53.
42. Enami M, Enami K. Influenza virus hemagglutinin and neuraminidase glycoproteins stimulate the membrane association of the matrix protein. *J Virol.* 1996;70(10):6653-7.
43. Jin H, Leser GP, Zhang J, Lamb RA. Influenza virus hemagglutinin and neuraminidase cytoplasmic tails control particle shape. *EMBO J.* 1997;16(6):1236-47.
44. Roberts PC, Lamb RA, Compans RW. The M1 and M2 proteins of influenza A virus are important determinants in filamentous particle formation. *Virology.* 1998;240(1):127-37.
45. Cheung TK, Poon LL. Biology of influenza A virus. *Ann N Y Acad Sci.* 2007;1102:1-25.
46. Pinto LH, Lamb RA. The M2 proton channels of influenza A and B viruses. *J Biol Chem.* 2006;281(14):8997-9000.
47. O'Neill RE, Talon J, Palese P. The influenza virus NEP (NS2 protein) mediates the nuclear export of viral ribonucleoproteins. *EMBO J.* 1998;17(1):288-96.
48. Vasin AV, Temkina OA, Egorov VV, Klotchenko SA, Plotnikova MA, Kiselev OI. Molecular mechanisms enhancing the proteome of influenza A viruses: an overview of recently discovered proteins. *Virus Res.* 2014;185:53-63.

49. Yamayoshi S, Watanabe M, Goto H, Kawaoka Y. Identification of a Novel Viral Protein Expressed from the PB2 Segment of Influenza A Virus. *J Virol*. 2016;90(1):444-56.
50. Rust MJ, Lakadamyali M, Zhang F, Zhuang X. Assembly of endocytic machinery around individual influenza viruses during viral entry. *Nat Struct Mol Biol*. 2004;11(6):567-73.
51. Godley L, Pfeifer J, Steinhauer D, Ely B, Shaw G, Kaufmann R, et al. Introduction of intersubunit disulfide bonds in the membrane-distal region of the influenza hemagglutinin abolishes membrane fusion activity. *Cell*. 1992;68(4):635-45.
52. Leiding T, Wang J, Martinsson J, DeGrado WF, Arskold SP. Proton and cation transport activity of the M2 proton channel from influenza A virus. *Proc Natl Acad Sci U S A*. 2010;107(35):15409-14.
53. Tripathi S, Batra J, Lal SK. Interplay between influenza A virus and host factors: targets for antiviral intervention. *Archives of virology*. 2015;160(8):1877-91.
54. Perez JT, Varble A, Sachidanandam R, Zlatev I, Manoharan M, Garcia-Sastre A, et al. Influenza A virus-generated small RNAs regulate the switch from transcription to replication. *Proc Natl Acad Sci U S A*. 2010;107(25):11525-30.
55. Huang TS, Palese P, Krystal M. Determination of influenza virus proteins required for genome replication. *J Virol*. 1990;64(11):5669-73.
56. Perales B, Ortin J. The influenza A virus PB2 polymerase subunit is required for the replication of viral RNA. *J Virol*. 1997;71(2):1381-5.
57. Zheng H, Lee HA, Palese P, Garcia-Sastre A. Influenza A virus RNA polymerase has the ability to stutter at the polyadenylation site of a viral RNA template during RNA replication. *J Virol*. 1999;73(6):5240-3.
58. Garfinkel MS, Katze MG. Translational control by influenza virus. Selective translation is mediated by sequences within the viral mRNA 5'-untranslated region. *J Biol Chem*. 1993;268(30):22223-6.
59. Rodriguez-Boulan E, Paskiet KT, Salas PJ, Bard E. Intracellular transport of influenza virus hemagglutinin to the apical surface of Madin-Darby canine kidney cells. *J Cell Biol*. 1984;98(1):308-19.
60. Bos TJ, Davis AR, Nayak DP. NH2-terminal hydrophobic region of influenza

virus neuraminidase provides the signal function in translocation. *Proc Natl Acad Sci U S A*. 1984;81(8):2327-31.

61. Sakaguchi T, Leser GP, Lamb RA. The ion channel activity of the influenza virus M2 protein affects transport through the Golgi apparatus. *J Cell Biol*. 1996;133(4):733-47.

62. Bui M, Whittaker G, Helenius A. Effect of M1 protein and low pH on nuclear transport of influenza virus ribonucleoproteins. *J Virol*. 1996;70(12):8391-401.

63. McCown MF, Pekosz A. The influenza A virus M2 cytoplasmic tail is required for infectious virus production and efficient genome packaging. *J Virol*. 2005;79(6):3595-605.

64. Ito T, Goto H, Yamamoto E, Tanaka H, Takeuchi M, Kuwayama M, et al. Generation of a highly pathogenic avian influenza A virus from an avirulent field isolate by passaging in chickens. *J Virol*. 2001;75(9):4439-43.

65. Simonsen L, Viboud C, Grenfell BT, Dushoff J, Jennings L, Smit M, et al. The genesis and spread of reassortment human influenza A/H3N2 viruses conferring adamantane resistance. *Mol Biol Evol*. 2007;24(8):1811-20.

66. Ottmann M, Duchamp MB, Casalegno JS, Frobert E, Moules V, Ferraris O, et al. Novel influenza A(H1N1) 2009 in vitro reassortant viruses with oseltamivir resistance. *Antivir Ther*. 2010;15(5):721-6.

67. Fujisaki S, Takashita E, Yokoyama M, Taniwaki T, Xu H, Kishida N, et al. A single E105K mutation far from the active site of influenza B virus neuraminidase contributes to reduced susceptibility to multiple neuraminidase-inhibitor drugs. *Biochem Biophys Res Commun*. 2012;429(1-2):51-6.

68. Taubenberger JK, Kash JC. Influenza virus evolution, host adaptation, and pandemic formation. *Cell Host Microbe*. 2010;7(6):440-51.

69. Rabadan R, Levine AJ, Robins H. Comparison of avian and human influenza A viruses reveals a mutational bias on the viral genomes. *J Virol*. 2006;80(23):11887-91.

70. Taubenberger JK, Reid AH, Lourens RM, Wang R, Jin G, Fanning TG. Characterization of the 1918 influenza virus polymerase genes. *Nature*. 2005;437(7060):889-93.

71. Scholtissek C, Rohde W, Von Hoyningen V, Rott R. On the origin of the human

influenza virus subtypes H2N2 and H3N2. *Virology*. 1978;87(1):13-20.

72. Kawaoka Y, Krauss S, Webster RG. Avian-to-human transmission of the PB1 gene of influenza A viruses in the 1957 and 1968 pandemics. *J Virol*. 1989;63(11):4603-8.
73. Nakajima K, Desselberger U, Palese P. Recent human influenza A (H1N1) viruses are closely related genetically to strains isolated in 1950. *Nature*. 1978;274(5669):334-9.
74. Smith GJ, Vijaykrishna D, Bahl J, Lycett SJ, Worobey M, Pybus OG, et al. Origins and evolutionary genomics of the 2009 swine-origin H1N1 influenza A epidemic. *Nature*. 2009;459(7250):1122-5.
75. Ambrose CS, Levin MJ. The rationale for quadrivalent influenza vaccines. *Hum Vaccin Immunother*. 2012;8(1):81-8.
76. Vijaykrishna D, Holmes EC, Joseph U, Fourment M, Su YC, Halpin R, et al. The contrasting phylodynamics of human influenza B viruses. *Elife*. 2015;4:e05055.
77. Paul Glezen W, Schmier JK, Kuehn CM, Ryan KJ, Oxford J. The burden of influenza B: a structured literature review. *Am J Public Health*. 2013;103(3):e43-51.
78. Dormitzer PR, Tsai TF, Del Giudice G. New technologies for influenza vaccines. *Hum Vaccin Immunother*. 2012;8(1):45-58.
79. Skowronski DM, Janjua NZ, De Serres G, Sabaiduc S, Eshaghi A, Dickinson JA, et al. Low 2012-13 influenza vaccine effectiveness associated with mutation in the egg-adapted H3N2 vaccine strain not antigenic drift in circulating viruses. *Plos One*. 2014;9(3):e92153.
80. Lee Y, Kim M, Han J, Yeom KH, Lee S, Baek SH, et al. MicroRNA genes are transcribed by RNA polymerase II. *EMBO J*. 2004;23(20):4051-60.
81. Borchert GM, Lanier W, Davidson BL. RNA polymerase III transcribes human microRNAs. *Nat Struct Mol Biol*. 2006;13(12):1097-101.
82. Cai X, Hagedorn CH, Cullen BR. Human microRNAs are processed from capped, polyadenylated transcripts that can also function as mRNAs. *Rna*. 2004;10(12):1957-66.
83. Winter J, Jung S, Keller S, Gregory RI, Diederichs S. Many roads to maturity: microRNA biogenesis pathways and their regulation. *Nat Cell Biol*. 2009;11(3):228-34.

84. Yi R, Qin Y, Macara IG, Cullen BR. Exportin-5 mediates the nuclear export of pre-microRNAs and short hairpin RNAs. *Genes Dev.* 2003;17(24):3011-6.
85. Lund E, Guttinger S, Calado A, Dahlberg JE, Kutay U. Nuclear export of microRNA precursors. *Science.* 2004;303(5654):95-8.
86. Gregory RI, Chendrimada TP, Cooch N, Shiekhattar R. Human RISC couples microRNA biogenesis and posttranscriptional gene silencing. *Cell.* 2005;123(4):631-40.
87. Haase AD, Jaskiewicz L, Zhang H, Laine S, Sack R, Gatignol A, et al. TRBP, a regulator of cellular PKR and HIV-1 virus expression, interacts with Dicer and functions in RNA silencing. *EMBO Rep.* 2005;6(10):961-7.
88. Lee Y, Hur I, Park SY, Kim YK, Suh MR, Kim VN. The role of PACT in the RNA silencing pathway. *EMBO J.* 2006;25(3):522-32.
89. MacRae IJ, Ma E, Zhou M, Robinson CV, Doudna JA. In vitro reconstitution of the human RISC-loading complex. *Proc Natl Acad Sci U S A.* 2008;105(2):512-7.
90. Ketting RF, Fischer SE, Bernstein E, Sijen T, Hannon GJ, Plasterk RH. Dicer functions in RNA interference and in synthesis of small RNA involved in developmental timing in *C. elegans*. *Genes Dev.* 2001;15(20):2654-9.
91. Khvorova A, Reynolds A, Jayasena SD. Functional siRNAs and miRNAs exhibit strand bias. *Cell.* 2003;115(2):209-16.
92. Ghildiyal M, Zamore PD. Small silencing RNAs: an expanding universe. *Nat Rev Genet.* 2009;10(2):94-108.
93. Friedman RC, Farh KK, Burge CB, Bartel DP. Most mammalian mRNAs are conserved targets of microRNAs. *Genome research.* 2009;19(1):92-105.
94. Ameres SL, Zamore PD. Diversifying microRNA sequence and function. *Nat Rev Mol Cell Biol.* 2013;14(8):475-88.
95. Bartel DP. MicroRNAs: target recognition and regulatory functions. *Cell.* 2009;136(2):215-33.
96. Eulalio A, Huntzinger E, Izaurralde E. Getting to the root of miRNA-mediated gene silencing. *Cell.* 2008;132(1):9-14.
97. Chekulaeva M, Filipowicz W. Mechanisms of miRNA-mediated post-transcriptional regulation in animal cells. *Curr Opin Cell Biol.* 2009;21(3):452-60.
98. Eulalio A, Behm-Ansmant I, Izaurralde E. P bodies: at the crossroads of post-

transcriptional pathways. *Nat Rev Mol Cell Biol.* 2007;8(1):9-22.

99. Parker R, Sheth U. P bodies and the control of mRNA translation and degradation. *Mol Cell.* 2007;25(5):635-46.

100. Fabian MR, Sonenberg N, Filipowicz W. Regulation of mRNA translation and stability by microRNAs. *Annu Rev Biochem.* 2010;79:351-79.

101. Gantier MP, Sadler AJ, Williams BR. Fine-tuning of the innate immune response by microRNAs. *Immunol Cell Biol.* 2007;85(6):458-62.

102. Poy MN, Eliasson L, Krutzfeldt J, Kuwajima S, Ma X, Macdonald PE, et al. A pancreatic islet-specific microRNA regulates insulin secretion. *Nature.* 2004;432(7014):226-30.

103. Jopling CL, Yi M, Lancaster AM, Lemon SM, Sarnow P. Modulation of hepatitis C virus RNA abundance by a liver-specific MicroRNA. *Science.* 2005;309(5740):1577-81.

104. Scheel TK, Luna JM, Liniger M, Nishiuchi E, Rozen-Gagnon K, Shlomai A, et al. A Broad RNA Virus Survey Reveals Both miRNA Dependence and Functional Sequestration. *Cell Host Microbe.* 2016;19(3):409-23.

105. Jopling CL, Schutz S, Sarnow P. Position-dependent function for a tandem microRNA miR-122-binding site located in the hepatitis C virus RNA genome. *Cell Host Microbe.* 2008;4(1):77-85.

106. Gao L, Guo XK, Wang L, Zhang Q, Li N, Chen XX, et al. MicroRNA 181 suppresses porcine reproductive and respiratory syndrome virus (PRRSV) infection by targeting PRRSV receptor CD163. *J Virol.* 2013;87(15):8808-12.

107. Chen Z, Ye J, Ashraf U, Li Y, Wei S, Wan S, et al. MicroRNA-33a-5p Modulates Japanese Encephalitis Virus Replication by Targeting Eukaryotic Translation Elongation Factor 1A1. *J Virol.* 2016;90(7):3722-34.

108. Ho BC, Yu SL, Chen JJ, Chang SY, Yan BS, Hong QS, et al. Enterovirus-induced miR-141 contributes to shutoff of host protein translation by targeting the translation initiation factor eIF4E. *Cell Host Microbe.* 2011;9(1):58-69.

109. Slonchak A, Shannon RP, Pali G, Khromykh AA. Human MicroRNA miR-532-5p Exhibits Antiviral Activity against West Nile Virus via Suppression of Host Genes SESTD1 and TAB3 Required for Virus Replication. *J Virol.* 2015;90(5):2388-402.

110. Rosenberger CM, Podyminogin RL, Diercks AH, Treuting PM, Peschon JJ, Rodriguez D, et al. miR-144 attenuates the host response to influenza virus by targeting the TRAF6-IRF7 signaling axis. *PLoS Pathog.* 2017;13(4):e1006305.
111. Kozomara A, Griffiths-Jones S. miRBase: annotating high confidence microRNAs using deep sequencing data. *Nucleic Acids Res.* 2014;42(Database issue):D68-73.
112. Makkoch J, Poomipak W, Saengchoowong S, Khongnomnan K, Praianantathavorn K, Jinato T, et al. Human microRNAs profiling in response to influenza A viruses (subtypes pH1N1, H3N2, and H5N1). *Exp Biol Med (Maywood).* 2016;241(4):409-20.
113. Mei Q, Li X, Meng YG, Wu ZQ, Guo MZ, Zhao YL, et al. A Facile and Specific Assay for Quantifying MicroRNA by an Optimized RT-qPCR Approach. *Plos One.* 2012;7(10).
114. Whelan JA, Russell NB, Whelan MA. A method for the absolute quantification of cDNA using real-time PCR. *J Immunol Methods.* 2003;278(1-2):261-9.
115. Alhoot MA, Wang SM, Sekaran SD. RNA interference mediated inhibition of dengue virus multiplication and entry in HepG2 cells. *Plos One.* 2012;7(3):e34060.
116. Rehmsmeier M, Steffen P, Hochsmann M, Giegerich R. Fast and effective prediction of microRNA/target duplexes. *Rna.* 2004;10(10):1507-17.
117. Campos-Melo D, Droppelmann CA, Volkening K, Strong MJ. Comprehensive luciferase-based reporter gene assay reveals previously masked up-regulatory effects of miRNAs. *Int J Mol Sci.* 2014;15(9):15592-602.
118. Labouesse MA, Polesel M, Clementi E, Muller F, Markkanen E, Mouttet F, et al. MicroRNA Expression Profiling in the Prefrontal Cortex: Putative Mechanisms for the Cognitive Effects of Adolescent High Fat Feeding. *Sci Rep.* 2018;8(1):8344.
119. Zhou B, Lin X, Wang W, Halpin RA, Bera J, Stockwell TB, et al. Universal influenza B virus genomic amplification facilitates sequencing, diagnostics, and reverse genetics. *J Clin Microbiol.* 2014;52(5):1330-7.
120. Zhou B, Donnelly ME, Scholes DT, St George K, Hatta M, Kawaoka Y, et al. Single-reaction genomic amplification accelerates sequencing and vaccine production for classical and Swine origin human influenza A viruses. *J Virol.* 2009;83(19):10309-

- 13.
121. Baccam P, Beauchemin C, Macken CA, Hayden FG, Perelson AS. Kinetics of influenza A virus infection in humans. *J Virol.* 2006;80(15):7590-9.
122. Control CfD. Seasonal Influenza Vaccine Supply for the U.S. 2019-2020 Influenza Season 2019 [Available from: <https://www.cdc.gov/flu/prevent/vaxsupply.htm>].
123. Ping J, Lopes TJS, Nidom CA, Ghedin E, Macken CA, Fitch A, et al. Development of high-yield influenza A virus vaccine viruses. *Nat Commun.* 2015;6:8148.
124. Stohr K, Bucher D, Colgate T, Wood J. Influenza virus surveillance, vaccine strain selection, and manufacture. *Methods Mol Biol.* 2012;865:147-62.
125. Mochalova L, Gambaryan A, Romanova J, Tuzikov A, Chinarev A, Katinger D, et al. Receptor-binding properties of modern human influenza viruses primarily isolated in Vero and MDCK cells and chicken embryonated eggs. *Virology.* 2003;313(2):473-80.
126. Zost SJ, Parkhouse K, Gumina ME, Kim K, Diaz Perez S, Wilson PC, et al. Contemporary H3N2 influenza viruses have a glycosylation site that alters binding of antibodies elicited by egg-adapted vaccine strains. *Proc Natl Acad Sci U S A.* 2017;114(47):12578-83.
127. Widjaja L, Ilyushina N, Webster RG, Webby RJ. Molecular changes associated with adaptation of human influenza A virus in embryonated chicken eggs. *Virology.* 2006;350(1):137-45.
128. Nicholls JM, Chan RW, Russell RJ, Air GM, Peiris JS. Evolving complexities of influenza virus and its receptors. *Trends Microbiol.* 2008;16(4):149-57.
129. Imai M, Kawaoka Y. The role of receptor binding specificity in interspecies transmission of influenza viruses. *Curr Opin Virol.* 2012;2(2):160-7.
130. Einfeld AJ, Neumann G, Kawaoka Y. Influenza A virus isolation, culture and identification. *Nat Protoc.* 2014;9(11):2663-81.
131. Control CfD. Cell-Based Flu Vaccines 2019 [Available from: https://www.cdc.gov/flu/prevent/cell-based.htm?CDC_AA_refVal=https%3A%2F%2Fwww.cdc.gov%2Fflu%2Fprotect%2F

vaccine%2Fcell-based.htm.

132. Agency EM. Flucelvax Tetra 2019 [Available from: <https://www.ema.europa.eu/en/medicines/human/EPAR/flucelvax-tetra#authorisation-details-section>].
133. Hegde NR. Cell culture-based influenza vaccines: A necessary and indispensable investment for the future. *Hum Vaccin Immunother.* 2015;11(5):1223-34.
134. Milian E, Kamen AA. Current and emerging cell culture manufacturing technologies for influenza vaccines. *Biomed Res Int.* 2015;2015:504831.
135. Hutter J, Rodig JV, Hoper D, Seeberger PH, Reichl U, Rapp E, et al. Toward animal cell culture-based influenza vaccine design: viral hemagglutinin N-glycosylation markedly impacts immunogenicity. *J Immunol.* 2013;190(1):220-30.
136. An Y, McCullers JA, Alymova I, Parsons LM, Cipollo JF. Glycosylation Analysis of Engineered H3N2 Influenza A Virus Hemagglutinins with Sequentially Added Historically Relevant Glycosylation Sites. *J Proteome Res.* 2015;14(9):3957-69.
137. Paules CI, Sullivan SG, Subbarao K, Fauci AS. Chasing Seasonal Influenza - The Need for a Universal Influenza Vaccine. *N Engl J Med.* 2018;378(1):7-9.
138. van der Ree MH, van der Meer AJ, de Bruijne J, Maan R, van Vliet A, Welzel TM, et al. Long-term safety and efficacy of microRNA-targeted therapy in chronic hepatitis C patients. *Antiviral Res.* 2014;111:53-9.
139. van der Ree MH, de Vree JM, Stelma F, Willemse S, van der Valk M, Rietdijk S, et al. Safety, tolerability, and antiviral effect of RG-101 in patients with chronic hepatitis C: a phase 1B, double-blind, randomised controlled trial. *Lancet.* 2017;389(10070):709-17.
140. El-Diwany R, Wasilewski LN, Witwer KW, Bailey JR, Page K, Ray SC, et al. Acute Hepatitis C Virus Infection Induces Consistent Changes in Circulating MicroRNAs That Are Associated with Nonlytic Hepatocyte Release. *J Virol.* 2015;89(18):9454-64.
141. Jin BX, Zhang YH, Jin WJ, Sun XY, Qiao GF, Wei YY, et al. MicroRNA panels as disease biomarkers distinguishing hepatitis B virus infection caused hepatitis and liver cirrhosis. *Sci Rep.* 2015;5:15026.
142. Yen YH, Huang CM, Wei KL, Wang JH, Lu SN, Lee CM, et al. MicroRNA-122

- as a predictor of HBsAg seroclearance in hepatitis B and C dual infected patients treated with interferon and ribavirin. *Sci Rep.* 2016;6:33816.
143. Brostoff T, Pesavento PA, Barker CM, Kenney JL, Dietrich EA, Duggal NK, et al. MicroRNA reduction of neuronal West Nile virus replication attenuates and affords a protective immune response in mice. *Vaccine.* 2016;34(44):5366-75.
144. Heiss BL, Maximova OA, Pletnev AG. Insertion of microRNA targets into the flavivirus genome alters its highly neurovirulent phenotype. *J Virol.* 2011;85(4):1464-72.
145. Kozomara A, Birgaoanu M, Griffiths-Jones S. miRBase: from microRNA sequences to function. *Nucleic Acids Res.* 2019;47(D1):D155-D62.
146. Zhao FR, Su S, Zhou DH, Zhou P, Xu TC, Zhang LQ, et al. Comparative analysis of microRNAs from the lungs and trachea of dogs (*Canis familiaris*) infected with canine influenza virus. *Infect Genet Evol.* 2014;21:367-74.
147. Zhu Z, Qi Y, Ge A, Zhu Y, Xu K, Ji H, et al. Comprehensive characterization of serum microRNA profile in response to the emerging avian influenza A (H7N9) virus infection in humans. *Viruses.* 2014;6(4):1525-39.
148. Nakamura S, Horie M, Daidoji T, Honda T, Yasugi M, Kuno A, et al. Influenza A Virus-Induced Expression of a GalNAc Transferase, GALNT3, via MicroRNAs Is Required for Enhanced Viral Replication. *J Virol.* 2016;90(4):1788-801.
149. Wang Y, Brahmakshatriya V, Lupiani B, Reddy SM, Soibam B, Benham AL, et al. Integrated analysis of microRNA expression and mRNA transcriptome in lungs of avian influenza virus infected broilers. *BMC Genomics.* 2012;13:278.
150. Buggele WA, Johnson KE, Horvath CM. Influenza A virus infection of human respiratory cells induces primary microRNA expression. *J Biol Chem.* 2012;287(37):31027-40.
151. Peng F, He Ja, Loo JFC, Kong SK, Li B, Gu D. Identification of serum MicroRNAs as diagnostic biomarkers for influenza H7N9 infection. *Virology Reports.* 2017;7:1-8.
152. Othumpangat S, Bryan NB, Beezhold DH, Noti JD. Upregulation of miRNA-4776 in Influenza Virus Infected Bronchial Epithelial Cells Is Associated with Downregulation of NFKBIB and Increased Viral Survival. *Viruses.* 2017;9(5).

153. Tambyah PA, Sepramaniam S, Mohamed Ali J, Chai SC, Swaminathan P, Armugam A, et al. microRNAs in circulation are altered in response to influenza A virus infection in humans. *Plos One*. 2013;8(10):e76811.
154. Trobaugh DW, Gardner CL, Sun C, Haddow AD, Wang E, Chapnik E, et al. RNA viruses can hijack vertebrate microRNAs to suppress innate immunity. *Nature*. 2014;506(7487):245-8.
155. Lecellier CH, Dunoyer P, Arar K, Lehmann-Che J, Eyquem S, Himber C, et al. A cellular microRNA mediates antiviral defense in human cells. *Science*. 2005;308(5721):557-60.
156. Bai XT, Nicot C. miR-28-3p is a cellular restriction factor that inhibits human T cell leukemia virus, type 1 (HTLV-1) replication and virus infection. *J Biol Chem*. 2015;290(9):5381-90.
157. Zheng Z, Ke X, Wang M, He S, Li Q, Zheng C, et al. Human microRNA hsa-miR-296-5p suppresses enterovirus 71 replication by targeting the viral genome. *J Virol*. 2013;87(10):5645-56.
158. Wen BP, Dai HJ, Yang YH, Zhuang Y, Sheng R. MicroRNA-23b inhibits enterovirus 71 replication through downregulation of EV71 VP1 protein. *Intervirology*. 2013;56(3):195-200.
159. Wang R, Zhang YY, Lu JS, Xia BH, Yang ZX, Zhu XD, et al. The highly pathogenic H5N1 influenza A virus down-regulated several cellular MicroRNAs which target viral genome. *J Cell Mol Med*. 2017;21(11):3076-86.
160. Kumar A, Kumar A, Ingle H, Kumar S, Mishra R, Verma MK, et al. MicroRNA hsa-miR-324-5p Suppresses H5N1 Virus Replication by Targeting the Viral PB1 and Host CUEDC2. *J Virol*. 2018;92(19).
161. Ingle H, Kumar S, Raut AA, Mishra A, Kulkarni DD, Kameyama T, et al. The microRNA miR-485 targets host and influenza virus transcripts to regulate antiviral immunity and restrict viral replication. *Sci Signal*. 2015;8(406):ra126.
162. Bavagnoli L, Campanini G, Forte M, Ceccotti G, Percivalle E, Bione S, et al. Identification of a novel antiviral micro-RNA targeting the NS1 protein of the H1N1 pandemic human influenza virus and a corresponding viral escape mutation. *Antiviral Res*. 2019;171:104593.

163. Peng S, Wang J, Wei S, Li C, Zhou K, Hu J, et al. Endogenous Cellular MicroRNAs Mediate Antiviral Defense against Influenza A Virus. *Mol Ther Nucleic Acids*. 2018;10:361-75.
164. Shimakami T, Yamane D, Jangra RK, Kempf BJ, Spaniel C, Barton DJ, et al. Stabilization of hepatitis C virus RNA by an Ago2-miR-122 complex. *Proc Natl Acad Sci U S A*. 2012;109(3):941-6.
165. Saetrom P, Heale BS, Snove O, Jr., Aagaard L, Alluin J, Rossi JJ. Distance constraints between microRNA target sites dictate efficacy and cooperativity. *Nucleic Acids Res*. 2007;35(7):2333-42.
166. Zhou P, Tu L, Lin X, Hao X, Zheng Q, Zeng W, et al. cfa-miR-143 Promotes Apoptosis via the p53 Pathway in Canine Influenza Virus H3N2-Infected Cells. *Viruses*. 2017;9(12).
167. Chen X, Zhou L, Peng N, Yu H, Li M, Cao Z, et al. MicroRNA-302a suppresses influenza A virus-stimulated interferon regulatory factor-5 expression and cytokine storm induction. *J Biol Chem*. 2017;292(52):21291-303.
168. Loveday EK, Diederich S, Pasick J, Jean F. Human microRNA-24 modulates highly pathogenic avian-origin H5N1 influenza A virus infection in A549 cells by targeting secretory pathway furin. *J Gen Virol*. 2015;96(Pt 1):30-9.
169. Wang K, Lai C, Gu H, Zhao L, Xia M, Yang P, et al. miR-194 Inhibits Innate Antiviral Immunity by Targeting FGF2 in Influenza H1N1 Virus Infection. *Front Microbiol*. 2017;8:2187.
170. Zhang S, Li J, Li J, Yang Y, Kang X, Li Y, et al. Up-regulation of microRNA-203 in influenza A virus infection inhibits viral replication by targeting DR1. *Sci Rep*. 2018;8(1):6797.
171. Maskey N, Li D, Xu H, Song H, Wu C, Hua K, et al. MicroRNA-340 inhibits invasion and metastasis by downregulating ROCK1 in breast cancer cells. *Oncol Lett*. 2017;14(2):2261-7.
172. Yuan J, Ji H, Xiao F, Lin Z, Zhao X, Wang Z, et al. MicroRNA-340 inhibits the proliferation and invasion of hepatocellular carcinoma cells by targeting JAK1. *Biochem Biophys Res Commun*. 2017;483(1):578-84.
173. Fujioka Y, Tsuda M, Nanbo A, Hattori T, Sasaki J, Sasaki T, et al. A Ca²⁺-

dependent signalling circuit regulates influenza A virus internalization and infection. *Nat Commun.* 2013;4:2763.

174. Hui KP, Li HS, Cheung MC, Chan RW, Yuen KM, Mok CK, et al. Highly pathogenic avian influenza H5N1 virus delays apoptotic responses via activation of STAT3. *Sci Rep.* 2016;6:28593.

175. Agarwal V, Bell GW, Nam JW, Bartel DP. Predicting effective microRNA target sites in mammalian mRNAs. *Elife.* 2015;4.

176. Zhao L, Zhang X, Wu Z, Huang K, Sun X, Chen H, et al. The Downregulation of MicroRNA hsa-miR-340-5p in IAV-Infected A549 Cells Suppresses Viral Replication by Targeting RIG-I and OAS2. *Mol Ther Nucleic Acids.* 2019;14:509-19.

177. Park H, Huang X, Lu C, Cairo MS, Zhou X. MicroRNA-146a and microRNA-146b regulate human dendritic cell apoptosis and cytokine production by targeting TRAF6 and IRAK1 proteins. *J Biol Chem.* 2015;290(5):2831-41.

178. Deng Y, Yan Y, Tan KS, Liu J, Chow VT, Tao ZZ, et al. MicroRNA-146a induction during influenza H3N2 virus infection targets and regulates TRAF6 levels in human nasal epithelial cells (hNECs). *Exp Cell Res.* 2017;352(2):184-92.

179. Ho BC, Yu IS, Lu LF, Rudensky A, Chen HY, Tsai CW, et al. Inhibition of miR-146a prevents enterovirus-induced death by restoring the production of type I interferon. *Nat Commun.* 2014;5:3344.

180. Wu S, He L, Li Y, Wang T, Feng L, Jiang L, et al. miR-146a facilitates replication of dengue virus by dampening interferon induction by targeting TRAF6. *J Infect.* 2013;67(4):329-41.

181. Sharma N, Verma R, Kumawat KL, Basu A, Singh SK. miR-146a suppresses cellular immune response during Japanese encephalitis virus JaOArS982 strain infection in human microglial cells. *J Neuroinflammation.* 2015;12:30.

182. Tang WF, Huang RT, Chien KY, Huang JY, Lau KS, Jheng JR, et al. Host MicroRNA miR-197 Plays a Negative Regulatory Role in the Enterovirus 71 Infectious Cycle by Targeting the RAN Protein. *J Virol.* 2016;90(3):1424-38.

183. Hutchinson EC, Fodor E. Transport of the influenza virus genome from nucleus to nucleus. *Viruses.* 2013;5(10):2424-46.

184. Chen Y, Yang C. miR1973-induced downregulation of lysine 63 deubiquitinase

- promotes cell proliferation and inhibits cell apoptosis in lung adenocarcinoma cell lines. *Mol Med Rep.* 2018;17(3):3921-7.
185. Nakhaei P, Genin P, Civas A, Hiscott J. RIG-I-like receptors: sensing and responding to RNA virus infection. *Semin Immunol.* 2009;21(4):215-22.
186. Friedman CS, O'Donnell MA, Legarda-Addison D, Ng A, Cardenas WB, Yount JS, et al. The tumour suppressor CYLD is a negative regulator of RIG-I-mediated antiviral response. *EMBO Rep.* 2008;9(9):930-6.
187. Zhang M, Wu X, Lee AJ, Jin W, Chang M, Wright A, et al. Regulation of IkappaB kinase-related kinases and antiviral responses by tumor suppressor CYLD. *J Biol Chem.* 2008;283(27):18621-6.
188. Ge G, Zhang W, Niu L, Yan Y, Ren Y, Zou Y. miR-215 functions as a tumor suppressor in epithelial ovarian cancer through regulation of the X-chromosome-linked inhibitor of apoptosis. *Oncol Rep.* 2016;35(3):1816-22.
189. Ye MX, Zhang J, Zhang J, Miao Q, Yao LB, Zhang J. Curcumin promotes apoptosis by activating the p53-miR-192-5p/215-XIAP pathway in non-small cell lung cancer. *Cancer Letters.* 2015;357(1):196-205.
190. Deveraux QL, Leo E, Stennicke HR, Welsh K, Salvesen GS, Reed JC. Cleavage of human inhibitor of apoptosis protein XIAP results in fragments with distinct specificities for caspases. *EMBO J.* 1999;18(19):5242-51.
191. Wurzer WJ, Planz O, Ehrhardt C, Giner M, Silberzahn T, Pleschka S, et al. Caspase 3 activation is essential for efficient influenza virus propagation. *EMBO J.* 2003;22(11):2717-28.
192. Shiozaki T, Iwai A, Kawaoka Y, Takada A, Kida H, Miyazaki T. Requirement for Siva-1 for replication of influenza A virus through apoptosis induction. *J Gen Virol.* 2011;92(Pt 2):315-25.
193. Iwai A, Shiozaki T, Miyazaki T. Relevance of signaling molecules for apoptosis induction on influenza A virus replication. *Biochem Biophys Res Commun.* 2013;441(3):531-7.
194. Ahlquist P. RNA-dependent RNA polymerases, viruses, and RNA silencing. *Science.* 2002;296(5571):1270-3.
195. Chen R, Holmes EC. Avian influenza virus exhibits rapid evolutionary

dynamics. *Mol Biol Evol.* 2006;23(12):2336-41.

196. Nobusawa E, Sato K. Comparison of the mutation rates of human influenza A and B viruses. *J Virol.* 2006;80(7):3675-8.

197. Boden D, Pusch O, Lee F, Tucker L, Ramratnam B. Human immunodeficiency virus type 1 escape from RNA interference. *J Virol.* 2003;77(21):11531-5.

198. Westerhout EM, Ooms M, Vink M, Das AT, Berkhout B. HIV-1 can escape from RNA interference by evolving an alternative structure in its RNA genome. *Nucleic Acids Res.* 2005;33(2):796-804.

199. Knossow M, Skehel JJ. Variation and infectivity neutralization in influenza. *Immunology.* 2006;119(1):1-7.

200. Lin Y, Wharton SA, Whittaker L, Dai M, Ermetal B, Lo J, et al. The characteristics and antigenic properties of recently emerged subclade 3C.3a and 3C.2a human influenza A(H3N2) viruses passaged in MDCK cells. *Influenza Other Respir Viruses.* 2017;11(3):263-74.

201. Li D, Saito R, Suzuki Y, Sato I, Zaraket H, Dapat C, et al. In vivo and in vitro alterations in influenza A/H3N2 virus M2 and hemagglutinin genes: effect of passage in MDCK-SIAT1 cells and conventional MDCK cells. *J Clin Microbiol.* 2009;47(2):466-8.

202. Raab N, Mathias S, Alt K, Handrick R, Fischer S, Schmieder V, et al. CRISPR/Cas9-Mediated Knockout of MicroRNA-744 Improves Antibody Titer of CHO Production Cell Lines. *Biotechnol J.* 2019;14(5):e1800477.

203. Teng Y, Luo M, Yu T, Chen L, Huang Q, Chen S, et al. CRISPR/Cas9-mediated deletion of miR-146a enhances antiviral response in HIV-1 infected cells. *Genes Immun.* 2019;20(4):327-37.

204. Jing W, Zhang X, Sun W, Hou X, Yao Z, Zhu Y. CRISPR/CAS9-Mediated Genome Editing of miRNA-155 Inhibits Proinflammatory Cytokine Production by RAW264.7 Cells. *Biomed Res Int.* 2015;2015:326042.

205. Chang H, Yi B, Ma R, Zhang X, Zhao H, Xi Y. CRISPR/cas9, a novel genomic tool to knock down microRNA in vitro and in vivo. *Sci Rep.* 2016;6:22312.

206. Waring BM, Sjaastad LE, Fiege JK, Fay EJ, Reyes I, Moriarity B, et al. MicroRNA-Based Attenuation of Influenza Virus across Susceptible Hosts. *J Virol.* 2018;92(2).

207. Ambion. pSilencer™ siRNA Expression Vectors 2006 [Available from: https://www.thermofisher.com/document-connect/document-connect.html?url=https%3A%2F%2Fassets.thermofisher.com%2FTFS-Assets%2FSLSG%2Fmanuals%2Ffm_7209.pdf&title=cFNpbGVuY2VyJnRyYWRI0yBzaVJOQSBFeHByZXNzaW9uIFZlY3RvcnMgSW5zdHJ1Y3Rpb24gTWfudWFs].
208. Promega. pmirGLO Dual-Luciferase miRNA Target Expression Vector 2016 [Available from: <https://worldwide.promega.com/products/luciferase-assays/genetic-reporter-vectors-and-cell-lines/pmirglo-dual-luciferase-mirna-target-expression-vector/?catNum=E1330>].





จุฬาลงกรณ์มหาวิทยาลัย
CHULALONGKORN UNIVERSITY

VITA

NAME Suthat Saengchoowong

DATE OF BIRTH 26 July 1983

PLACE OF BIRTH Bangkok, Thailand

INSTITUTIONS ATTENDED D.V.M. Faculty of Veterinary Science, Chulalongkorn University

HOME ADDRESS 19/13 Sathupradit Road,
Bangphongphang, Yannawa, Bangkok
10120 Thailand

PUBLICATION

1. Chavalit T, Nimsamer P, Khongnomnan K, Anuntakarun S, Saengchoowong S, Tangkijvanich P, Payungporn S. 2019. Hepatitis B Virus-Encoded MicroRNA (HBV-miR-3) Regulates Host Gene PPM1A Related to Hepatocellular Carcinoma. *Microna*.
2. Saengchoowong S, Khongnomnan K, Poomipak W, Praianantathavorn K, Poovorawan Y, Zhang Q, Payungporn S. 2019. High-Throughput MicroRNA Profiles of Permissive Madin-Darby Canine Kidney Cell Line Infected with Influenza B Viruses. 11(11). pii: E986.
3. Khongnomnan K, Poomipak W, Praianantathavorn K, Saengchoowong S, Pisitkun T, Poovorawan Y, Payungporn S. 2018. Human MicroRNAs Expression Profiles in Influenza B Virus-Infected Cells based on Illumina MiSeq Platform. *Microna*. 7(3):204-214.
4. Makkoch J, Poomipak W, Saengchoowong S, Khongnomnan K, Jinato T, Praianantathavorn K, Poovorawan Y, Payungporn S. 2016. Human MicroRNAs Profiling in Response to Influenza A Viruses (Subtypes pH1N1, H3N2 & H5N1). *Exp Biol Med (Maywood)*. 241(4):409-20.
5. Siengsan-Lamont J, Robertson ID, Blacksell SD, Ellis T, Saengchoowong S, Suwanpukdee S, Yongyuttawichai P, Cheewajorn K, Jangjaras J, Chaichoun K, Wiriyarat W, Ratanakorn P. 2013. A Study of Risk Factors for Infection with HPAI H5N1 in Small Poultry Farms in Thailand Using a Questionnaire Survey. *Zoonoses Public Health*. 60(3):209-14.
6. Siengsan-Lamont J, Robertson I, Blacksell SD, Ellis

T, Fenwick S, Saengchoowong S, Suwanpukdee S, Yongyuttawichai P, Sariya L, Prompiram P, Chaichoun K, Wiriyarat W, Pothieng D, Ratanakorn P. 2011. Virological and Molecular Epidemiological Investigations into the Role of Wild Birds in the Epidemiology of Influenza A/H5N1 in Central Thailand. *Vet Microbiol.* 148(2-4):213-8.

AWARD RECEIVED

- The 100th Anniversary Chulalongkorn University Fund for Doctoral Scholarship, Graduate School, Chulalongkorn University, 2014-2018.
- Young Scientist Award, Merck Ltd., Thailand, 2015.
- Young Ambassador of Science to Thailand, American Society for Microbiology (ASM), 2016-2018.
- Young Scientist Award (Travel Fellowship), the 6th ESWI Influenza Conference, Latvia, 2017.
- Thailand delegate selected by H.R.H Princess Sirindhorn, Global Young Scientists Summit, Singapore, 2018.
- Good Award MSc/PhD Graduate Research Competition 2019, Graduate Affairs, Faculty of Medicine, Chulalongkorn University, 2019.